

**API Ballot 6634  
TG DSE**

<b>Work Item Number</b>	7038
<b>Title of Work Item</b>	Double Shouldered Connections
<b>Ballot Revision Level</b>	
<b>Type of Ballot</b> (Initial, Comment, Comment resolution (reference API ballot#), 1 <sup>st</sup> Re-ballot, 2 <sup>nd</sup> Re-ballot, etc.)	Initial
<b>Submitter Name(s)</b>	Jackie Smith
<b>API Document Modified</b>	New TR 7DSC
<b>Impacted Documents</b>	None
<b>Revision Key</b>	

**Work Item Charge:** Identify the charge of the work group for this item, based on the approved SRRR form.

**Ballot Rationale:** The TR is an intermediate product to document the development process, enabling updates of the relevant standards, 7-2, 7G-2, 7G-1 and eventually 5DP.

**Ballot Text:**

This is for the release of a new TR documenting the development, qualification and design rules for double-shouldered connections, based on Preferred Connections in specification 7-2.

Document is attached:

# **DOUBLE SHOULDER CONNECTION**

API TECHNICAL REPORT 7DSC  
FIRST EDITION, [M] [Y]

## 1 Scope

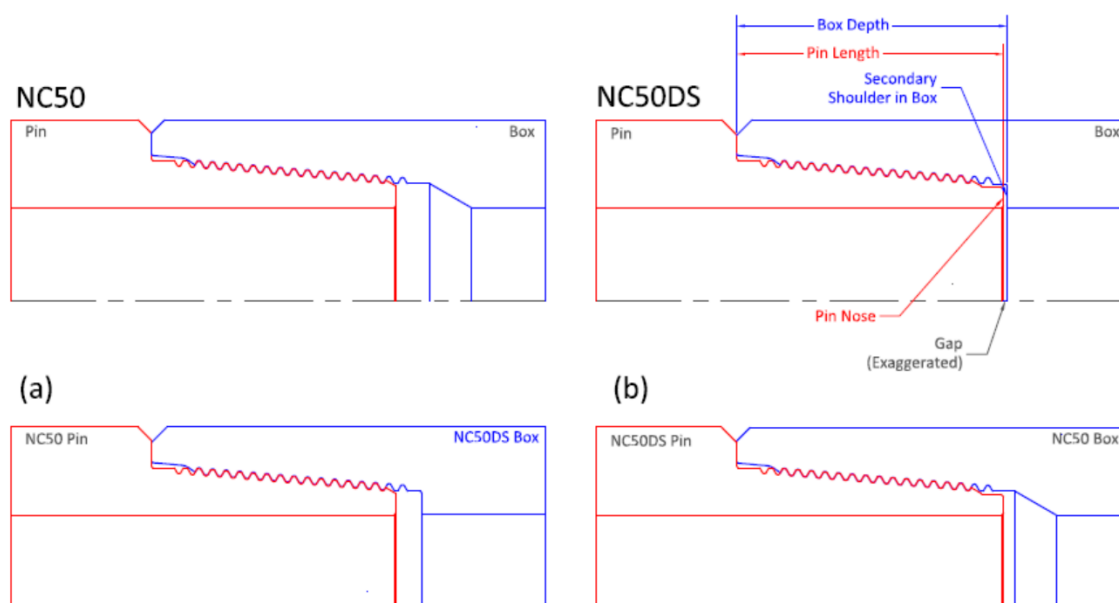
The objective was to design three sizes of double shoulder tool joints (connections) that would interchange with the same style API tool joints; double shoulder pin to API box and API pin to double shoulder box.

Further to that goal:

- The connections are expected to span the drill pipe market.
- The connections show increased torsional strength so the bore diameter can be increased for better hydraulics.
- The introduction of the connections as API products can be an easy process for existing manufacturers of double shoulder connections.
- The connections meet existing field inspection requirements.

The connections selected for development and testing were the NC26DS, NC50DS, and 6-5/8 FHDS.

Figure 1 below shows an NC50 and an NC50DS made-up with each other.



NOTE Top row shows side-by-side comparison of NC50 and NC50DS; the bottom row shows interchangeability.

**Figure 1—Comparison of NC50 and NC50DS**

## 2 6-5/8 X 3-1/2 NC50DS

### 2.1 General

Several manufacturers that produced drill pipe with double shoulder connections capable of make-up with the same size and style API tool joints agreed to share the pin length and box depth dimensions of their connections. The resulting pin length and box depth dimensions and tolerances are shown in Table 1 below.

**Table 1—Pin and Box Dimensions by Contributing Manufacturers**

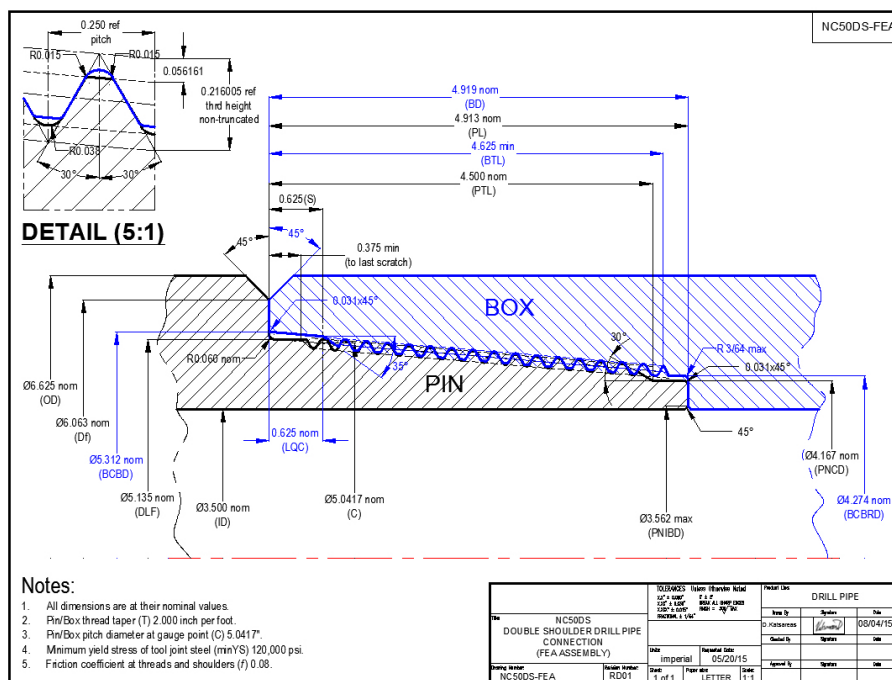
Connection Style and Size	Pin Length	Box Depth
	LPCDS +0.003 -0.000	LBCDS +0.003 -0.000
NC50DS	4.913	4.919

## 2.2 NC50DS Finite Element Analysis

There is a history of double shoulder tool joints going back to 1985, and possibly before. Since then, the design has rapidly evolved so that most connections produced today are different, primarily to make them shorter. The concept of double shoulder tool joints “sat on the shelf” for years because it was felt that tolerances could not be held close enough to machine pins and boxes with and constantly small gap at the secondary shoulder to prevent tensile yielding of the pin when the connection was made-up.

Then, a connection was designed with a two inch long pin base and one inch long pin nose that allowed a reasonable machining tolerance to prevent yielding. It was soon learned there was no damage done to the connections if the combined axial deflection of the pin and box was enough to close a 0.020 in. or greater gap. The fatigue history of double shoulder connections is good according to fatigue tests and observation of double shoulder connections in service. Therefore, the timing and the load sharing of the secondary shoulder with an FEA actual tests using the NC50DS.

A finite element analysis (FEA) was conducted on the NC50DS shown in Figure 2. The dimensions for the pin length, pin nose diameter, box depth, and box thread in the region of the secondary shoulder were picked based on the double shoulder connection manufacturers provided. The rest of the dimensions are the same as those of the NC50. The yield stress was 120 ksi.



NOTE In this configuration, the primary shoulder faces are only touching; i.e. no interference, no load.

**Figure 2—Assembly Drawing of NC50DS with Nominal Dimensions**



The FEA considered only the make-up torque (MUT) in this analysis. An analysis was not conducted for yield torque. The initial condition of the pin and box for the yield torque analysis was “hand tight” with the primary shoulders just touching. Make-up was increased gradually by simulating rotation in increments of 0.005 in. interference at the primary shoulder while advancing the pin into the box. The incremental increases continued until the mean axial stress at the critical cross section of the pin reached 72,000 psi which is 60 % of minimum yield strength recommended in API 7G.

### 2.3 Torque Shoulder Contact Pressure

As shown in Figure 3 below, the mean contact pressure for the primary shoulder is 110,656 psi. The mean contact pressure for the secondary shoulder is 119,460 psi. The added shoulder provides a place for make-up torque to become additional torsional strength. The additional shoulder also impedes pin stretching and box swelling. The FEA report is in Annex A.

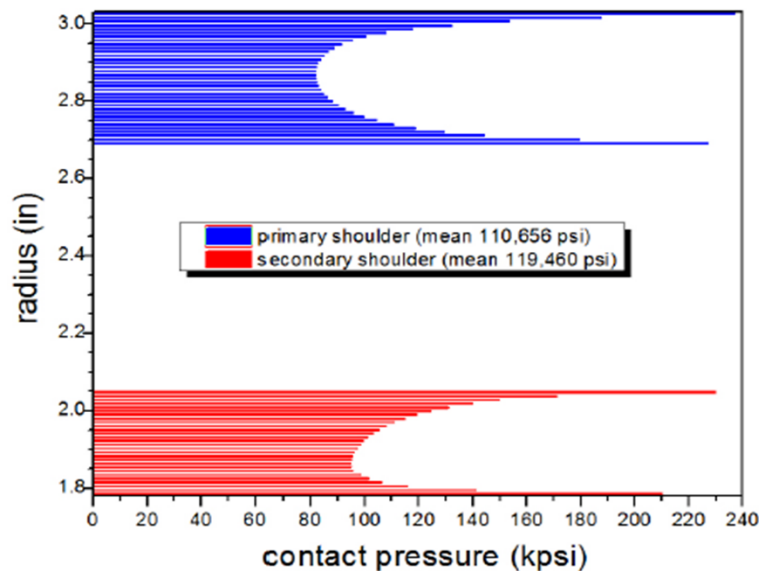


Figure 3—Contact Pressure Distribution over the Primary and Secondary Shoulders

## 3 NC50DC Connection Tests

### 3.1 Break-in Procedure

Make-up each set of connections two times to smooth the tool marks on the thread flanks and induce stress in the thread roots. Use Kopr-Kote thread compound with a 1.15 friction factor. The calculated make-up torque is given for each connection and includes an additional 15 % to account for the thread compound friction factor. The break-in procedure consists of the following steps.

1. Clean, visually inspect and measure shoulder to shoulder pin thread length, shoulder to shoulder box thread length, pin nose OD, and box counterbore ID. Make-up connection to specified make-up torque and break-out.
2. The make-up and break-out was repeated once for a total of two makes and breaks with no inspection or redoping. Make-up and break-up torque was recorded each time.
3. Remove connection from machine.
4. Visually inspect for thread damage, photograph and measure the required connection features.

### 3.2 Torque-to-yield Procedure

The torque-to-yield procedure consists of the following steps.

1. Make-up each connection until slope of torque-turn curve decreases to zero.
2. Break-out connection. Record make-up and break-out torque.
3. Remove connection from machine.
4. Visually inspect, photograph, and measure the required connection features.

### **3.3 NC50DS Torque-turn Test: Break-in**

Break-in and torque-to-yield tests on the NC50DS connections were performed using the tongs shown in Figure 4. The secondary shoulders of new connections should contact during make-up with the calculated make-up torque.



**Figure 4—Tongs Used to Conduct Torsion Tests on NC50DS Connections**

### **3.4 NC50DS Torque-turn Curve, Torque-to-failure**

The first NC50DS make-up and break-out charts are shown below in Figures 5 and 6. The applied torque and compressive stress in the pin nose and box counterbore are plotted vs. time. After the torque reached its predetermined value and the load was released, the strain gauges continued to show compressive stress because the connection was still made-up. Figure 7 on the following page shows a closer view of the timing of contact of both sets of shoulders. Figure 8 shows the timing of the next make-up. The charts show that the secondary shoulders did contact in time to contribute to the torsional strength of the connection.

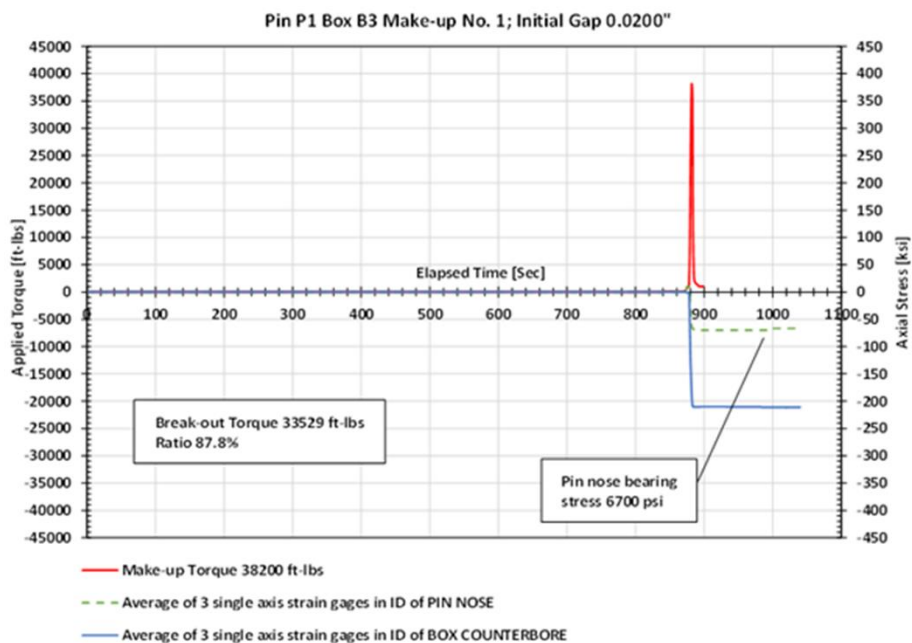


**Figure 5—NC50DS P1–B3 Break-in Cycle, Make-up No. 1**

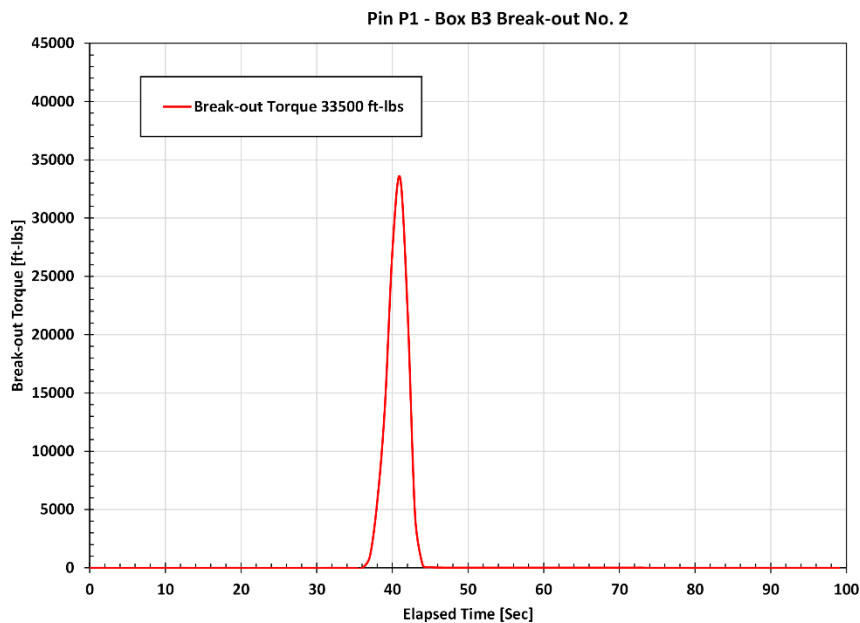


**Figure 6—NC50DS P1–B3 Break-in Cycle, Break-out No. 1**

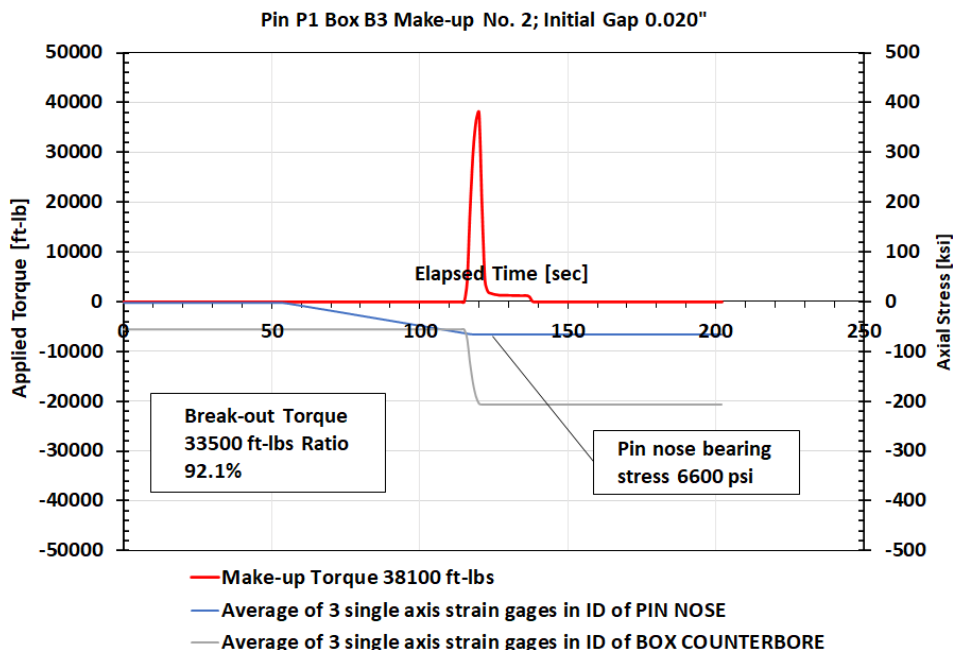


**Figure 7—NC50DS P1-B3 Break-in Cycle, Make-up No. 2**

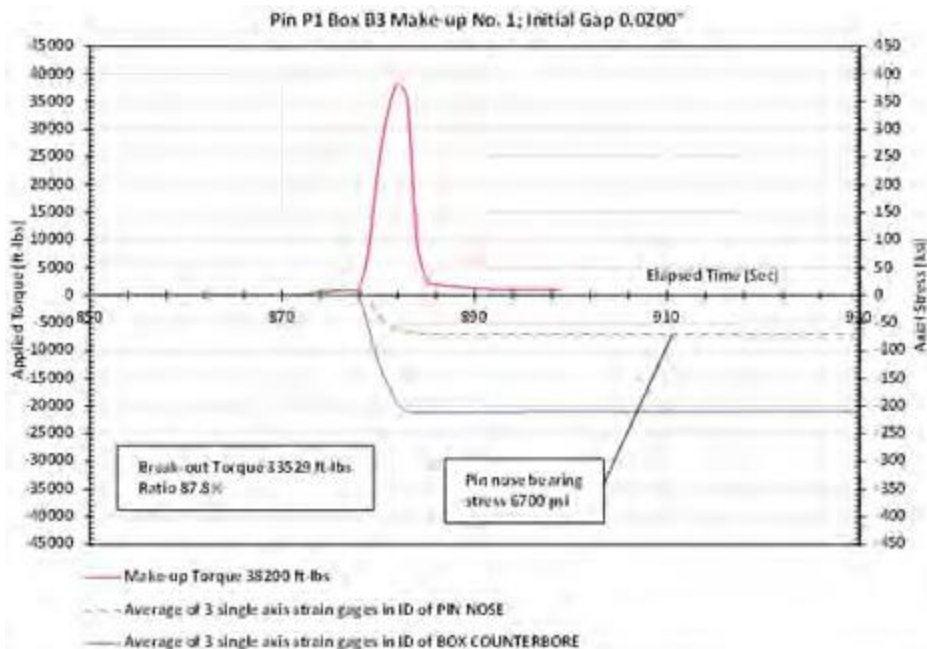


**Figure 8—NC50DS P1-B3 Expanded Time-scale with Timing of Secondary Shoulder Contact**

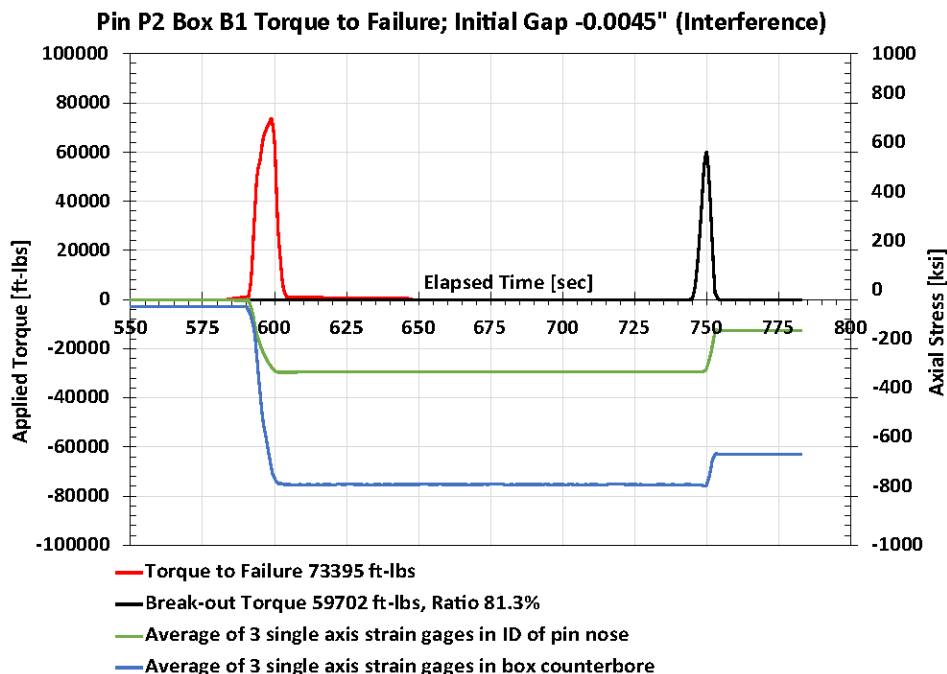


**Figure 9—NC50DS P1–B3 Torque-to-yield and Break-out Curves**

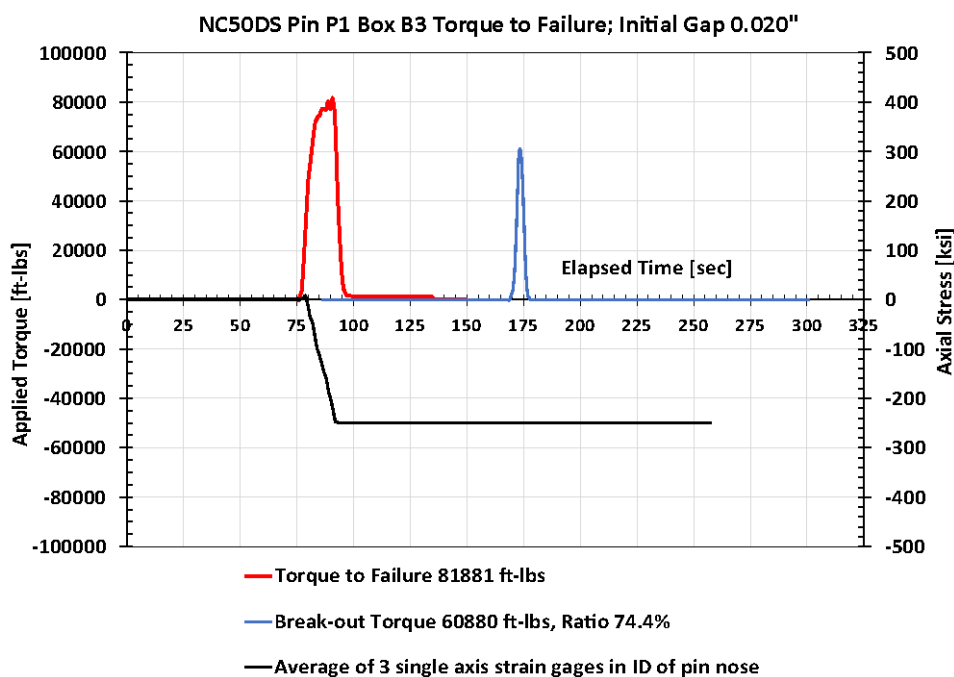


**Figure 10—NC50DS P2–B1 Torque-to-yield and Break-out Curves**





**Figure 11—NC50DS Pin P3 for Torque-to-yield Test**

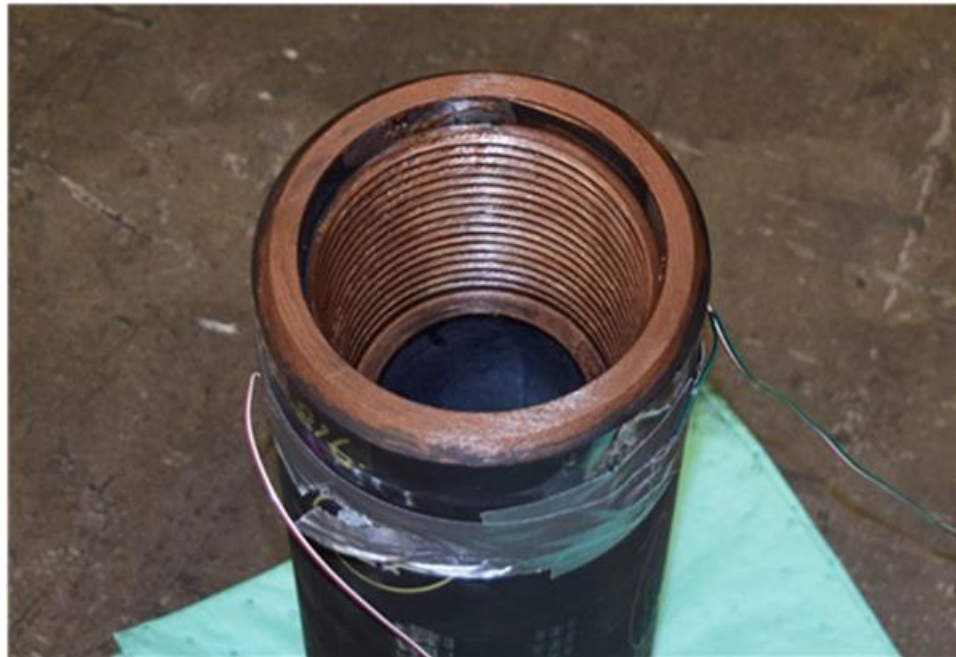


**Figure 12—NC50DS Box for Made-up and Testing**

## **4      3-3/8 X 1-3/4 NC26DS**

### **4.1    General**

The design of the NC26DS followed the design of the NC50DS. The hand-tight gap widths and tolerances are the same even though distance between the primary shoulders on the pin and box are less than they are on the NC50DS. The decision to proceed with testing with no FEA was based on a history of double shoulder NC26, double shoulder 2-7/8 PAC, and other proprietary double shoulder connections of the same size or similar size. Drawings of the NC26DS are in Figures 17 and 18.

Strain gauges were not used in the NC26DS tests. The timing and load of the secondary shoulder contact had been verified in the testing of the NC50DS. The bucking unit produced the torque turn curve and the related data at the time of the test. Photographs of the unit are shown in Figures 15 and 16.

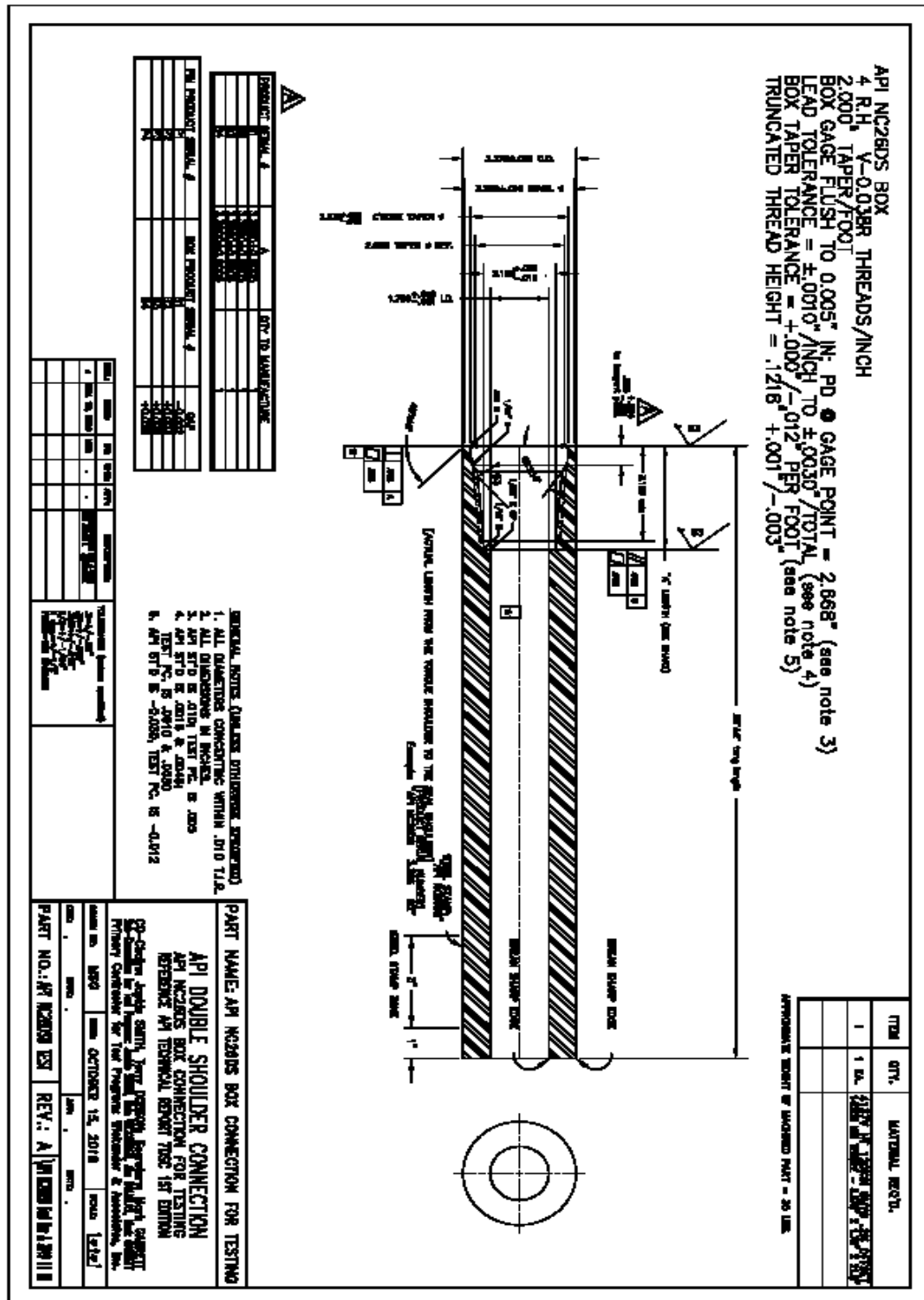
### **4.2    NC26DS Torque-turn Tests**



**Figure 13—Bucking Unit with Torque of 200,000 ft-lb**

### 14—NC26DS Pin Drawing Used in Tests





15—NC26DS Box Drawing Used in Tests

#### 4.4 NC26DS Torque-Turn Curves

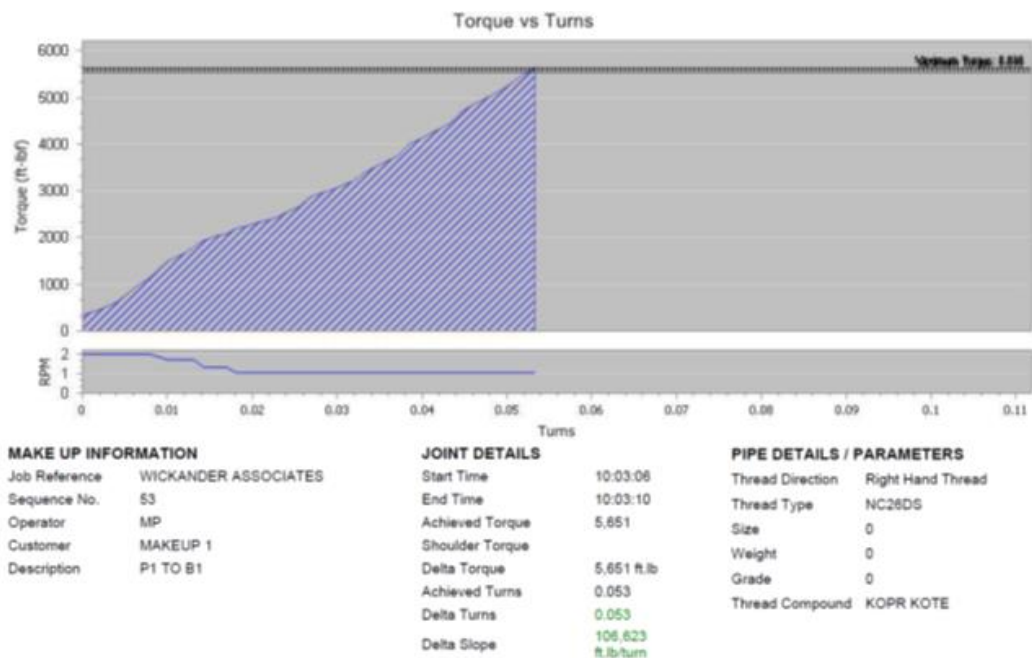


Figure 16—NC26DS P1-B1 Break-in Cycle, Make-up No. 1

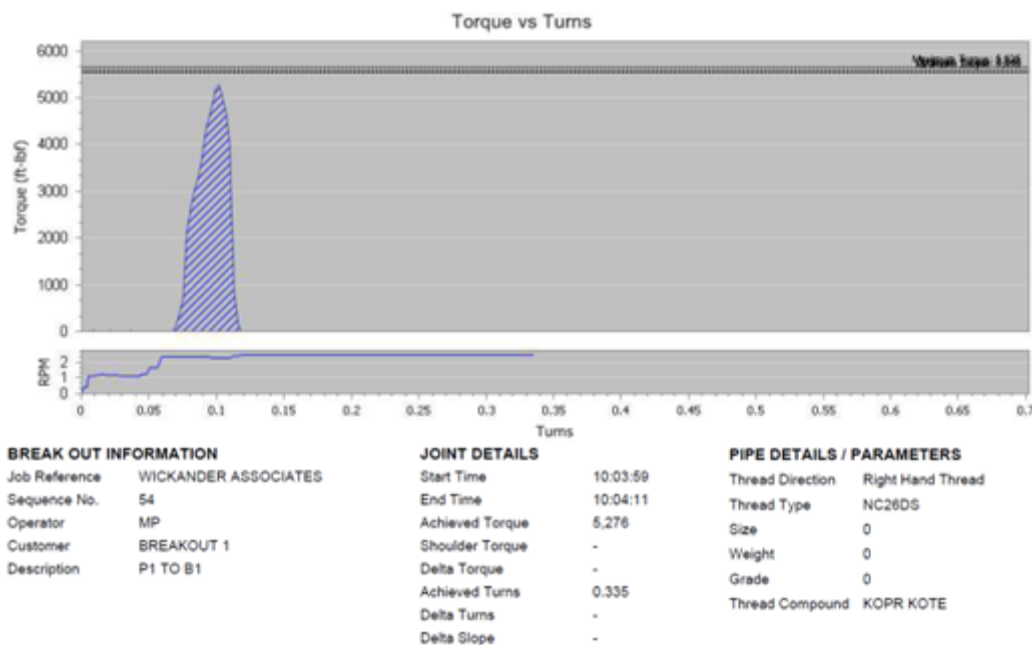


Figure 17—NC26DS P1-B1 Break-in Cycle, Break-out No. 1

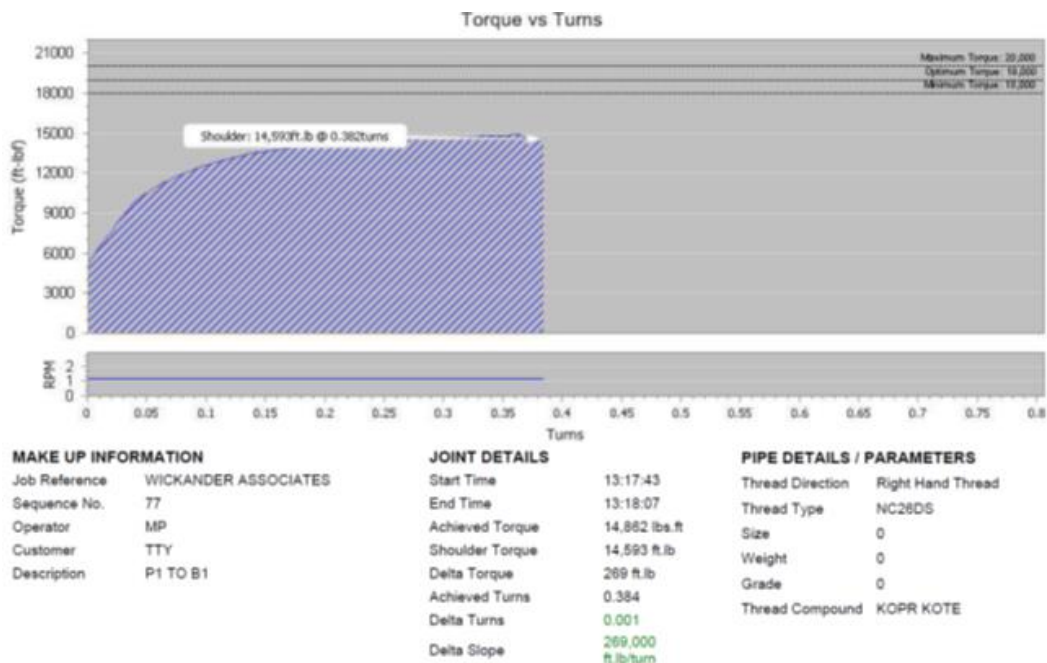


Figure 18—NC26DS P1–B1 Torque-to-Yield, Max Torque 14,862 ft-lb

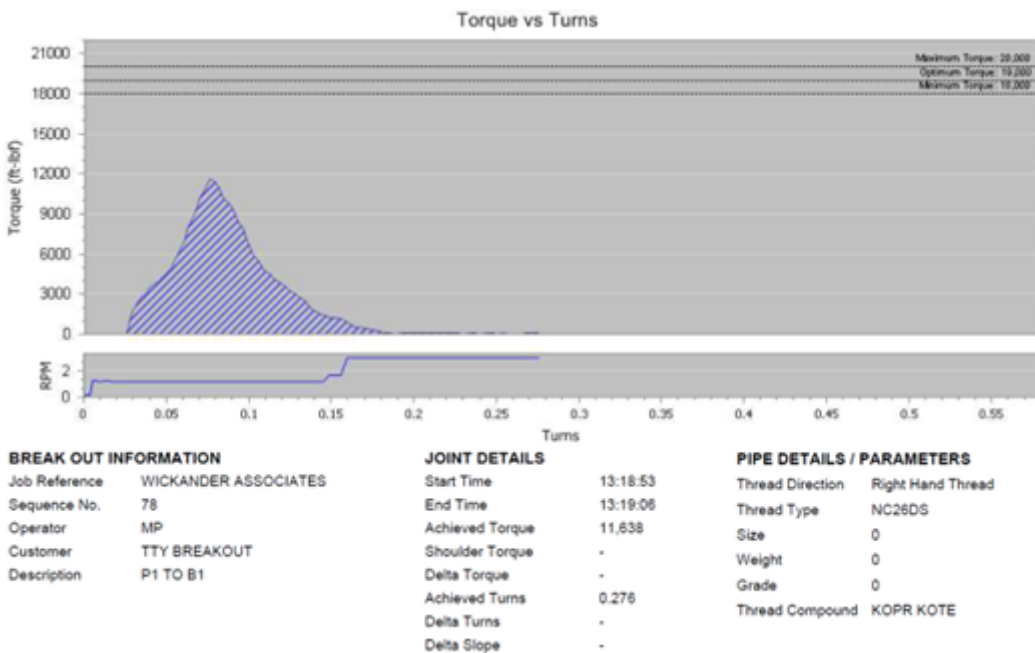


Figure 19—NC26DS P1–B1 Torque-to-yield, Break-out Torque 11,638 ft-lb

## 4.5 NC26DS Photographs



NOTE The “finning” on the pin nose’s perimeter results from high compressive stress by the secondary shoulder.

**Figure 20—NC26DS Pin P2 after Make-up to 14,070 ft-lb in Torque-to-failure Test**



NOTE Despite torquing to 14,070 ft-lb and the box belling, the pipe may still possibly be fished without an overshot.

**Figure 21—NC26DS Box B1 after Torque-to-yield Test**

## **5      8 x 4-3/4 6-5/8 FHDS**

### **5.1      General**

Like the NC26DS, the 6-5/8 FHDS was designed with the same hand-tight gap width and tolerances as the NC50DS even though, in this case, the pin length and box depth are larger. Drawings of the connection are in Figures 31 and 32.

### **5.2      Photographs of 6-5/8 FHDS**

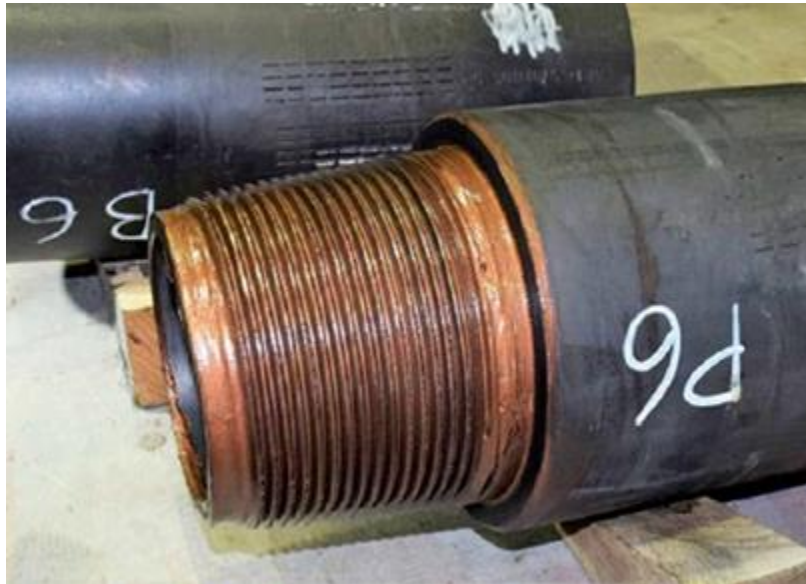


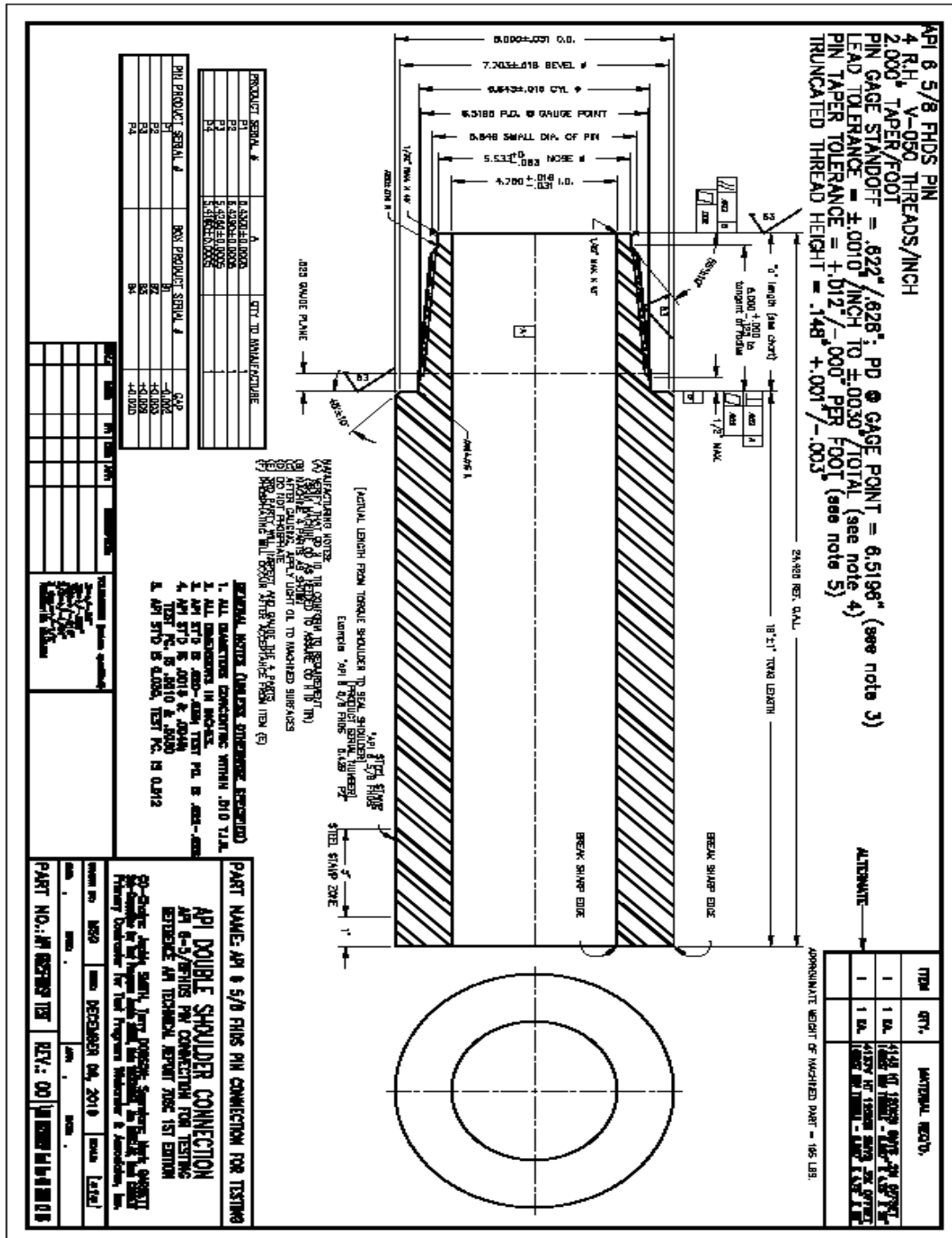
**Figure 22—6-5/8 FHDS Pin P6 after Break-in Cycle Make-up**



**Figure 23—6-5/8 FHDS Box B6 after Break-in Cycle Make-up**

### 5.3 Drawings of 6-5/8 FHDS

Figure 24—6-5/8 FHDS Pin Drawing Used in Tests





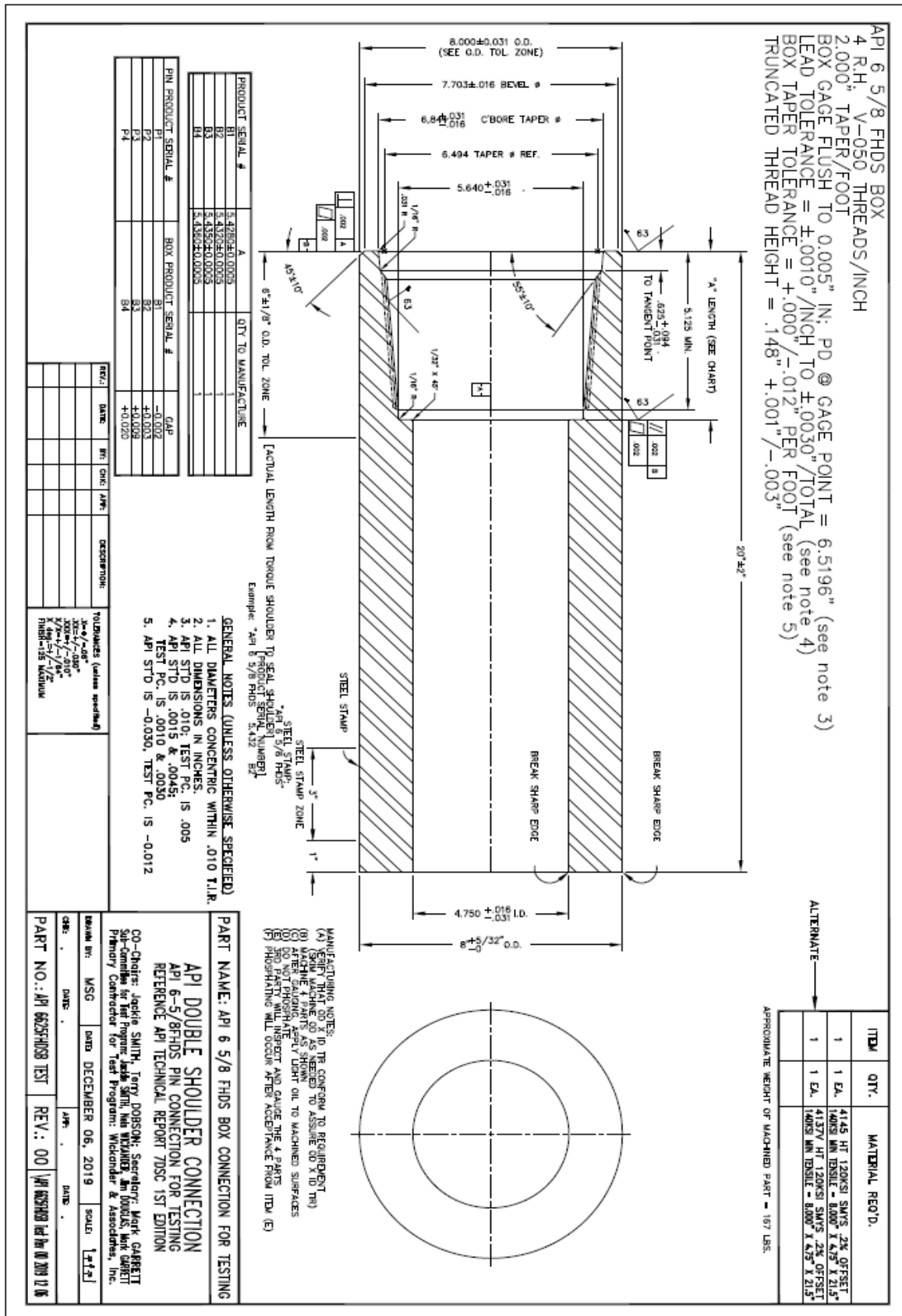


Figure 25—6 5/8 FHDS Box Drawing Used in Tests

## 5.4 6-5/8 FHDS Torque-Turn Curves, Break-in

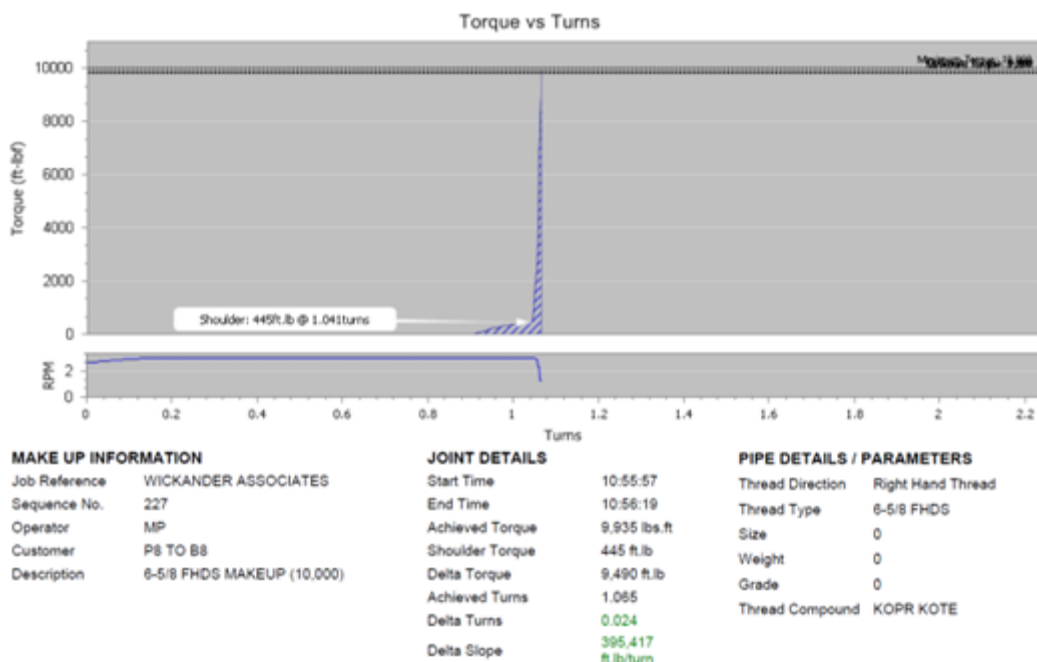


Figure 26—6-5/8 FHDS P8–B8 Break-in Cycle, Make-up No. 1

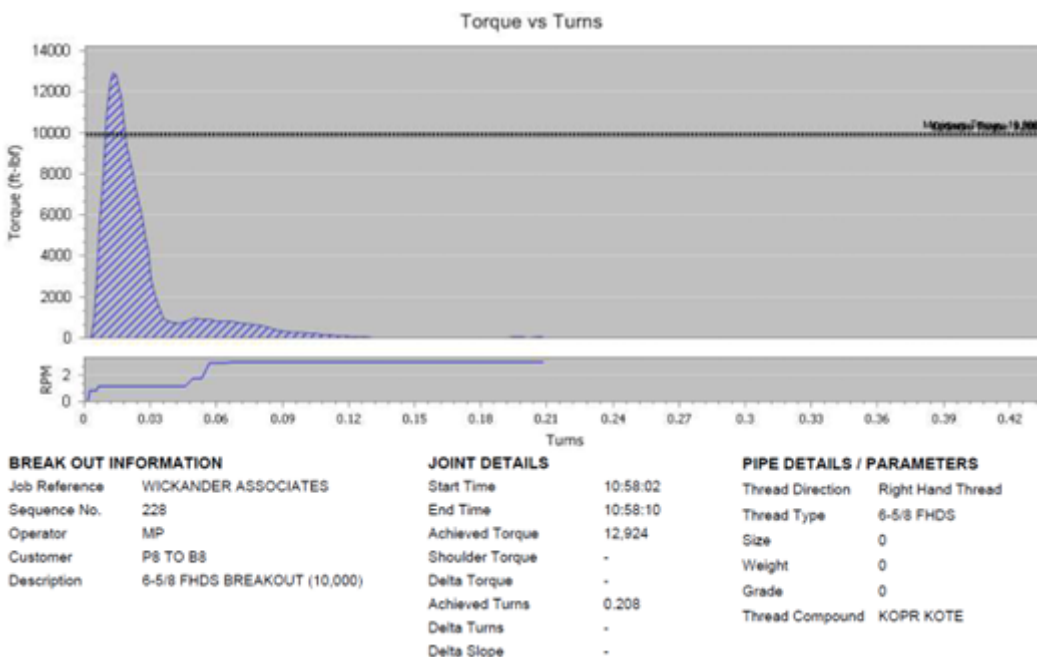


Figure 27—6-5/8 FHDS P8–B8 Break-in Cycle, Break-out No. 1



## 5.5 6-5/8 FHDS Torque to Yield Curves

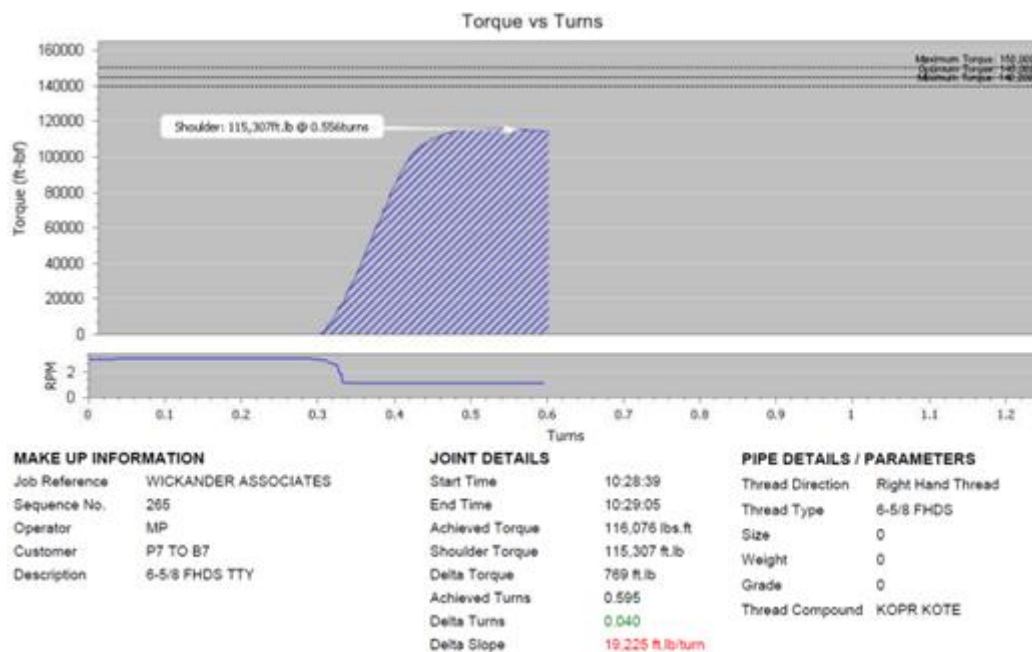


Figure 28—6-5/8 FHDS P7—B7 Torque-to-yield, Max Torque 116,076 ft-lb

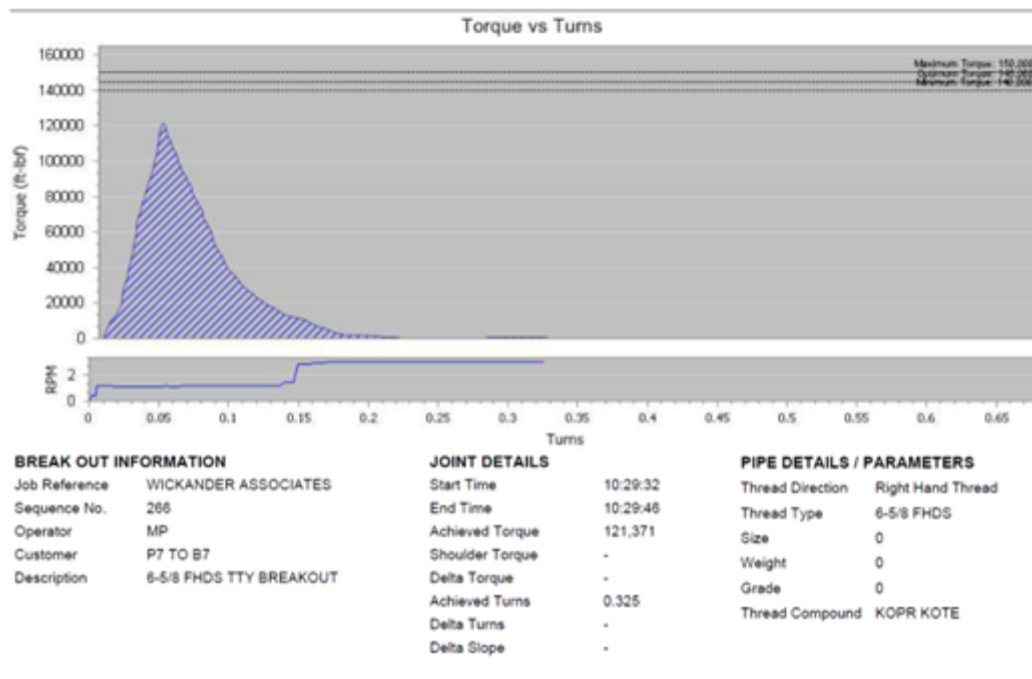


Figure 29—6-5/8 FHDS P7—B7 Torque-to-yield, Break-out Torque 121,371 ft-lb

## 6 Torque-Turn Torque and Measurement Data

### 6.1 General

The following tables summarize the results of the Torque-turn tests. They contain the torsional strength results along with the dimensional changes of the key features of the double shoulder connections.

### 6.2 DS Tabular Data

**Table 2—NC50DS Test Results Data: Pin P1, Box B3**

	<b>Make-up Torque (ft-lb)</b>	<b>Break-out Torque (ft-lb)</b>	<b>Break-out to Make-up Ratio</b>		
<b>Make-up 1</b>	38,200	33,500	87.7 %		
<b>Make-up 2</b>	38,500	33,500	87.0 %		
<b>Torque-to-Yield</b>	81,900	60,900	74.4 %		
	<b>Pin Nose Diameter (in.)</b>	<b>Box C'bore Diameter (in.)</b>	<b>Pin Length (in.)</b>	<b>Box Depth (in.)</b>	<b>Gap (in.)</b>
<b>New</b>	4.1580	5.3110	4.8985	4.9185	0.0200
<b>Make-up 1</b>	4.1445	5.3020	4.8985	4.9185	0.0200
<b>Make-up 2</b>	4.1445	5.3020	4.8985	4.9185	0.0200
<b>Torque-to-Yield</b>	4.1520	5.3080	4.8970	4.9140	0.0170

**Table 3—NC50DS Test Results Data: Pin P2, Box B1**

	<b>Make-up Torque (ft-lb)</b>	<b>Break-out Torque (ft-lb)</b>	<b>Break-out to Make-up Ratio</b>		
<b>Make-up 1</b>	38,600	30,900	80.1 %		
<b>Make-up 2</b>	38,100	32,300	84.8 %		
<b>Torque-to-Yield</b>	73,400	59,700	81.3 %		
	<b>Pin Nose Diameter (in.)</b>	<b>Box C'bore Diameter (in.)</b>	<b>Pin Length (in.)</b>	<b>Box Depth (in.)</b>	<b>Gap (in.)</b>
<b>New</b>	4.1580	5.3070	4.9130	4.9220	0.0090
<b>Make-up 1</b>	4.1590	5.2950	4.9135	4.9215	0.0080
<b>Make-up 2</b>	4.1380	5.2950	4.9135	4.9220	0.0085
<b>Torque-to-Yield</b>	4.1520	5.2950	4.9135	4.9235	0.0090

**Table 4—NC50DS Test Results Data: Pin P3, Box B5**

	<b>Make-up Torque (ft-lb)</b>	<b>Break-out Torque (ft-lb)</b>	<b>Break-out to Make-up Ratio</b>		
<b>Make-up 1</b>	38,600	33,800	87.6 %		
<b>Make-up 2</b>	38,600	34,100	88.3 %		
<b>Torque-to-Yield</b>	79,000	63,200	80.0 %		
	<b>Pin Nose Diameter (in.)</b>	<b>Box C'bore Diameter (in.)</b>	<b>Pin Length (in.)</b>	<b>Box Depth (in.)</b>	<b>Gap (in.)</b>

<b>New</b>	4.1450	5.2950	4.8925	4.9190	0.0265
<b>Make-up 1 <sup>a</sup></b>	—	—	—	—	—
<b>Make-up 2</b>	4.1450	5.2950	4.8925	4.9190	0.0265
<b>Torque-to-Yield</b>	4.1450	5.2950	4.8940	4.9150	0.0210

<sup>a</sup> No measurements taken after make-up 1.

**Table 5—NC26DS Test Results: Pin P1, Box B1**

	<b>Make-up Torque (ft-lb)</b>	<b>Break-out Torque (ft-lb)</b>	<b>Break-out to Make-up Ratio</b>		
<b>Make-up 1</b>	5651	5276	93.4 %		
<b>Make-up 2</b>	5604	5354	95.5 %		
<b>Make-up 3</b>	5739	5192	90.5 %		
<b>Torque-to-Yield</b>	14,862	11,638	78.3 %		
	<b>Pin Nose Diameter (in.)</b>	<b>Box C'bore Diameter (in.)</b>	<b>Pin Length (in.)</b>	<b>Box Depth (in.)</b>	<b>Gap (in.)</b>
<b>New</b>	2.0490	2.9380	3.3840	3.3830	-0.0010
<b>Make-up 1</b>	2.0630	3.3780	3.3840	3.3830	-0.0010
<b>Make-up 2</b>	2.0660	3.3780	3.3810	3.3845	0.0035
<b>Torque-to-Yield</b>	2.1050	3.4730	3.3210	3.3626	0.0416

**Table 6—NC26DS Test Results: Pin P2, Box B2**

	<b>Make-up Torque (ft-lb)</b>	<b>Break-out Torque (ft-lb)</b>	<b>Break-out to Make-up Ratio</b>		
<b>Make-up 1</b>	5837	5350	91.7 %		
<b>Make-up 2</b>	5608	5648	100.7 %		
<b>Make-up 3</b>	5680	5518	97.1 %		
<b>Torque-to-Yield</b>	14,070	10,972	78.0 %		
	<b>Pin Nose Diameter (in.)</b>	<b>Box C'bore Diameter (in.)</b>	<b>Pin Length (in.)</b>	<b>Box Depth (in.)</b>	<b>Gap (in.)</b>
<b>New</b>	2.0490	2.9380	3.3830	3.3870	0.0040
<b>Make-up 1</b>	2.0630	3.3780	3.3830	3.3870	0.0040
<b>Make-up 2</b>	2.0640	3.3780	3.3830	3.3870	0.0040
<b>Torque-to-Yield</b>	2.0740	3.4580	3.3508	3.3508	0.0040

**Table 7—NC26DS Test Results Data: Pin P3, Box B3**

	<b>Make-up Torque (ft-lb)</b>	<b>Break-out Torque (ft-lb)</b>	<b>Break-out to Make-up Ratio</b>		
<b>Make-up 1</b>	5633	5453	96.8 %		
<b>Make-up 2</b>	5735	5524	96.3 %		
<b>Make-up 3</b>	5680	5552	97.7 %		
<b>Torque-to-Yield</b>	13,367	10,739	80.3 %		

	<b>Pin Nose Diameter (in.)</b>	<b>Box C'bore Diameter (in.)</b>	<b>Pin Length (in.)</b>	<b>Box Depth (in.)</b>	<b>Gap (in.)</b>
<b>New</b>	2.0490	2.9380	3.3800	3.3890	0.0090
<b>Make-up 1</b>	2.0630	3.4000	3.3830	3.3900	0.0070
<b>Make-up 2</b>	2.0640	2.3900	3.3790	3.3900	0.0110
<b>Torque-to-Yield</b>	2.0720	3.3610	3.3610	3.3610	0.0000

**Table 8—NC26DS Test Results Data: Pin P4, Box B4**

	<b>Make-up Torque (ft-lb)</b>	<b>Break-out Torque (ft-lb)</b>	<b>Break-out to Make-up Ratio</b>		
<b>Make-up 1</b>	5608	5475	97.6 %		
<b>Make-up 2</b>	5651	5881	104.1 %		
<b>Make-up 3</b>	5600	5484	97.9 %		
<b>Torque-to-Yield</b>	12,963	10,459	80.7 %		
	<b>Pin Nose Diameter (in.)</b>	<b>Box C'bore Diameter (in.)</b>	<b>Pin Length (in.)</b>	<b>Box Depth (in.)</b>	<b>Gap (in.)</b>
<b>New</b>	2.0490	2.9380	3.3910	3.3910	0.0000
<b>Make-up 1</b>	2.0625	2.0625	3.3695	3.3910	0.0215
<b>Make-up 2</b>	2.0625	2.3900	3.3700	3.3900	0.0200
<b>Torque-to-Yield</b>	2.0670	3.3610	3.3510	3.3910	0.0000

**Table 9—6-5/8 FHDS Test Results Data: Pin P5, Box B5**

	<b>Make-up Torque (ft-lb)</b>	<b>Break-out Torque (ft-lb)</b>	<b>Break-out to Make-up Ratio</b>		
<b>New</b>	80,027	80,273	100.3 %		
<b>Make-up 1</b>	79,880	81,479	102.0 %		
<b>Make-up 2</b>	79,635	81,004	101.7 %		
<b>Torque-to-Yield</b>	116,254	118,909	102.3 %		
	<b>Pin Nose Diameter (in.)</b>	<b>Box C'bore Diameter (in.)</b>	<b>Pin Length (in.)</b>	<b>Box Depth (in.)</b>	<b>Gap (in.)</b>
<b>New</b>	5.5040	8.0085	5.4305	5.4280	-0.0025
<b>Make-up 1 <sup>a</sup></b>	—	—	—	—	—
<b>Make-up 2</b>	5.5050	8.0095	5.4305	5.4285	-0.0020
<b>Torque-to-Yield</b>	5.4850	8.0915	5.4100	5.4177	0.0077

<sup>a</sup> No measurements taken after make-up 1.

**Table 10—6-5/8 FHDS Test Results Data: Pin P6, Box B6**

	<b>Make-up Torque (ft-lb)</b>	<b>Break-out Torque (ft-lb)</b>	<b>Break-out to Make-up Ratio</b>		
<b>New</b>	79,525	80,178	100.8 %		
<b>Make-up 1</b>	80,375	82,082	102.1 %		

<b>Make-up 2</b>	79,819	81,770	102.4 %		
<b>Torque-to-Yield</b>	116,654	121,712	104.3 %		
	<b>Pin Nose Diameter (in.)</b>	<b>Box C'bore Diameter (in.)</b>	<b>Pin Length (in.)</b>	<b>Box Depth (in.)</b>	<b>Gap (in.)</b>
<b>New</b>	5.5060	8.0120	5.4295	5.4320	0.0025
<b>Make-up 1 <sup>a</sup></b>	—	—	—	—	—
<b>Make-up 2</b>	5.5065	8.0130	5.4295	5.4320	0.0025
<b>Torque-to-Yield</b>	5.4935	8.0790	5.4140	5.4225	0.0085

<sup>a</sup> No measurements taken after make-up 1.

**Table 11—6-5/8 FHDS Test Results Data: Pin P7, Box B7**

	<b>Make-up Torque (ft-lb)</b>	<b>Break-out Torque (ft-lb)</b>	<b>Break-out to Make-up Ratio</b>		
<b>New</b>	80,186	82,909	103.4 %		
<b>Make-up 1</b>	81,294	84,734	104.2 %		
<b>Make-up 2</b>	79,440	83,830	105.5 %		
<b>Torque-to-Yield</b>	116,076	121,371	104.6 %		
	<b>Pin Nose Diameter (in.)</b>	<b>Box C'bore Diameter (in.)</b>	<b>Pin Length (in.)</b>	<b>Box Depth (in.)</b>	<b>Gap (in.)</b>
<b>New</b>	5.5045	8.0095	5.4245	5.4350	0.0105
<b>Make-up 1 <sup>a</sup></b>	—	—	—	—	—
<b>Make-up 2</b>	5.5050	8.0115	5.4245	5.4340	0.0095
<b>Torque-to-Yield</b>	5.4890	8.0890	5.4170	5.4240	0.0070

<sup>a</sup> No measurements taken after make-up 1.

**Table 12—6-5/8 FHDS Test Results Data: Pin P8, Box B8**

	<b>Make-up Torque (ft-lb)</b>	<b>Break-out Torque (ft-lb)</b>	<b>Break-out to Make-up Ratio</b>		
<b>New</b>	79,894	78,730	98.5 %		
<b>Make-up 1</b>	81,006	80,634	99.5 %		
<b>Make-up 2</b>	79,224	79,737	100.6 %		
<b>Torque-to-Yield</b>	116,468	119,161	102.3 %		
	<b>Pin Nose Diameter (in.)</b>	<b>Box C'bore Diameter (in.)</b>	<b>Pin Length (in.)</b>	<b>Box Depth (in.)</b>	<b>Gap (in.)</b>
<b>New</b>	5.5040	8.0085	5.4165	5.4360	0.0195
<b>Make-up 1 <sup>a</sup></b>	—	—	—	—	—
<b>Make-up 2</b>	5.5055	8.0180	5.4165	5.4340	0.0175
<b>Torque-to-Yield</b>	5.4860	8.0970	5.4095	5.4230	0.0135

<sup>a</sup> No measurements taken after make-up 1.

## 7 Performance Properties

### 7.1 General

This section includes the calculation of the following performance properties of the NC50 and NC50DS from API 7G (16<sup>th</sup> Edition).

- A.8.3 (pre-Addendum): Combined Torsion and Tension-to-yield and a Rotary Shouldered Connection

NOTE With a 1.1 safety factor.

- A.9.1: Torque to Yield a Rotary Shouldered Connection

- A.9.2: Make-up Torque for Rotary Shouldered Connections

- A.10.2 (post-Addendum): Combined Torsion and Tension to Yield Rotary Shouldered Connection and Drill Pipe Body

NOTE Where the applied torque may exceed the make-up torque and no safety factor.

These calculations are included to show the similarities between the single and double shoulder equations in the calculation of their performance properties. The calculations shown here will follow API 7G except the software manages the units; therefore, the “12” is not needed to convert in.-lbs to ft-lbs and will not show up in the equations, and lbf instead of lb is used for force.

### 7.2 Double Shoulder Connection Torque Formula

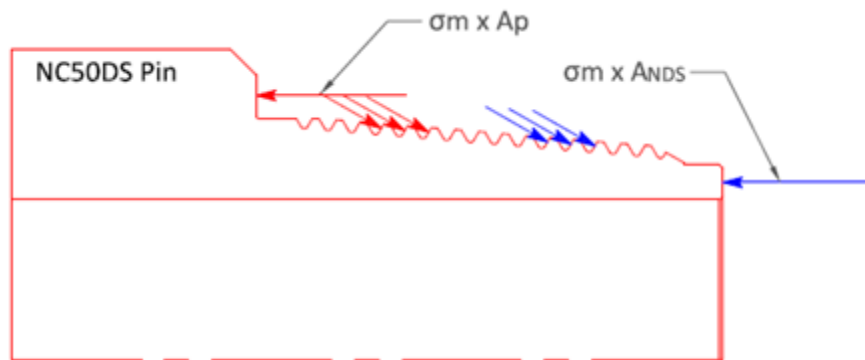
*NC50DS Torsional Strength Formula*

$$T_{NC50} = \sigma_m \cdot A_p \cdot \left( \frac{p}{2 \cdot \pi} + f \cdot \left( \frac{R_T}{\cos(\theta)} + R_S \right) \right)$$

*NC50DS Torsional Strength Formula (nomenclature is on the following page)*

$$T_{NC50DS} = \sigma_m \cdot A_p \cdot \left( \frac{p}{2 \cdot \pi} + f \cdot \left( \frac{R_T}{\cos(\theta)} + R_S \right) \right) + A_{NDS} \cdot \sigma_m \cdot \left( \frac{p}{2 \cdot \pi} + f \cdot \left( \frac{R_T}{\cos(\theta)} + R_{NDS} \right) \right)$$

The first set of terms in the NCDS formula is the same as the NC50 formula. The  $\sigma_m \cdot A_p$  is the force term and the terms in the parentheses are the moment arm or radius terms. The force in the first term acts only on the primary shoulder and is reacted by forces on the “load” flank of the threads. The second term is a result of the secondary shoulder. It’s force term acts on the secondary shoulder and on the load flank of the threads. The radius terms for both connections are the same, except on the NC50DS, the radius of the secondary shoulder takes the place of the radius of the primary shoulder. The forces on the shoulders are independent of each other. When high tensile loads are encountered, the bearing stress on the primary shoulder will decrease but the force on the secondary shoulder will remain the very near the same. Figure 46 illustrates the area difference typical in API double shoulder connections.



Note 1 The primary and secondary shoulders forces on the threads are separated for clarity

Note 2 The forces on the shoulders are independent of each other

**Figure 30—Forces on Connection from Make-up**

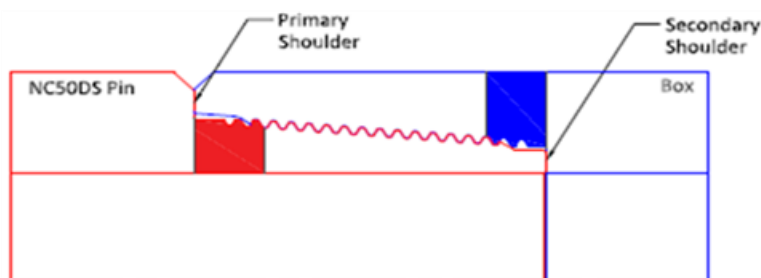


**Figure 31—Cross-sectional Area Difference between Critical Tensile Area of Pin and Box**

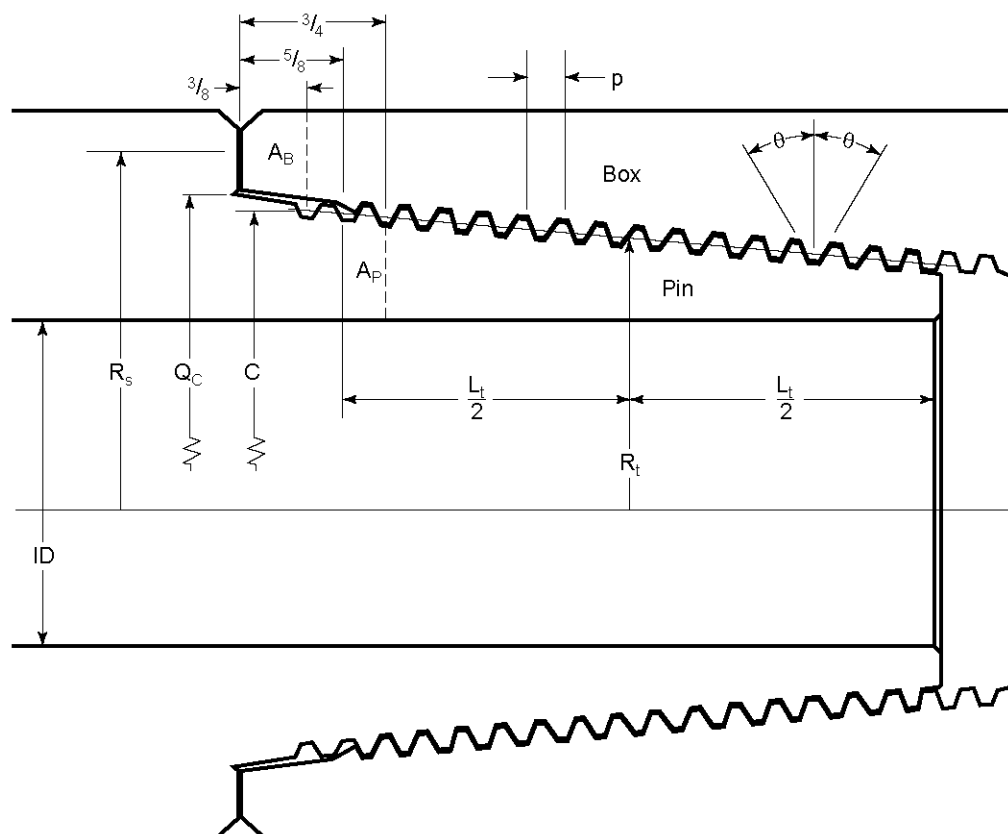


Figure 32—API 7G, Figure A.2: Rotary Shouldered Connection

### 7.3 Combined Torsion and Tension for NC50 and NC50DS

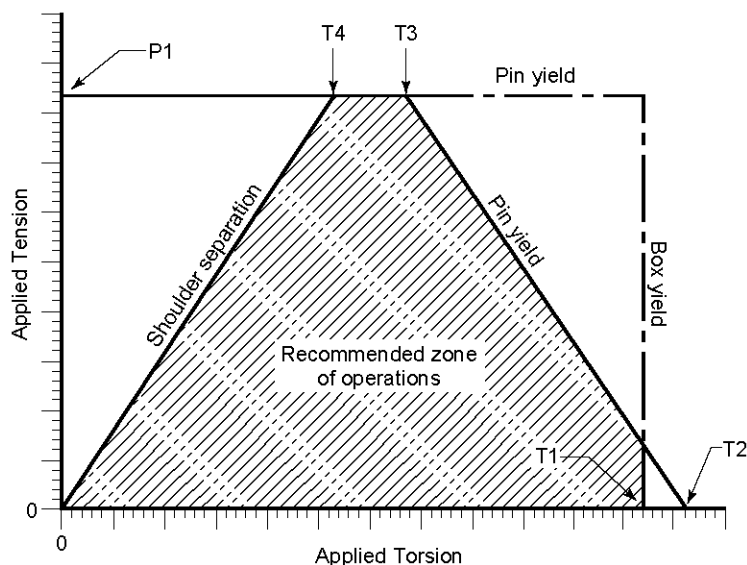


Figure 33—API 7G, Figure A.3: Limits for Combined Torsion and Tension for a Rotary Shouldered Connection

#### Nomenclature—Applies to NC50 and NC50DS

$C := 5.0417 \text{ in}$	Pitch dia at gage point	$p := 0.250 \text{ in}$	Thread pitch
$D := 6.625 \text{ in}$	Outside dia of connection	$Q_C := 5.312 \text{ in}$	Box counterbore dia
$d := 3.500 \text{ in}$	Inside dia of connection	$S_{rs} := 0.0380 \text{ in}$	Thread root radius
$\theta := 30 \text{ deg}$	Thread flank angle	$t_{pr} := 2.000 \frac{\text{in}}{\text{ft}}$	Taper
$f := 0.08$	Coefficient of friction	$Y_m := 120000 \text{ psi}$	Material yield strength
$H := 0.216005 \text{ in}$	Untruncated thread height	$L_{PC} := 4.500 \text{ in}$	Length of pin threads NC50 & NC50DS



$B := 2 \cdot \left( \left( \frac{H}{2} - S_{rs} \right) + tpr \cdot \frac{\text{in}}{8} \right)$	constant in Calculation of $A_p$	$B = 0.182 \text{ in}$
$A_p := \frac{\pi}{4} \cdot \left( (C - B)^2 - d^2 \right)$	CSA at LET of Pin	$A_p = 8.9299 \text{ in}^2$
$E := tpr \cdot \frac{3}{8} \cdot \text{in}$	Constant in Calculation of $A_b$	$E = 0.063 \text{ in}$
$A_b := \frac{\pi}{4} \cdot \left( D^2 - (Q_C - E)^2 \right)$	CSA of Box C' bore	$A_b = 12.828 \text{ in}^2$
$R_S := \frac{D + Q_C}{4}$	Mean (primary) shoulder radius	$R_S = 2.984 \text{ in}$
$R_T := \frac{C - \left( L_{PC} - \frac{5}{8} \cdot \text{in} \right) \cdot tpr}{2}$	Mean thread radius	$R_T = 2.359 \text{ in}$

#### 7.4 Torsional Strength and Make-up Torque for NC50

$A_p = 8.9299 \text{ in}^2$	$A_b = 12.828 \text{ in}^2$	$\min(A_p, A_b) = 8.9299 \text{ in}^2$
$T_{NC50} := A_p \cdot Y_m \cdot \left( \frac{p}{2 \cdot \pi} + f \cdot \left( \frac{R_T}{\cos(\theta)} + R_S \right) \right)$		$T_{NC50} = 44335 \text{ ft} \cdot \text{lb}$
$MUT := 0.6 \cdot T_{NC50}$		$MUT = 26601 \text{ ft} \cdot \text{lb}$
$T_{aNC50} := MUT$		$T_{aNC50} = 26601 \text{ ft} \cdot \text{lb}$
$T_{DH} := 0.75 \cdot 58112 \text{ lb} \cdot \text{ft}$	TDH: Downhole torque = 75% of torsional strength of 5", 19.50 ppf, S-135, premium class drill pipe.	
		$T_{DH} = 43584 \text{ ft} \cdot \text{lb}$
$P1 := Y_m \cdot A_p$	Yield strength of tool joint pin at 5/8" from the make-up shoulder	$P1 = 1071586 \text{ lb}$

$$P_o := \frac{(A_b + A_p) \cdot MUT}{A_b \cdot \left( \frac{p}{2 \cdot \pi} + f \cdot \left( \frac{R_T}{\cos(\theta)} + R_S \right) \right)}$$

Tension required to separate the shoulders after Ta (make-up torque) is applied. Po is represented by the line from the origin to the point T4. Do not use this formula if Ta is greater than T4 since Po will be greater than P1.

$$P_o = 1090518 \text{ lbf}$$

$$P_{T4T2} := (A_b + A_p) \cdot \left( Y_m - \frac{MUT}{A_p \cdot \left( \frac{p}{2 \cdot \pi} + f \cdot \left( \frac{R_T}{\cos(\theta)} + R_S \right) \right)} \right)$$

Tension required to yield pin after MUT is applied. PT4T2 is represented by the line from T4 to T2.

$$P_{T4T2} = 1044388 \text{ lbf}$$

$$P_{T3T2} := \frac{Y_m \cdot A_p \cdot \left( \frac{p}{2 \cdot \pi} + f \cdot \left( \frac{R_T}{\cos(\theta)} + R_S \right) \right) - MUT}{R_S \cdot f}$$

Tension required to yield pin after MUT is applied. PT4T2 is represented by the line from T4 to T2.

$$P_{T3T2} = 891381 \text{ lbf}$$

$$T1 := A_b \cdot Y_m \cdot \left( \frac{p}{2 \cdot \pi} + f \cdot \left( \frac{R_T}{\cos(\theta)} + R_S \right) \right)$$

Torsional strength of the box and is represented by a vertical line at that value on the x-axis.

$$T1 = 63689 \text{ lbf} \cdot \text{ft}$$

$$T2 := A_p \cdot Y_m \cdot \left( \frac{p}{2 \cdot \pi} + f \cdot \left( \frac{R_T}{\cos(\theta)} + R_S \right) \right)$$

Torsional strength of the pin

$$T2 = 44335 \text{ lbf} \cdot \text{ft}$$

$$T3 := A_p \cdot Y_m \cdot \left( \frac{p}{2 \cdot \pi} + f \cdot \left( \frac{R_T}{\cos(\theta)} \right) \right)$$

Torsional strength required to produce additional make-up when the shoulders are separated by a tensile load on the pipe that produces yield stress in the pin.

$$T3 = 23016 \text{ lbf} \cdot \text{ft}$$

$$T4 := Y_m \cdot \left( \frac{A_b \cdot A_p}{A_p + A_b} \right) \cdot \left( \frac{p}{2 \cdot \pi} + f \cdot \left( \frac{R_T}{\cos(\theta)} + R_S \right) \right)$$

Make-up torque at which pin yield and shoulder separation occur simultaneously with an externally applied tensile load.

$$T4 = 26139 \text{ ft} \cdot \text{lbf}$$

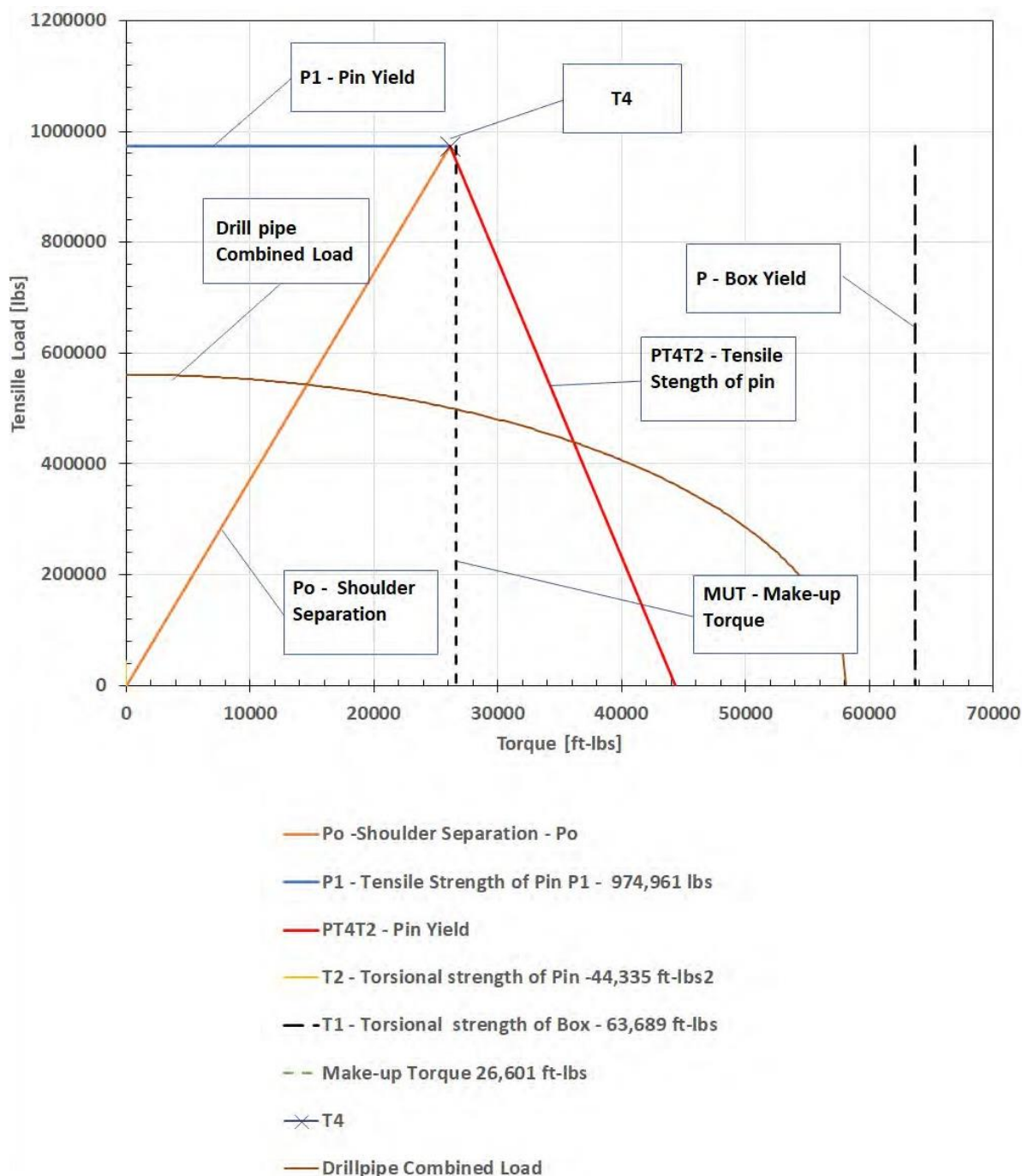


Figure 34—NC50 Combined Load Chart (Make-up Torque THEN Tension)

## 7.5 Torsional Strength and Make-up Torque for NC50DS with 120 ksi Material

$$T_{NC50DS} := \left( A_p \cdot Y_m \cdot \left( \frac{p}{2 \cdot \pi} + f \cdot \left( \frac{R_T}{\cos(\theta)} + R_S \right) \right) + A_{NDS} \cdot Y_m \cdot \left( \frac{p}{2 \cdot \pi} + f \cdot \left( \frac{R_T}{\cos(\theta)} + R_{NDS} \right) \right) \right)$$

$$T_{NC50DS} = 60846 \text{ lbf} \cdot \text{ft}$$

$$MUT_{NC50DS} := 0.6 \cdot T_{NC50DS}$$

$$MUT_{NC50DS} = 36508 \text{ ft} \cdot \text{lbf}$$

$$T_{DH} := 0.75 \cdot 58112 \text{ lbf} \cdot \text{ft} \quad \text{Same as NC50.}$$

$$T_{DH} = 43584 \text{ ft} \cdot \text{lbf}$$

$$P1 := Y_m \cdot A_p \quad \text{Same as NC50.}$$

$$P1 = 1071586 \text{ lbf}$$

$$P_o := \frac{(A_b + A_p) \cdot \left( 1 - \frac{A_{NDS}}{A_p} \right) \cdot MUT_{NC50DS}}{A_b \cdot \left( \frac{p}{2 \cdot \pi} + f \cdot \left( \frac{R_T}{\cos(\theta)} + R_S \right) \right)}$$

$$P_o = 823487 \text{ lbf}$$

$$P_{T4T2} := (A_b + A_p) \cdot \left( Y_m - \frac{MUT_{NC50DS}}{A_p \cdot \left( \frac{p}{2 \cdot \pi} + f \cdot \left( \frac{R_T}{\cos(\theta)} + R_S \right) \right) + A_{NDS} \cdot \left( \frac{p}{2 \cdot \pi} + f \cdot \left( \frac{R_T}{\cos(\theta)} + R_{NDS} \right) \right)} \right)$$

$$P_{T4T2} = 1044388 \text{ lbf}$$

$$T1 := A_b \cdot Y_m \cdot \left( \frac{p}{2 \cdot \pi} + f \cdot \left( \frac{R_T}{\cos(\theta)} + R_S \right) \right) + A_{NDS} \cdot Y_m \cdot \left( \frac{p}{2 \cdot \pi} + f \cdot \left( \frac{R_T}{\cos(\theta)} + R_{NDS} \right) \right)$$

$$T1 = 80200 \text{ lbf} \cdot \text{ft}$$

$$T2 := A_p \cdot Y_m \cdot \left( \frac{p}{2 \cdot \pi} + f \cdot \left( \frac{R_T}{\cos(\theta)} + R_S \right) \right) + A_{NDS} \cdot Y_m \cdot \left( \frac{p}{2 \cdot \pi} + f \cdot \left( \frac{R_T}{\cos(\theta)} + R_{NDS} \right) \right)$$

$$T2 = 60846 \text{ lbf} \cdot \text{ft}$$

$$T3 := A_p \cdot Y_m \cdot \left( \frac{p}{2 \cdot \pi} + f \cdot \left( \frac{R_T}{\cos(\theta)} \right) \right) + A_{NDS} \cdot Y_m \cdot \left( \frac{p}{2 \cdot \pi} + f \cdot \left( \frac{R_T}{\cos(\theta)} + R_{NDS} \right) \right)$$

$$T3 = 39527 \text{ lbf} \cdot \text{ft}$$

$$T4 := Y_m \cdot \left( \frac{A_b \cdot A_p}{A_p + A_b} \right) \cdot \left( \frac{p}{2 \cdot \pi} + f \cdot \left( \frac{R_T}{\cos(\theta)} + R_S \right) \right) + A_{NDS} \cdot Y_m \cdot \left( \frac{p}{2 \cdot \pi} + f \cdot \left( \frac{R_T}{\cos(\theta)} + R_{NDS} \right) \right)$$

$$T4 = 42650 \text{ ft} \cdot \text{lbf}$$



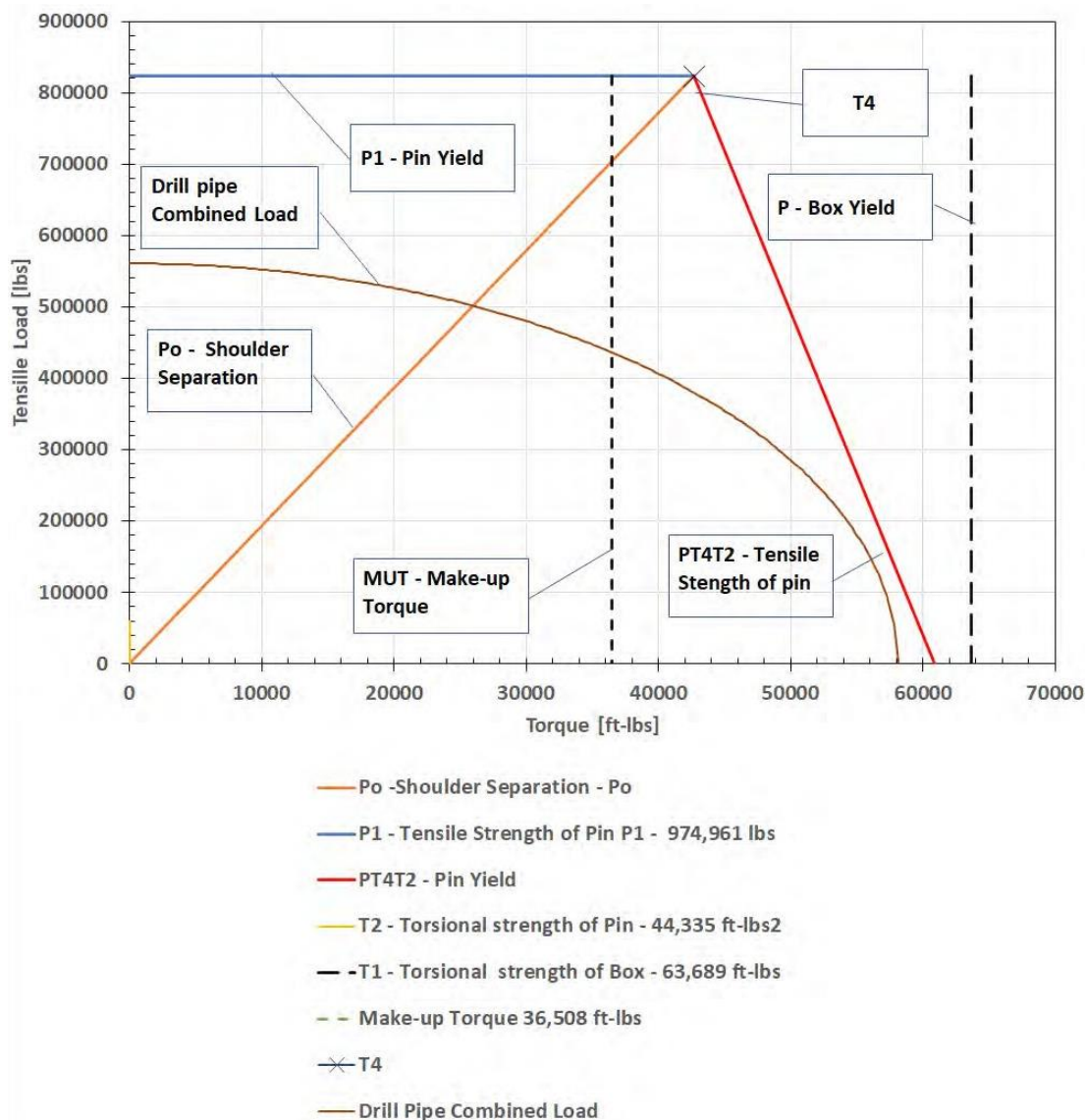


Figure 35—NC50DS Combined Load Chart (Make-up Torque THEN Tension)

## 8 Commentary

### 8.1 History and Attributes

The first modern day double shoulder connection was put into service in 1985. The motivation for designing the connection was to increase the torsional strength of tool joints. An obvious attribute was minimizing stretched pins but that was not the principal motivation.

It took about two decades for the connection to have enough usage to begin noticing other benefits, the most of which appeared to be hydraulics. With the increased torsional strength, bore diameters could increase and still provide adequate torsional strength. Furthermore, these connections could be welded to a larger size pipe which improved annular velocities and resulted in lower pressures losses inside the pipe. This led to the introduction of 5-7/8 in. pipe.

Unaware of any data, it looks as if the double shoulder connection is less likely to fail in fatigue. Thus, it is thought this is true because the secondary shoulder closes the axial gap between the pin and the box ID on conventional joints and instead of a point of flexure that can fatigue boxes, the connection becomes stiffer beam. This could be a real benefit for heavy wall drill string components. Until now, only a few strings of drill collars and heavy weight have had double shoulder connections which is the real test for fatigue but there are more drill collars now using double shoulder connections.

Dimensional tolerances for the pin length and box depth are not a problem either for machine shops with manual machines, the connection's performance or for field inspections. From information supplied by manufacturers, values 0.003 in. tolerance on pin length and box depth were selected, and tested up to 0.022 in. gap size and 0.004 in. interference.

When some conventional tool joints are grossly over-torqued, NC38 and N50 are worst, the boxes can severely bell preventing fishing with on overshot. With double shoulder connections, severe bellings does not occur. The boxes bulge over the juncture of the box counter-bore cylinder and the threads as shown in Figure 30. If bellings does occur, it tends to be minor with no milling required.

### 8.2 Torsional Performance

Table 13 below contains a summary of the torque to yield tests results compared with the calculated torsional strength values. The material strength of the test samples was verified with tensile tests and revised the calculations accordingly. The torque was adjusted by including the friction factor of the thread compound in the equation. An obvious inconsistency in data is the increasing difference between the calculated and the actual torque seen in the last row of data in the table. This difference covers nearly the entire size spectrum of RSC's used in oil and gas well drilling.

**Table 13—Torsional Yield from Torque-turn Tests**

	<b>NC26DS</b>	<b>NC50DS</b>	<b>6-5/8 FHDS</b>
<b>Make-up 1 <sup>a</sup></b>	14,862	81,900	116,254
<b>Make-up 2 <sup>a</sup></b>	14,070	73,400	116,654
<b>Make-up 3 <sup>a</sup></b>	13,367	79,000	116,076
<b>Make-up 4 <sup>a</sup></b>	12,963	—	116,468
<b>Average Torsional Strength <sup>a</sup></b>	13,816	78,100	116,363
<b>Average Break-out Torque <sup>a</sup></b>	10,952	60,291	120,290
<b>Calculated Torque <sup>b</sup></b>	8912	60,846	117,186
<b>Material Strength <sup>c</sup> (ksi)</b>	133	148	132.9
<b>Corrected for Material Strength <sup>a</sup></b>	9907	74,841	129,783

<b>Corrected for Thread Compound 1.15 FF<sup>a,d</sup></b>	11,393	86,067	149,251
<b>Different (calculated – actual)/actual</b>	-18 %	10 %	28 %
<sup>a</sup> Values in ft-lb. <sup>b</sup> Torque calculated using 120 ksi material strength and 0.08 coefficient of friction. <sup>c</sup> Values from the material certifications for the test pieces. <sup>d</sup> Test connections were tested with thread compound with a 1.15 friction factor (not the same as coefficient of friction); 1.15 friction factor multiplies torque by 1.15 times.			

The last line in Table 13 is the difference between the calculated and actual torsional strength values. The errors for the calculated values increased with the size of the connections. While the errors for the NC26DS and 6-5/8 FHDS were large, the error on the NC50DS could be considered within tolerance. The increase in break-out torque with connection size is apparently because the helix angle decreases as the connection size increases (see Figure 32); the torque formula does not account for that.

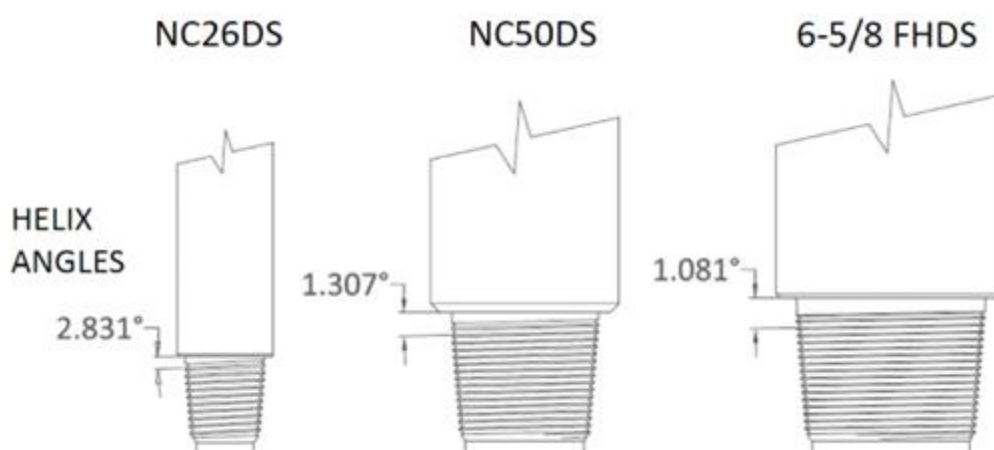


**Figure 36—Helix Angles of the DSCs Tested**

The helix angle defined by the equation on the left.

$$\alpha = \tan \left( \frac{p}{2 \times \pi \times R_t} \right)$$

$\alpha$  -Helix angle

$p$  -Thread pitch

$R_t$  -Radius of thread

$$T = A_p \cdot Y_m \left( \frac{p}{2 \cdot \pi} + f \cdot \left( \frac{R_t}{\cos(\theta)} + R_s \right) \right)$$

The circled term had  $R_t$  in the denominator during the derivation of the Torque Formula but later in the derivation it became the  $R_t$  term in the box.

The tool joint torque equation addresses the thread pitch but not the helix angle as shown in the equation above. In the derivation of the equation, the  $R_t$  term was part of the  $p$  over  $2 \pi$  term circled in red but was moved in an algebraic operation which removed its effect in the torque calculation as contributing to the helix angle.

A decision on whether to correct this oversight (if it is an oversight) in the torque formula was beyond the work scope and it has no bearing on the performance of the double shoulder connections. The derivation of the torque formula, on which the API tool joint torque formula is based, is given in Annex G.

Finally, Table 14 shows a comparison of the torsional strengths from Table 13 of the DSCs with the same size single shoulder connections. The values for the 3-3/8 X 1-3/4 NC26 and 6-5/8 X 3-1/2 NC50 were taken from API 7G; the value for the 8 X 4-3/4 was calculated because that size was not in the 7G-tables.

**Table 14—Comparison of Torsional Strengths of Single Shoulder Connections with DSCs**

	<b>Calculated Torsional Strength (ft-lb)</b>	<b>Make-up Torque (ft-lb)</b>
<b>NC26</b>	6875	4125
<b>NC26DS</b>	11,677	7006
<b>NC50</b>	52,257	31,356
<b>NC50DS</b>	83,980	50,388
<b>6-5/8 FH</b>	85,496	51,298
<b>6-5/8 FHDS</b>	119,036	71,422

### 8.3 Discussion of Dimensional Changes in Torsion Tests

Tables 15-25 below contain dimensions of the pin length, box depth, pin nose diameter and box counterbore diameter measured as manufactured and after each make-up (the 6-5/8 FHDS was measured after the 2<sup>nd</sup> and torque-to-yield only) and after the torsional yield test. These measurements act as an alert to down-hole make-up or over-torquing. The measurements can also warn us of pin nose swelling and swelling of the counterbore section of the box which are also symptoms of the above.

Experience over the last 25 years of double shoulder use tells us that when the same pin and box are made-up repeatedly with each other (i.e., in the same string for an extended period) they tend to conform dimensionally, so that the hand tight gap disappears, and the primary and secondary shoulders are loaded more equally.

Extreme changes in pin length or box depth or extreme changes in the diameter measurements indicate a manufacturing problem or over-torque.

### 8.4 6-5/8 X 3-1/2 NC50DS Dimensional Changes

**Table 15—NC50DS Test Results Data: Pin P1, Box B3**

	<b>Pin Nose Diameter (in.)</b>	<b>Box C'bore Diameter (in.)</b>	<b>Pin Length (in.)</b>	<b>Box Depth (in.)</b>	<b>Gap (in.)</b>
<b>New</b>	4.1580	5.3110	4.8985	4.9185	0.0200
<b>Make-up 1</b>	4.1445	5.3020	4.8985	4.9185	0.0200
<b>Make-up 2</b>	4.1445	5.3020	4.8985	4.9185	0.0200
<b>Torque-to-Yield</b>	4.1520	5.3080	4.8970	4.9140	0.0170
<b>Dimensional Change after M-U #1</b>	-0.0135	-0.0090	0.0000	0.0000	0.0000
<b>Dimensional Change after M-U #2</b>	0.0000	0.0000	0.0000	0.0000	0.0000
<b>Dimensional Change after TTY</b>	0.0075	0.0060	-0.0015	-0.0015	-0.0030

**Table 16—NC50DS Test Results Data: Pin P2, Box B1**



	<b>Pin Nose Diameter (in.)</b>	<b>Box C'bore Diameter (in.)</b>	<b>Pin Length (in.)</b>	<b>Box Depth (in.)</b>	<b>Gap (in.)</b>
<b>New</b>	4.1580	5.3070	4.9130	4.9220	0.0090
<b>Make-up 1</b>	4.1590	5.2950	4.9135	4.9215	0.0080
<b>Make-up 2</b>	4.1380	5.2950	4.9135	4.9220	0.0085
<b>Torque-to-Yield</b>	4.1520	5.2950	4.9145	4.9235	0.0090
<b>Dimensional Change after M-U #1</b>	0.0010	-0.0120	0.0005	-0.0005	-0.0010
<b>Dimensional Change after M-U #2</b>	-0.0210	0.0000	0.0000	0.0005	0.0005
<b>Dimensional Change after TTY</b>	0.0140	0.0000	0.0010	0.0015	0.0005

**Table 17—NC50DS Test Results Data: Pin P3, Box B5**

	<b>Pin Nose Diameter (in.)</b>	<b>Box C'bore Diameter (in.)</b>	<b>Pin Length (in.)</b>	<b>Box Depth (in.)</b>	<b>Gap (in.)</b>
<b>New</b>	4.1580	5.3100	4.9160	4.9190	0.0030
<b>Make-up 1</b>	4.1620	5.3010	4.9160	4.9190	0.0030
<b>Make-up 2</b>	4.1450	5.2950	4.8920	4.9190	0.0270
<b>Torque-to-Yield</b>	4.1450	5.2910	4.8925	4.9190	0.0265
<b>Dimensional Change after M-U #1</b>	0.0040	-0.0090	0.0000	0.0000	0.0000
<b>Dimensional Change after M-U #2</b>	-0.0170	-0.0060	-0.0240	0.0000	0.0240
<b>Dimensional Change after TTY</b>	0.0000	-0.0040	0.0005	0.0000	-0.0005

## **8.5 NC26DS Measurement Results Data**

**Table 18—NC26DS Test Results Data: Pin P1, Box B1**

	<b>Pin Nose Diameter (in.)</b>	<b>Box C'bore Diameter (in.)</b>	<b>Pin Length (in.)</b>	<b>Box Depth (in.)</b>	<b>Gap (in.)</b>
<b>New</b>	2.0490	3.3780	3.3840	3.3820	-0.0020
<b>Make-up 1</b>	2.0630	3.3780	3.3840	3.3820	-0.0010
<b>Make-up 2</b>	2.0660	3.3780	3.3840	3.3845	0.0005
<b>Torque-to-Yield</b>	2.1050	3.4730	3.3840	3.3626	-0.0214
<b>Dimensional Change after M-U #1</b>	0.0140	0.4400	3.3840	0.0010	-3.383

<b>Dimensional Change after M-U #2</b>	0.0170	0.4400	3.3840	0.0025	-3.3815
<b>Dimensional Change after TTY</b>	0.0560	0.5350	3.3840	-0.0194	-3.4034

**Table 19—NC26DS Test Results Data: Pin P2, Box B2**

	<b>Pin Nose Diameter (in.)</b>	<b>Box C'bore Diameter (in.)</b>	<b>Pin Length (in.)</b>	<b>Box Depth (in.)</b>	<b>Gap (in.)</b>
<b>New</b>	2.0490	3.3780	3.3830	3.3870	0.0040
<b>Make-up 1</b>	2.0630	3.3780	3.3830	3.3870	0.0040
<b>Make-up 2</b>	2.0640	3.3780	3.3830	3.3870	0.0040
<b>Torque-to-Yield</b>	2.0740	3.4580	3.3508	3.3508	0.0000
<b>Dimensional Change after M-U #1</b>	0.0140	0.4400	0.0000	0.0000	0.0000
<b>Dimensional Change after M-U #2</b>	0.0150	0.4400	0.0000	0.0000	0.0000
<b>Dimensional Change after TTY</b>	0.0250	0.5200	-0.0322	-0.0362	-0.0040

**Table 20—NC26DS Test Results Data: Pin P3, Box B3**

	<b>Pin Nose Diameter (in.)</b>	<b>Box C'bore Diameter (in.)</b>	<b>Pin Length (in.)</b>	<b>Box Depth (in.)</b>	<b>Gap (in.)</b>
<b>New</b>	2.0490	2.9380	3.3800	3.3890	0.0090
<b>Make-up 1</b>	2.0630	3.4000	3.3830	3.3900	0.0070
<b>Make-up 2</b>	2.0640	3.4040	3.3790	3.3900	0.0110
<b>Torque-to-Yield</b>	2.0720	3.4730	3.3610	3.3610	0.0000
<b>Dimensional Change after M-U #1</b>	0.0140	0.4620	0.0030	0.0010	-0.0020
<b>Dimensional Change after M-U #2</b>	0.0150	0.4660	-0.0010	0.0010	0.0020
<b>Dimensional Change after TTY</b>	0.0230	0.5350	-0.0190	-0.0280	-0.0090

**Table 21—NC26DS Test Results Data: Pin P3, Box B3**

	<b>Pin Nose Diameter (in.)</b>	<b>Box C'bore Diameter (in.)</b>	<b>Pin Length (in.)</b>	<b>Box Depth (in.)</b>	<b>Gap (in.)</b>
<b>New</b>	2.0490	3.4000	3.3800	3.3890	0.0090
<b>Make-up 1</b>	2.0630	3.4000	3.3830	3.3900	0.0070
<b>Make-up 2</b>	2.0640	3.4040	3.3790	3.3900	0.0110

<b>Torque-to-Yield</b>	2.0720	3.4730	3.3610	3.3610	0.0000
<b>Dimensional Change after M-U #1</b>	0.0140	0.4620	0.003	0.0010	-0.002
<b>Dimensional Change after M-U #2</b>	0.0150	0.466	-0.0010	0.0010	0.0020
<b>Dimensional Change after TTY</b>	0.0230	0.5350	-0.0190	-0.0280	-0.0090

**Table 22—NC26DS Test Results Data: Pin P4, Box B4**

	<b>Pin Nose Diameter (in.)</b>	<b>Box C'bore Diameter (in.)</b>	<b>Pin Length (in.)</b>	<b>Box Depth (in.)</b>	<b>Gap (in.)</b>
<b>New</b>	2.0490	3.3780	3.3910	3.3910	0.0000
<b>Make-up 1</b>	2.0625	3.3780	3.3695	3.3910	0.0215
<b>Make-up 2</b>	2.0625	3.3840	3.3700	3.3900	0.0200
<b>Torque-to-Yield</b>	2.0670	3.4720	3.3510	3.3510	0.0000
<b>Dimensional Change after M-U #1</b>	0.0135	0.4400	-0.0215	0.0000	0.0215
<b>Dimensional Change after M-U #2</b>	0.0135	0.4460	-0.0210	-0.0010	0.0200
<b>Dimensional Change after TTY</b>	0.0180	0.5340	-0.0400	-0.0400	0.0000

## 8.6 8 X 4-1/4 6-5/8 FHDS Dimensional Changes

**Table 23—6-5/8 FHDS Test Results Data: Pin P5, Box B5**

	<b>Pin Nose Diameter (in.)</b>	<b>Box C'bore Diameter (in.)</b>	<b>Pin Length (in.)</b>	<b>Box Depth (in.)</b>	<b>Gap (in.)</b>
<b>New</b>	5.5040	8.0085	5.4305	5.4280	-0.0025
<b>Make-up 1 <sup>a</sup></b>	—	—	—	—	—
<b>Make-up 2</b>	5.5050	8.0095	5.4305	5.4280	-0.0025
<b>Torque-to-Yield</b>	5.4850	8.0915	5.4100	5.4177	0.0077
<b>Dimensional Change after M-U #1 <sup>a</sup></b>	—	—	—	—	—
<b>Dimensional Change after M-U #2</b>	0.0010	0.0010	0.0000	0.0000	0.0000
<b>Dimensional Change after TTY</b>	-0.0190	0.0830	-0.0205	-0.0103	0.0102

<sup>a</sup> No measurements taken after make-up 1.

**Table 24—6-5/8 FHDS Test Results Data: Pin P7, Box B7**

	<b>Pin Nose Diameter (in.)</b>	<b>Box C'bore Diameter (in.)</b>	<b>Pin Length (in.)</b>	<b>Box Depth (in.)</b>	<b>Gap (in.)</b>
<b>New</b>	5.5045	8.0095	5.4245	5.4350	0.0105
<b>Make-up 1 <sup>a</sup></b>	—	—	—	—	—
<b>Make-up 2</b>	5.5050	8.0115	5.4245	5.4340	0.0095
<b>Torque-to-Yield</b>	5.4890	8.0890	5.4170	5.4240	0.0070
<b>Dimensional Change after M-U #1 <sup>a</sup></b>	—	—	—	—	—
<b>Dimensional Change after M-U #2</b>	0.0005	0.0020	0.0000	-0.0010	-0.0010
<b>Dimensional Change after TTY</b>	-0.0155	0.0795	-0.0075	-0.0110	-0.0035
<sup>a</sup> No measurements taken after make-up 1.					

**Table 25—6-5/8 FHDS Test Results Data: Pin P8, Box B8**

	<b>Pin Nose Diameter (in.)</b>	<b>Box C'bore Diameter (in.)</b>	<b>Pin Length (in.)</b>	<b>Box Depth (in.)</b>	<b>Gap (in.)</b>
<b>New</b>	5.5040	8.0085	5.4165	5.4360	0.0195
<b>Make-up 1 <sup>a</sup></b>	—	—	—	—	—
<b>Make-up 2</b>	5.5055	8.0180	5.4165	5.4340	0.0175
<b>Torque-to-Yield</b>	5.4860	8.0970	5.4095	5.4230	0.0135
<b>Dimensional Change after M-U #1 <sup>a</sup></b>	—	—	—	—	—
<b>Dimensional Change after M-U #2</b>	0.0015	0.0095	0.0000	-0.0020	-0.0020
<b>Dimensional Change after TTY</b>	-0.0180	0.0885	-0.0070	-0.0130	-0.0060
<sup>a</sup> No measurements taken after make-up 1.					

## **9 Conclusions**

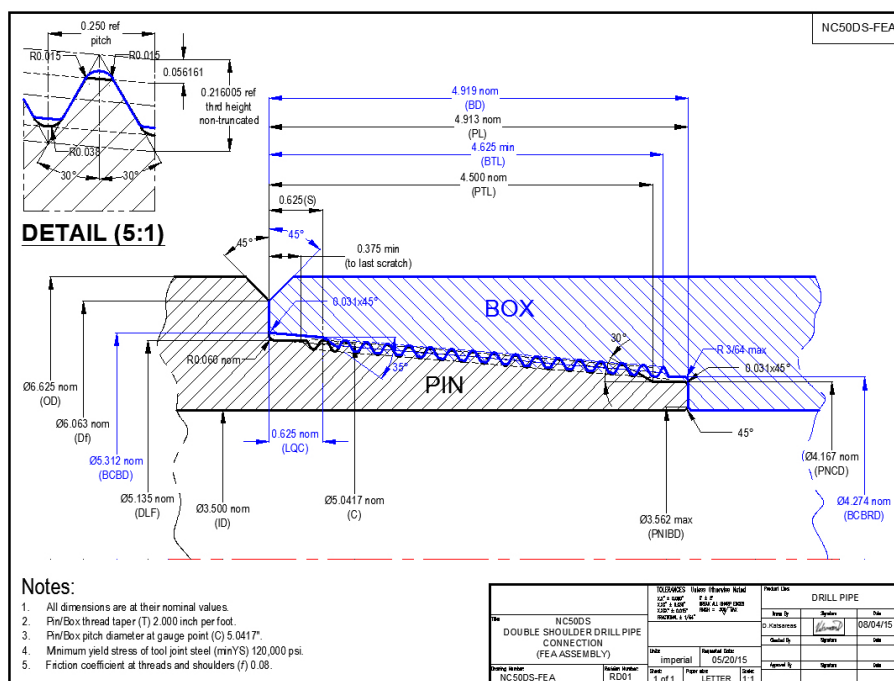
The foremost concern about double shoulder tool joints, and the concern that kept them on the shelf from 1940 until the 1980s, is maintaining the lengths of the pin and box threads so that both shoulders contact without yielding the pin in tension. While the tests in this WI were limited in terms of number of samples, and the breadth of the tests: we have confirmed, we have witnessed and participated in manufacturers and users testing, and we have seen in practice the following.

- 1) Large gaps and interference gaps are not detrimental to the performance or durability of the double shoulder connections. We tested gaps of 0.020 in. and interference of 0.004 in. We know of manufacturers' field inspection criteria with similar specifications, and we have seen in practice that a gap of 0.020 in. and larger and interference at the secondary shoulder can be used without problems.
- 2) Out-of-tolerance pin lengths and box depths change to conform to each other when the pipe is used.
- 3) Pipe can get mixed on the pipe rack; thus, field inspection gaps may differ from manufactured gaps.
- 4) The double shoulder connection has an excellent history of fatigue resistance on drill pipe based on the rarity of reported failures and the fatigue tests witnessed by members of the work group.
- 5) Fatigue tests are expensive and information on product performance in service can be very useful.
- 6) Budget constraints prevented conducting interchangeability and compatibility testing between single shoulder and double connections; however, successful tests have been conducted by users and witnessed by members of the work group.

## Annex A (informative) Finite Element Analysis of NC50DS

### Introduction

A finite element analysis (FEA) was conducted on the NC50DS drill pipe connection, depicted in Figure A.1. Both pin and box were drawn using nominal dimensions. In Figure A.1, the pin primary torque shoulder is only touching the box face, so the connection bears no loads (there is no interference).



**NOTE** In this configuration, the primary shoulder faces are only touching; i.e. no interference, no load.

**Figure A.1—Assembly Drawing of NC50DS with Nominal Dimensions**

### Material Properties

The yield stress used in the finite element model, was set at the minimum yield stress for API drill pipe tool joints, which is min YS=120,000 psi. Modulus of Elasticity was set at E = 30,000 kpsi, Poisson's ratio at  $\nu = 0.3$ . The generic stress-strain curve that was used is shown in Figure A.2.

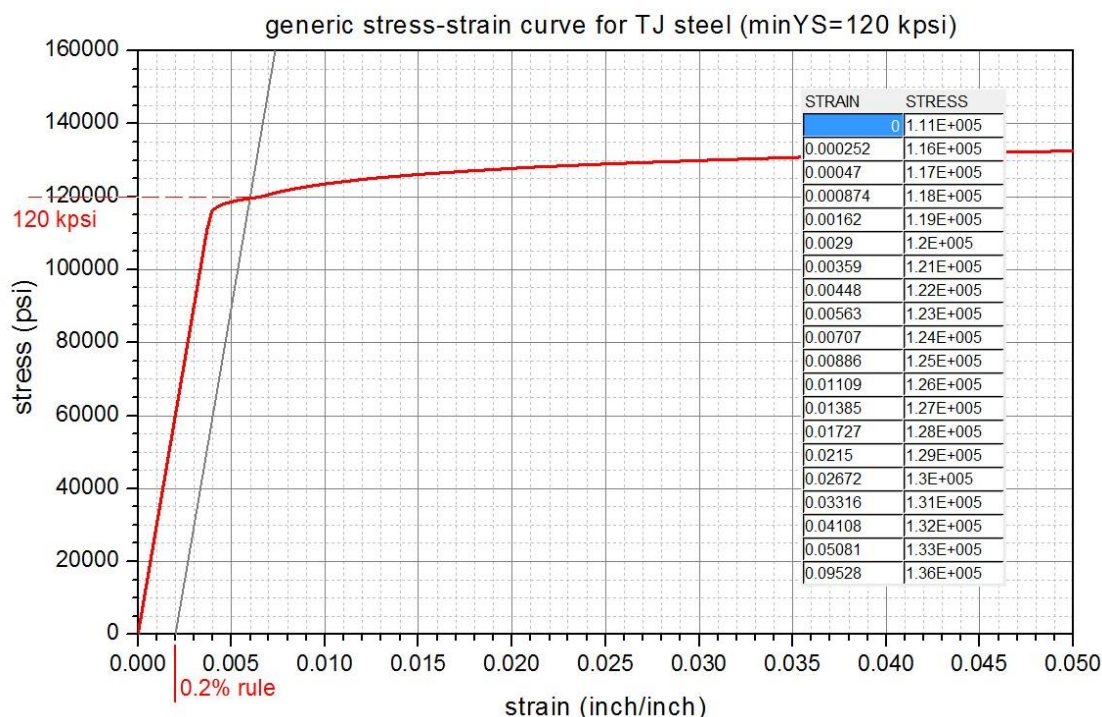


**Figure A.2—Stress-strain Curve for Tool Joint Steel with Yield Stress of 120,000 psi**

The friction coefficient was based on API 7G and was set to  $f=0.08$ .

## Loading

Only make-up load was considered in this analysis. Specifically, the make-up torque MUT was increased gradually until mean axial stress  $S_{ax}$ , at pin or box critical cross-sections, reached 60 % of min YS (72,000 psi). According to API 7G, the critical pin cross-section is 3/4 in. from the primary torque shoulder and the critical box cross-section is 3/8 in. from the primary torque shoulder, for a single shouldered connection.

In two-dimensional FEA (only a longitudinal section of the connection is modeled), the gradually increasing MUT is simulated as an increasing interference at the primary and eventually secondary torque shoulders. So starting with the primary torque shoulder only touching (this is a no-interference / no-load situation), we have redrawn the box made up by a 1/50<sup>th</sup> of a turn, which corresponds to 0.005 in. interference at the primary torque shoulder. At this load case there is no interference at the secondary torque shoulder (actually there is still a clearance of 0.001 in.), but there is some radial interference in the threads, due to the 2 in. per ft taper. The next load step involved a box made up by 2/50<sup>th</sup> of a turn and so on and so forth, until mean  $S_{ax} = 72,000$  psi at the pin or box critical cross-sections, whichever first.

## Finite Element Model

The finite element mesh used in this analysis is shown in Figure 3. Only a longitudinal section of the connection is modeled, assuming axi-symmetry, meaning the full 3-D geometry, material properties, loading and supports can be generated by sweeping the section around the centerline, by 360°.

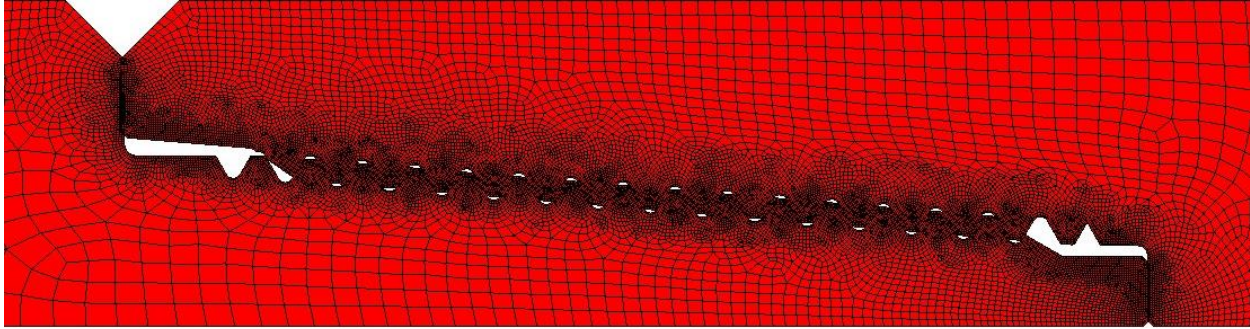


**Figure A.3—Finite Element Model used in the present FEA (shown in hand-tight make-up)**

This is not entirely true because threads are helical and not just grooves, but the assumption is considered legitimate (after a long debating in the literature). In this sense, both the model and FEA are two-dimensional instead of three-dimensional.

Some technical information regarding the finite element model, which is important for the analyst:

- a) The model depicted in Figure 3, corresponds to a box made up by 3/50<sup>th</sup> of a turn. The interference at the primary torque shoulder is 0.015 in.
- b) The model consists of 20,803 8-node axi-symmetric quadrilateral elements and 61,182 nodes. Generally, the larger the number of elements (in other words, the denser the mesh) the higher the accuracy of the FEA, but also the longer it takes to do it. That is why different mesh densities need be checked (this is called a mesh convergence check) and the optimum mesh used (reasonable accuracy in reasonable time). An element size of 0.010 in. was used on all contacting surfaces. Then it was gradually increased over the bevels (14 elements) and tool joint OD (98 elements) and ID (67 elements). A mesh convergence check has not been done yet.
- c) Special contact elements are used on the pin and box contact surfaces. These include torque shoulders and threads. The problem is treated and solved as an interference problem. Wherever is interference box contact elements "penetrate" pin contact elements, initially. Then the solver gradually deforms the material (of both pin and box), bringing it to a state of equilibrium, where no "penetration" occurs, only touching. During this process, penetrating/contacting surfaces deform but also slide against each other.
- d) The material model used is a multi-linear kinematic hardening material model, based on the generic stress-strain curve, shown in Figure 2.
- e) The model is much longer than it shows in Figure 3. To ensure that edge effects are negligible, tool joint pin/box lengths and upset lengths, based on API, were added to the model. This keeps the end supports (no axial displacement is permitted) away from the connection.

### **Stress at Critical Cross-sections**

Multiple analyses with increasing torque shoulder interference, has shown that when the box is made up by 3/50<sup>th</sup> of a turn (0.015 in. interference), mean axial stress  $S_{ax}$  reaches 72 kpsi at the pin critical cross-section first. Figure A.4, illustrates axial stress distributions, at pin and box critical cross-sections, for this particular load case.



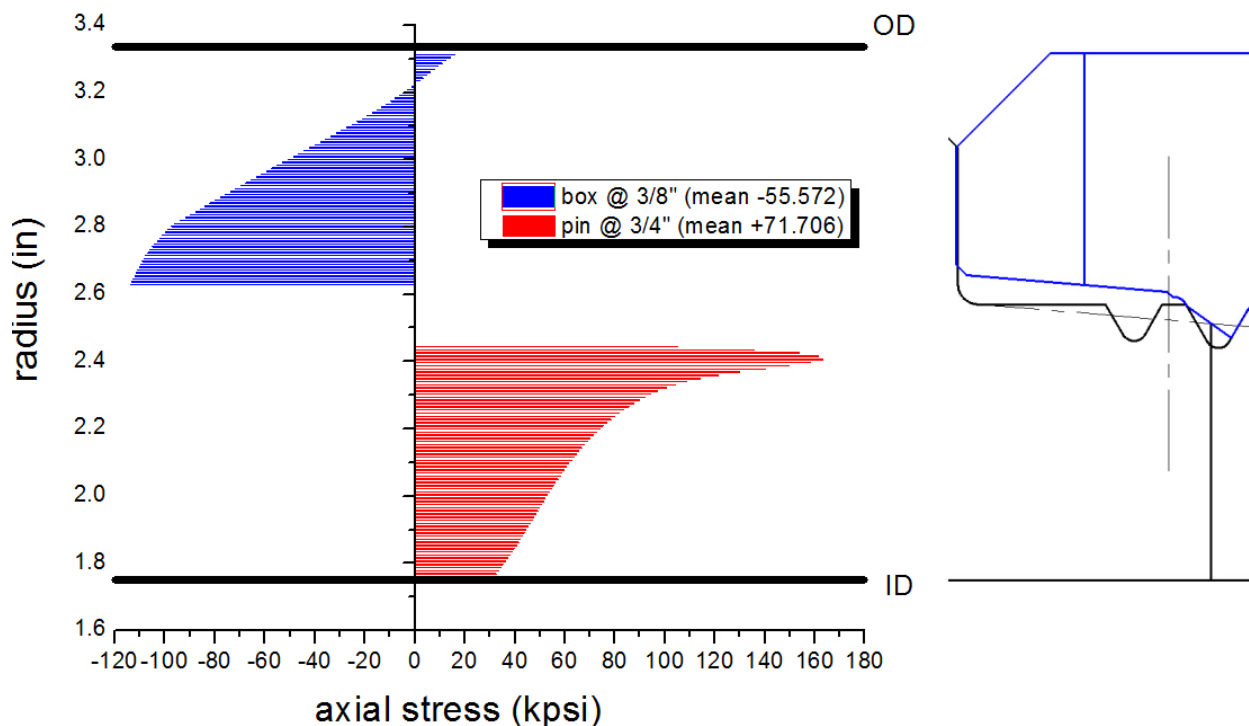


**Figure A.4—Axial Stress Distribution at Pin/Box Critical Cross-sections (right sketch) for Box Made-up by 3/50<sup>th</sup> of a turn (0.015 in. primary torque shoulder interference)**

As expected, axial stress in the pin is tensile, peaking close to the thread root and compressive in the box, again peaking close to the thread root. Mean axial stress for the pin is +71,706 psi and for the box -55,572 psi.

Figures A.1 to A.5 show contour plots of the axial, radial, hoop and Von Mises stress and equivalent plastic strain, respectively. Figures A.6 and A.7 show axial and hoop strain distributions along the pin ID and box OD, respectively.

## Make-up Torque

Figure A.5 shows an overview of the contact pressure distribution along all contacting surfaces. The total torque generated by this contact pressure distribution is 37,037 ft-lbf, for a friction coefficient  $f = 0.08$ . The total contact area is 29.951 sq. in.

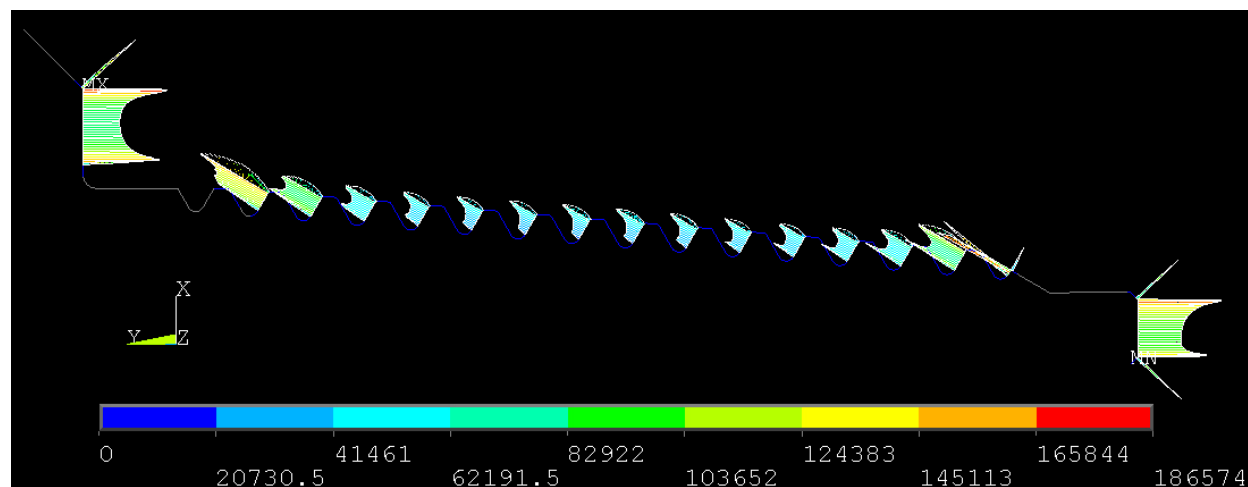


**Figure A.5—Contact Pressure Distribution over All Contacting Surfaces of Box Made-up by 3/50<sup>th</sup> of a turn (0.015 in. primary torque shoulder interference)**

The make-up torque for single shouldered connections, based on API 7G (16<sup>th</sup> Edition) is,

$$Ta = \frac{S}{12} A_M \left( \frac{p}{2\pi} + \frac{R_t f}{\cos \theta} + R_s f \right) \quad (A.1)$$

where  $A_M$  is the smallest of the two load bearing cross-sectional areas  $AB$  or  $AP$ ,  $S$  is the recommended make-up stress level ( $S = 72,000$  psi),  $p$  is the thread pitch,  $f$  is the friction coefficient on mating surfaces, threads and shoulder(s),  $\theta$  is the thread angle,  $AB$  is the load bearing cross-sectional area of the box, calculated 3/8 in. from the shoulder contact surface,

$$A_B = \frac{\pi}{4} [OD^2 - (Q_C - E)^2] \quad (A.2)$$

$A_P$  is the load bearing cross-sectional area of the pin, calculated 3/4 in. from the shoulder contact surface,

$$A_P = \frac{\pi}{4} [(C - B)^2 - ID^2] \quad (A.3)$$

$$R_t = \frac{C - \frac{(L_{PC} - 5/8) tpr}{2}}{2} \quad (A.4)$$

$$R_s = \frac{OD + Q_C}{4} \quad (A.5)$$

$OD$  is the outer diameter of the box,  $L_{PC}$  is the pin length,  $QC$  is the box counterbore, and

$$E = \frac{tpr}{12} \frac{3}{8} \quad (A.6)$$

$tpr$  being the thread taper,  $ID$  is the internal diameter of the pin,  $C$  is the pitch diameter at gauge point,

$$B = 2 \left( \frac{H}{2} - S_{rs} \right) + \frac{tpr}{12} \frac{1}{8} \quad (A.7)$$

$H$  is the non-truncated thread height and  $S_{rs}$  is the thread root truncation.

For the dimensions shown in Figure 1, the make-up torque according to equation (1) is  $Ta = 27,076$  ft-lbf.

If we use the double shoulder equation,

$$Ta = \frac{S}{12} A_M \left( \frac{p}{2\pi} + \frac{R_t f}{\cos \theta} + R_s f + R_{ss} f \right) \quad (A.8)$$

where (see Figure 1),

$$R_{ss} = \frac{PNIBD + PNCD}{4} \quad (A.9)$$

then the make-up torque is  $Ta = 35,506$  ft-lbf.

## Contact Pressure

A better resolution of the predicted pressure distributions on the primary (external) and secondary (internal) torque shoulders, is depicted in Figure 6. Mean contact pressure for the primary shoulder is 110,656 psi. Shoulder contact area is 6.195 sq. in. and the axial force is calculated to be 685,514 lbf. The friction force, for a friction coefficient of 0.08 is 54,841 lbf and the torque is 13,092 ft-lbf. If we calculate this using Equation (8) we get 13,020 ft-lbf.

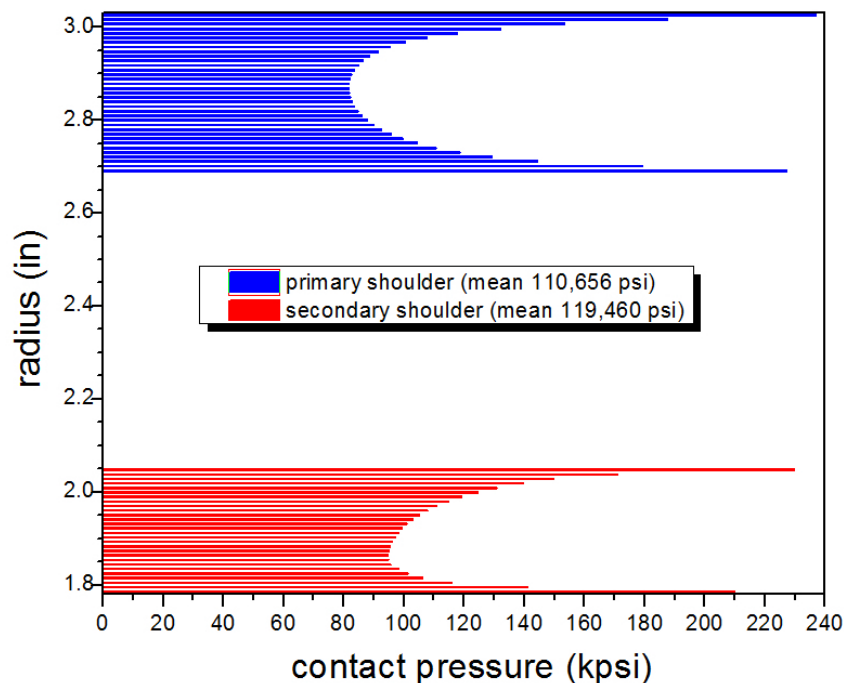


**Figure A.6—Contact Pressure Distribution over Primary and Secondary Torque Shoulders**

Mean contact pressure for the secondary shoulder is 119,460 psi. Contact area is 3.27 sq.in. and the axial force is calculated to be 392,634 lbf. The friction force is 31,251 lbf and the torque is 5037 ft-lbf. Calculating this torque using equation (8) we get 8430 ft-lbf.

## Follow-up

The dimensional configuration of the assembled connection analyzed is nominal. Extreme dimensional configurations (max pin length / min box depth, min pin length / max box depth) need also be investigated.

From the FEA point of view, the finite element mesh used in the present analysis needs be validated via a mesh convergence check.

## ADDITIONAL FIGURES

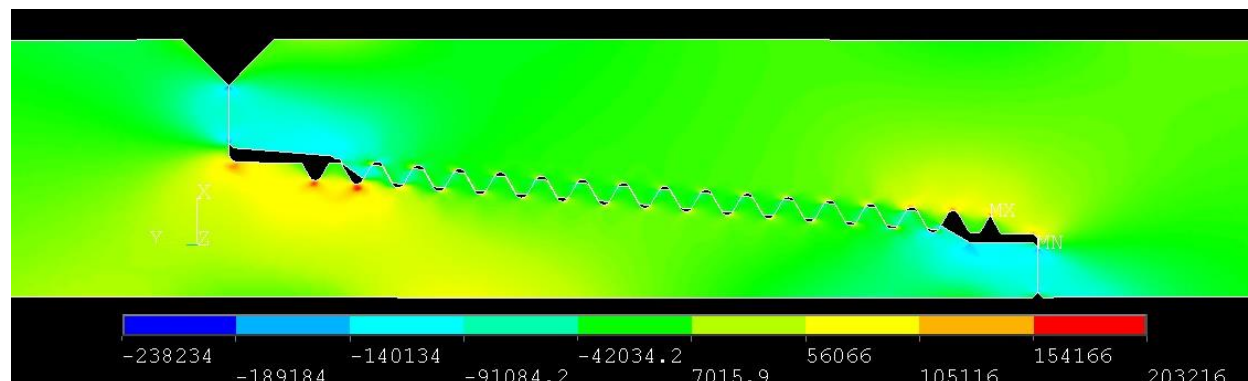


**Figure A.7—Axial Stress  $S_{ax}$  Distribution at 3/50<sup>th</sup> of a turn Make-up**

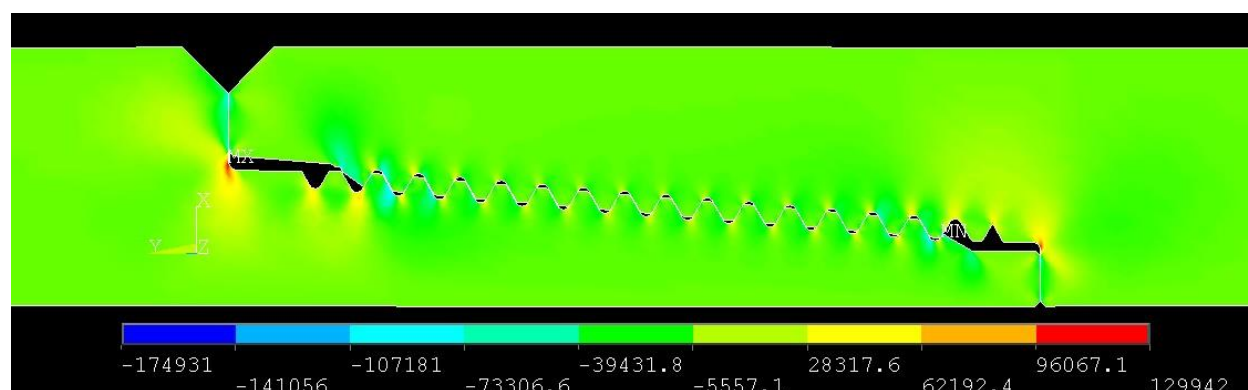


**Figure A.8—Radial Stress  $S_{ra}$  Distribution at 3/50<sup>th</sup> of a turn Make-up**

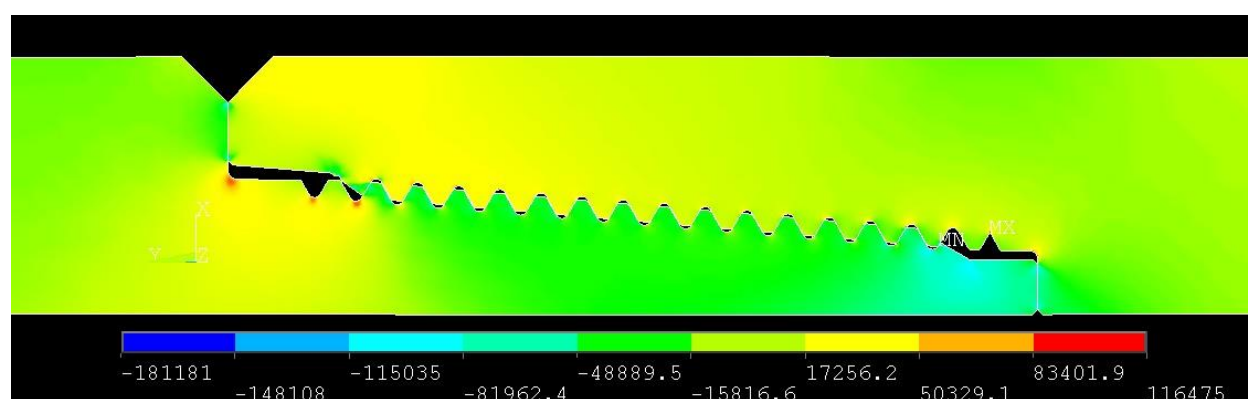


**Figure A.9—Hoop Stress  $S_{ho}$  Distribution at 3/50<sup>th</sup> of a turn Make-up**

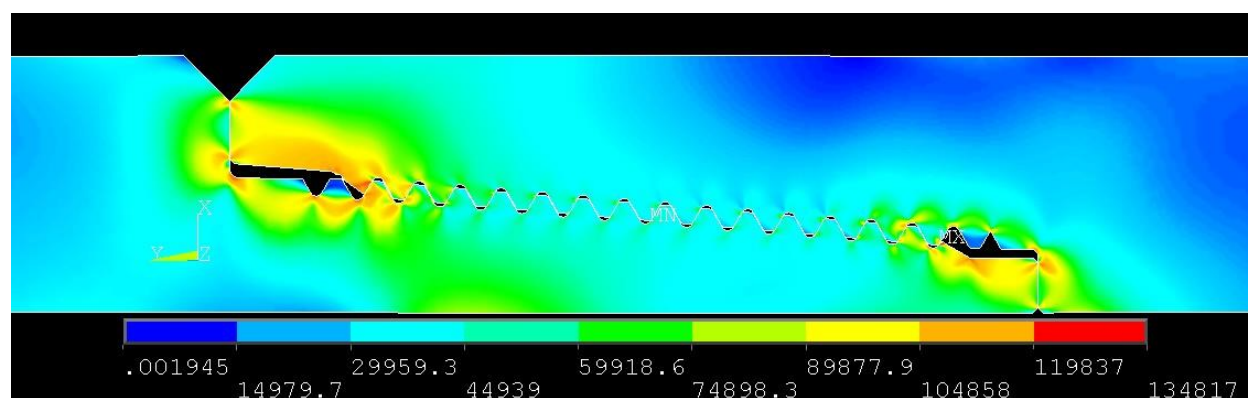


**Figure A.10—Von Mises (equivalent) Stress  $S_{eq}$  Distribution at 3/50<sup>th</sup> of a turn Make-up**

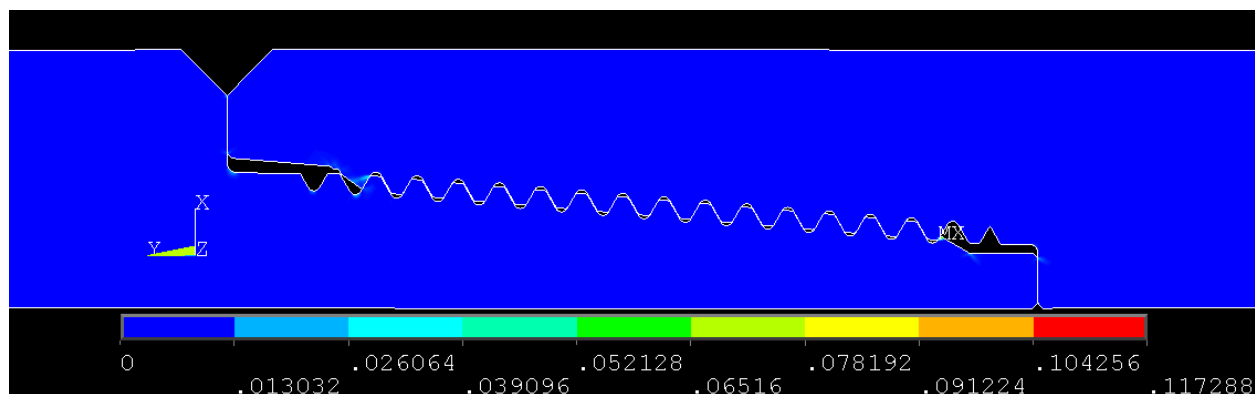


**Figure A.11—Equivalent Plastic Strain  $\epsilon_{p\text{leq}}$  Distribution at 3/50<sup>th</sup> of a turn Make-up**

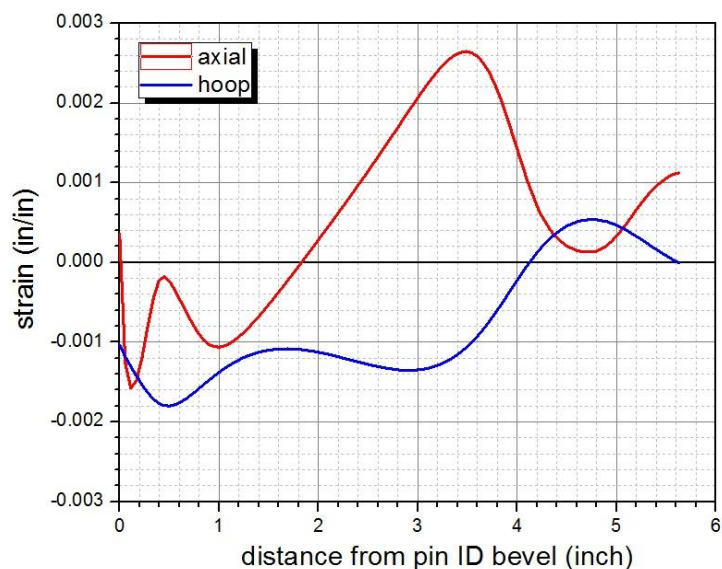


**Figure A.12—Axial and Hoop Strain Distributions along Pin ID (measured from Pin ID Bevel)**

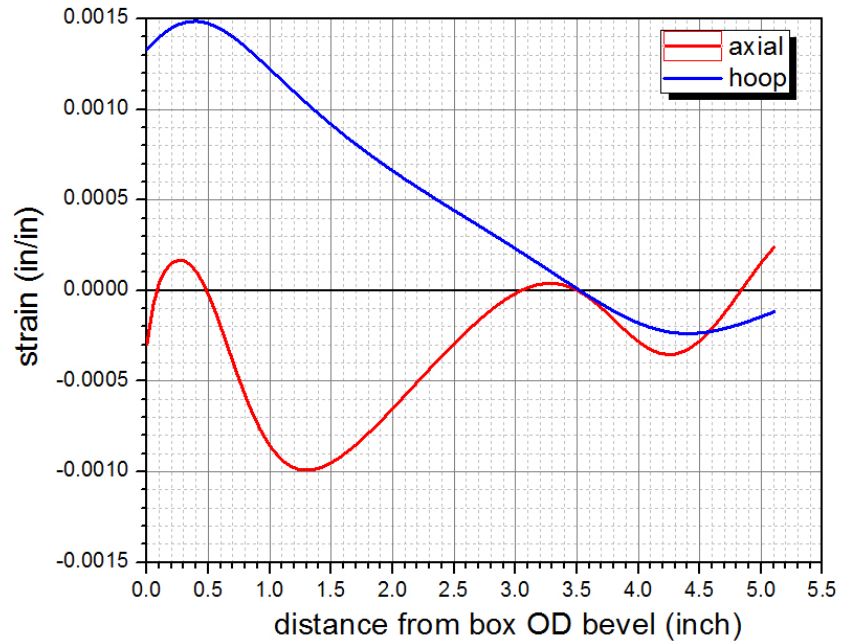


**Figure A.13—Axial and Hoop Strain Distributions along Box OD (measured from Box OD Bevel)**

## Annex B (informative) NC26DS Break-in Curves

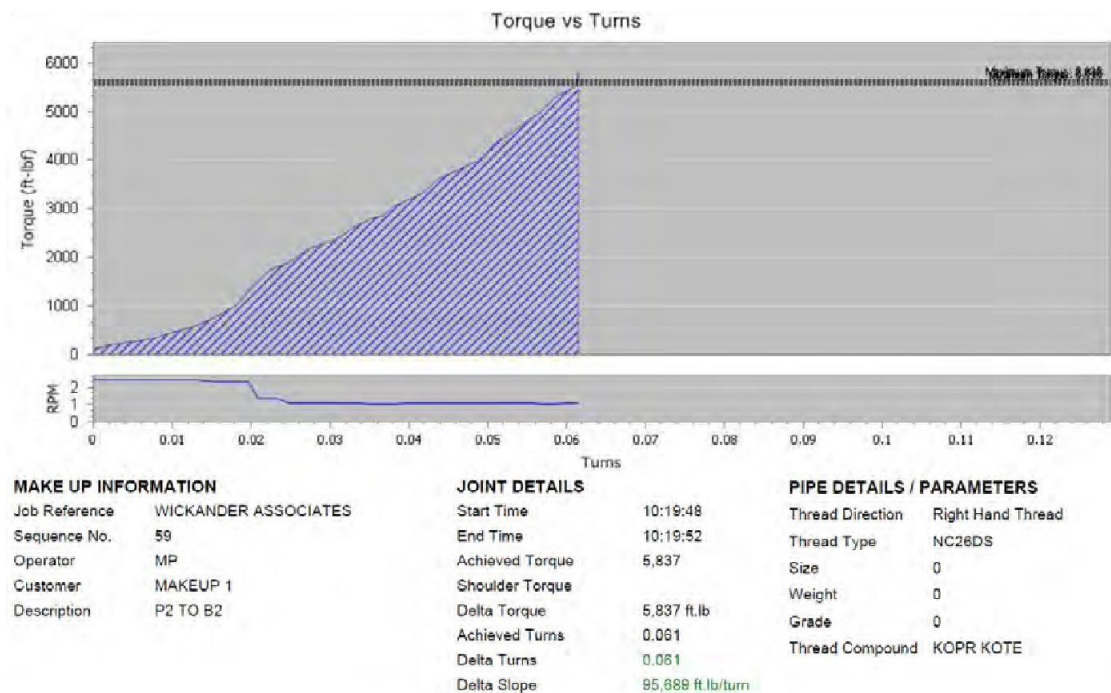


Figure B.1—NC26DS P2–B2 Break-in Cycle, Make-up No. 1

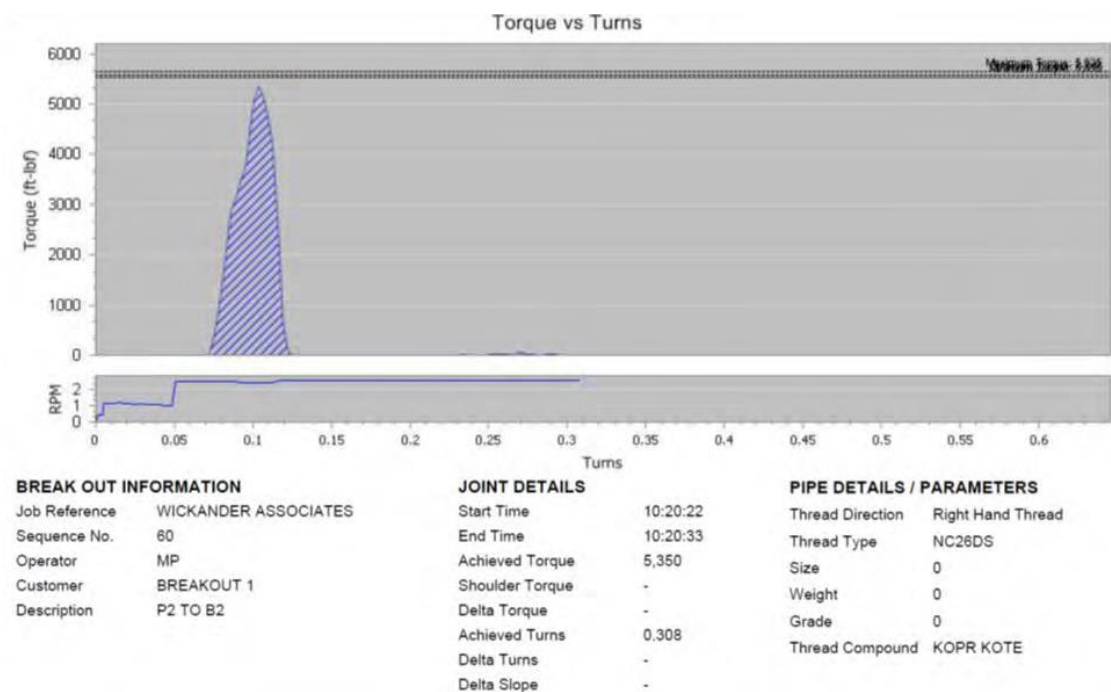


Figure B.2—NC26DS P2–B2 Break-in Cycle, Break-out No. 1



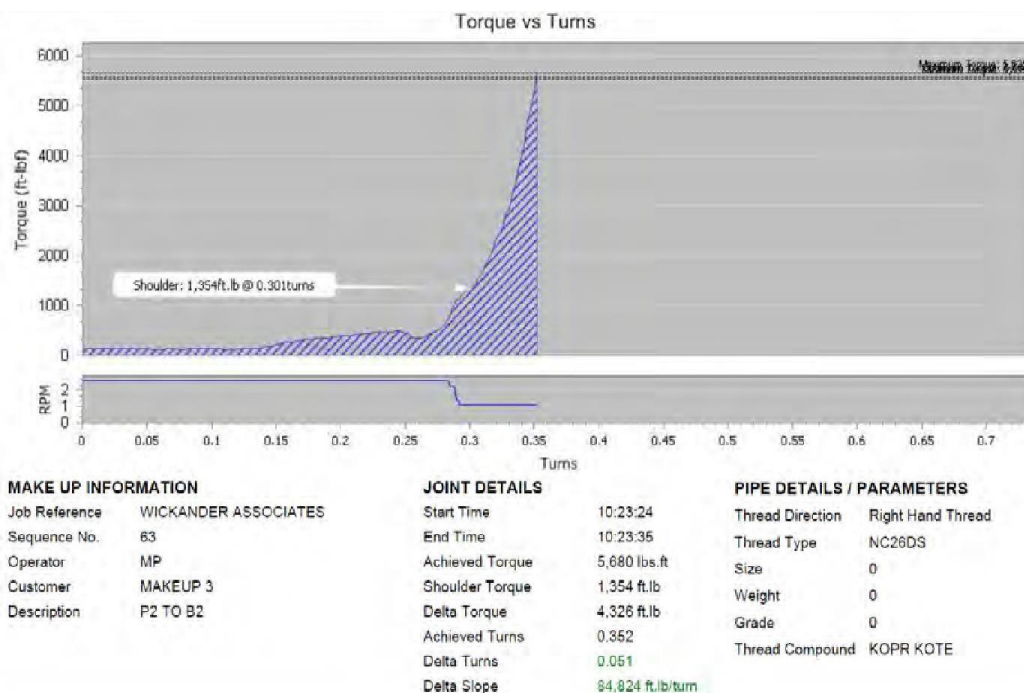
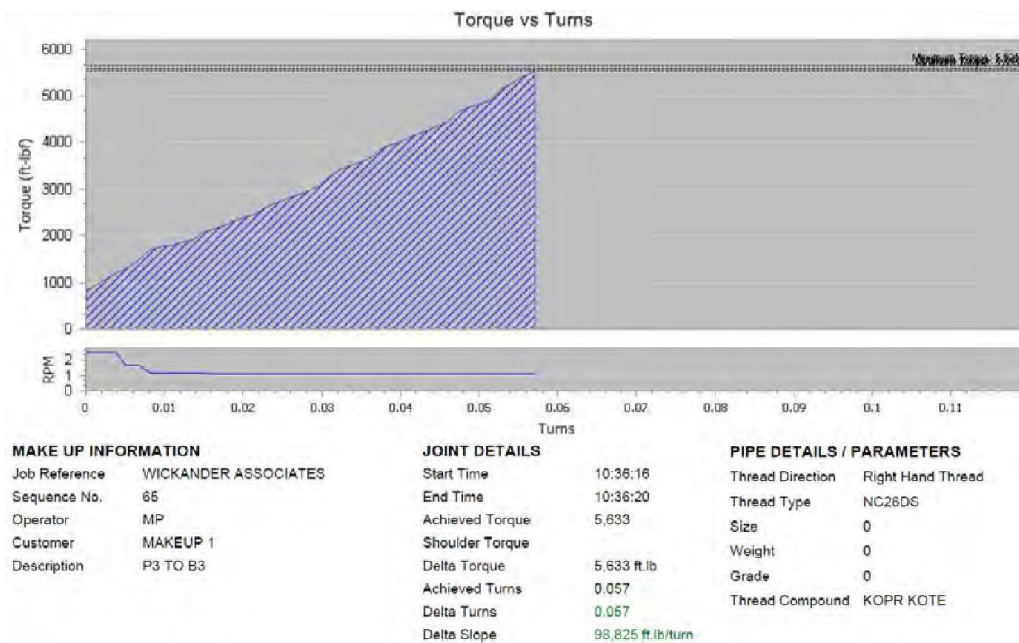


Figure B.3—NC26DS P2–B2 Break-in Cycle, Make-up No. 2

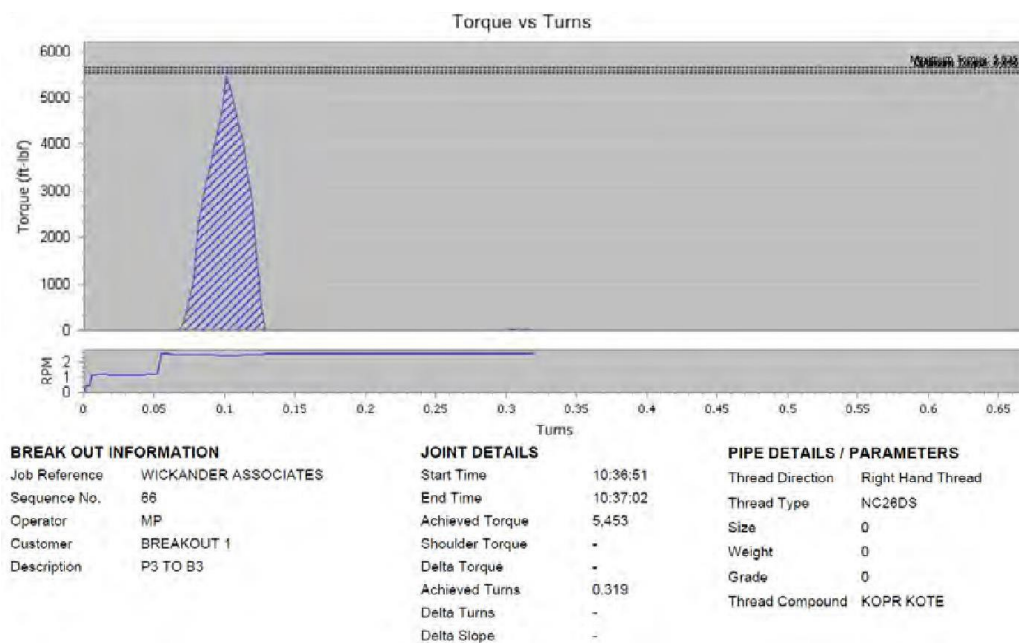


Figure B.4—NC26DS P2–B2 Break-in Cycle, Break-out No. 2





**Figure B.5—NC26DS P3–B3 Break-in Cycle, Make-up No. 1**



**Figure B.6—NC26DS P3–B3 Break-in Cycle, Break-out No. 1**

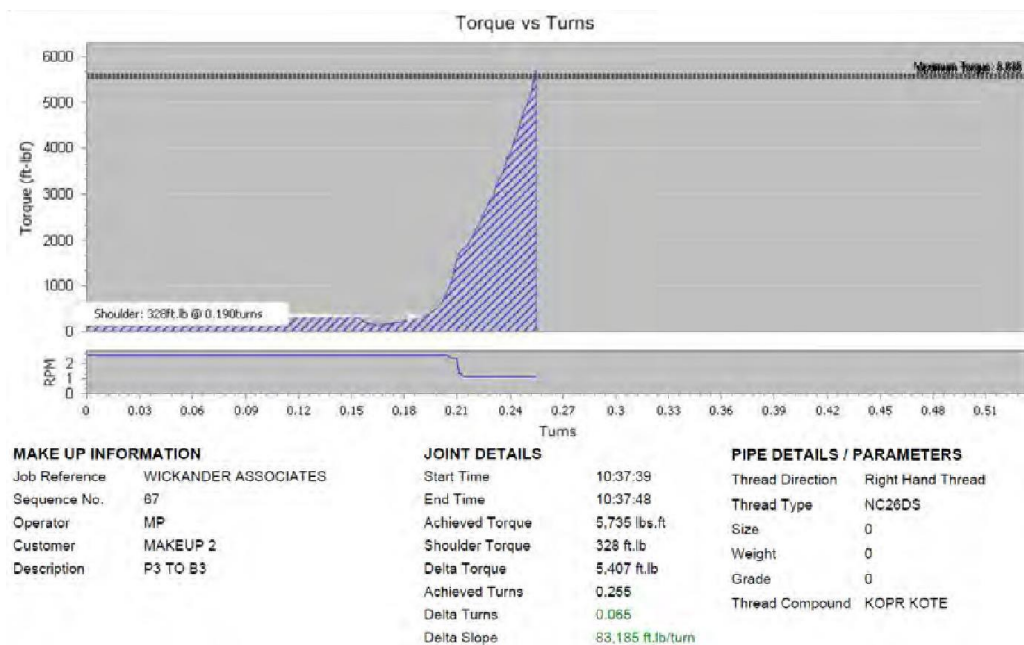


**Figure B.7—NC26DS P3–B3 Break-in Cycle, Make-up No. 2**

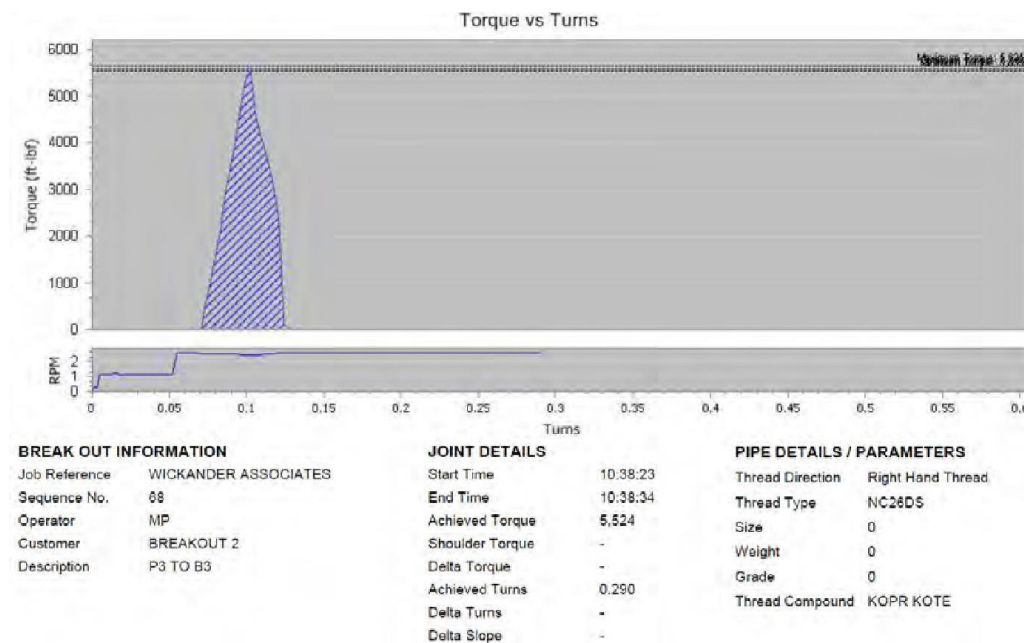


**Figure B.8—NC26DS P3–B3 Break-in Cycle, Break-out No. 2**

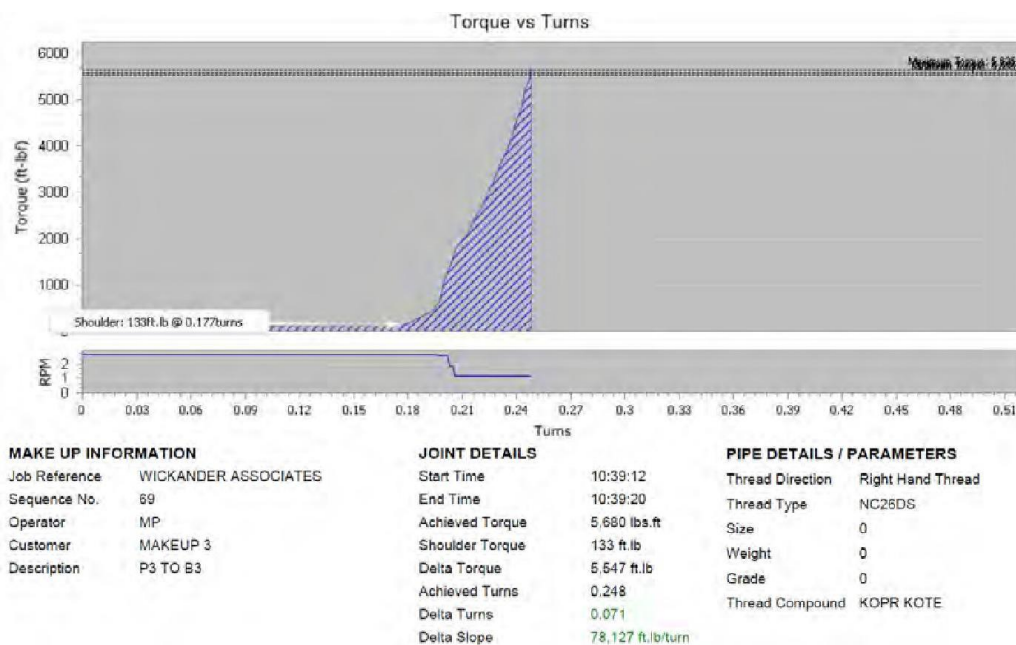


**Figure B.9—NC26DS P3–B3 Break-in Cycle, Make-up No. 3**

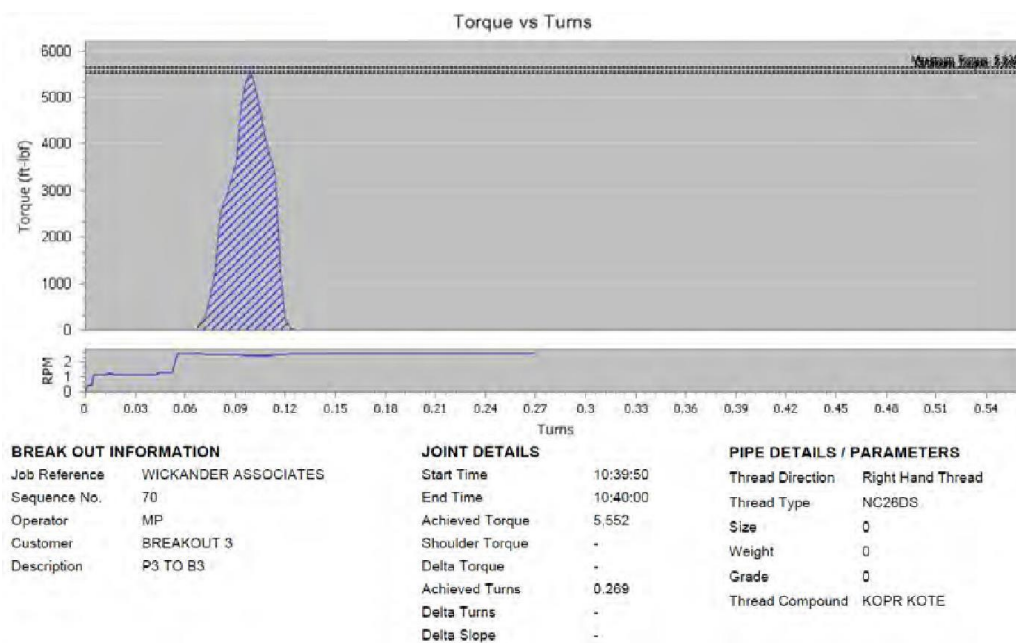


**Figure B.10—NC26DS P3–B3 Break-in Cycle, Break-out No. 3**

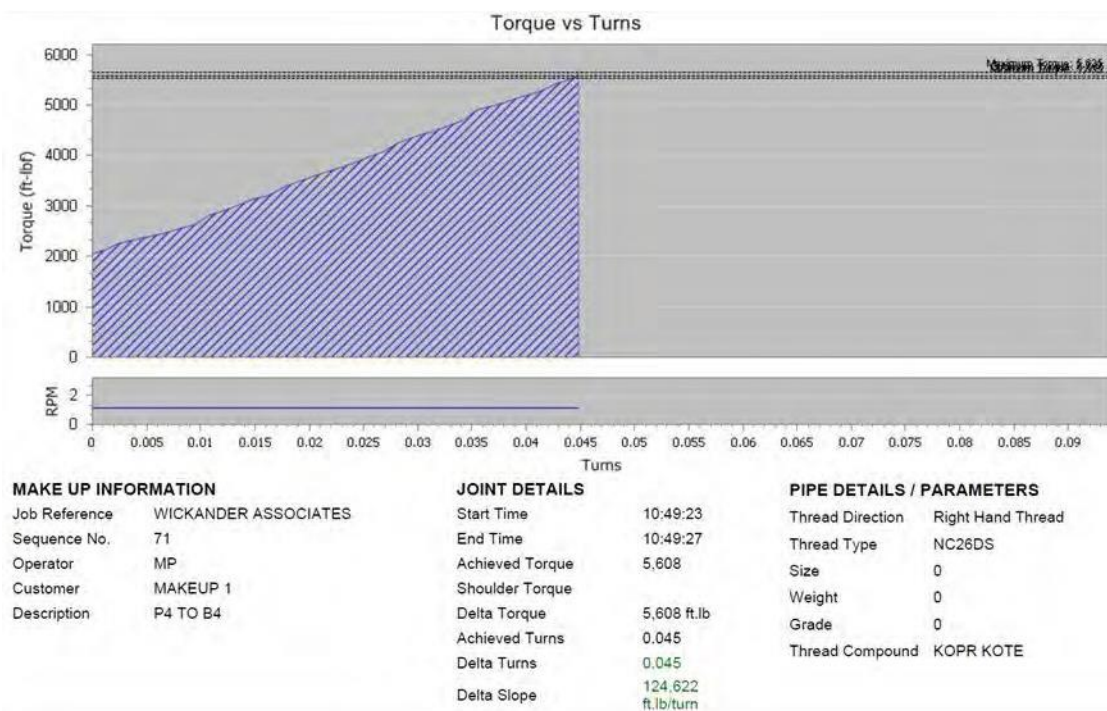


**Figure B.11—NC26DS P4–B4 Break-in Cycle, Make-up No. 1**

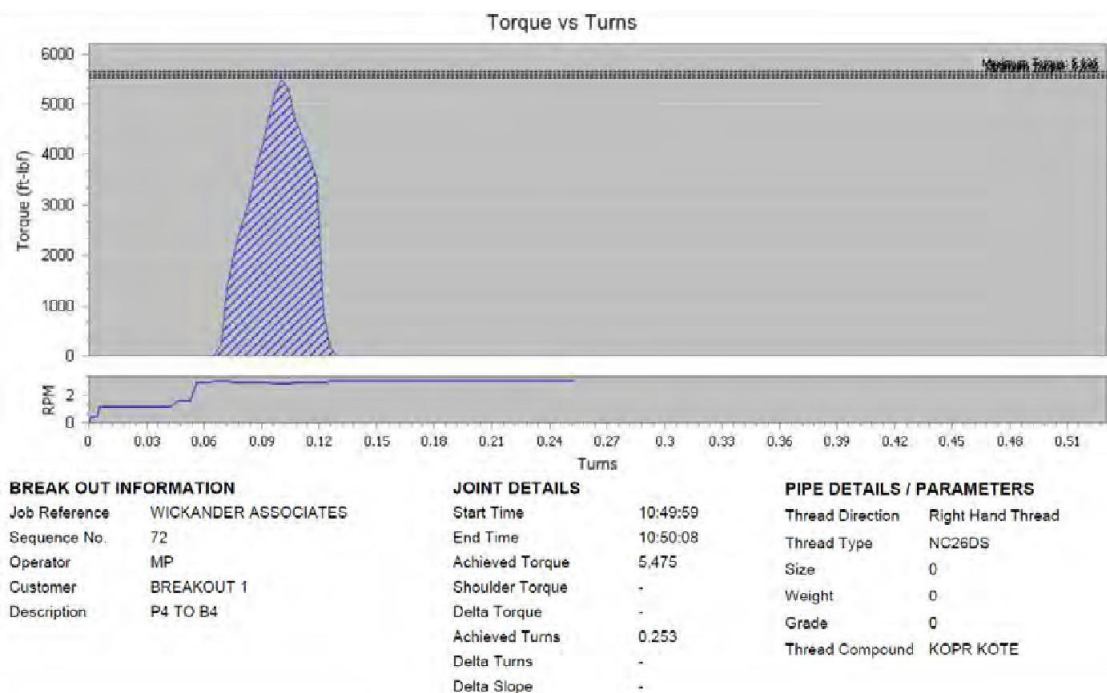


**Figure B.12—NC26DS P4–B4 Break-in Cycle, Break-out No. 1**



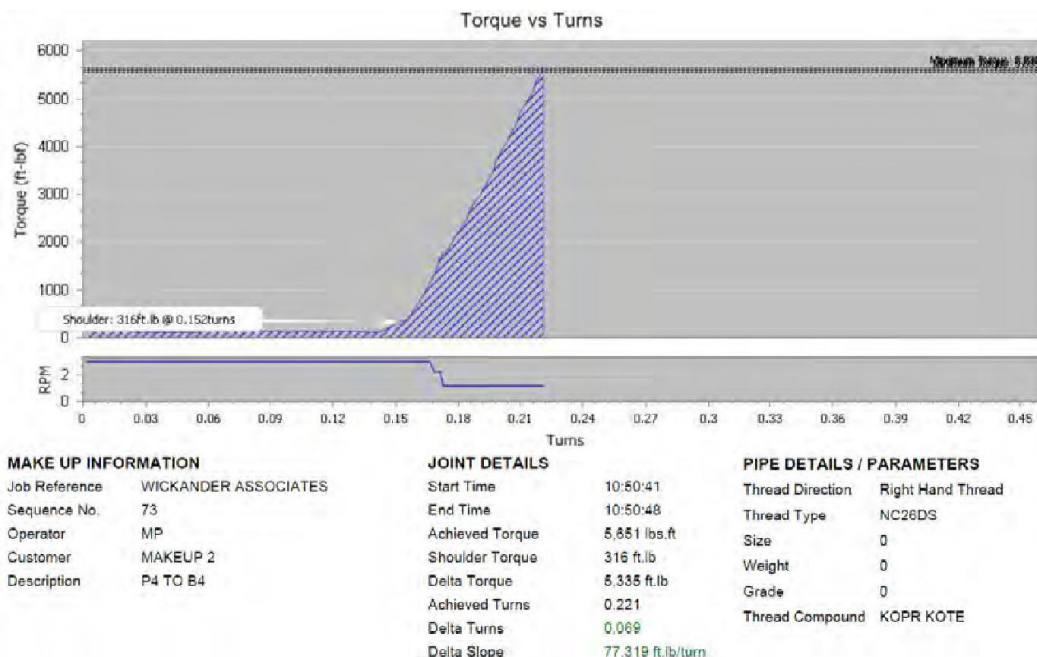


Figure B.13—NC26DS P4–B4 Break-in Cycle, Make-up No. 2

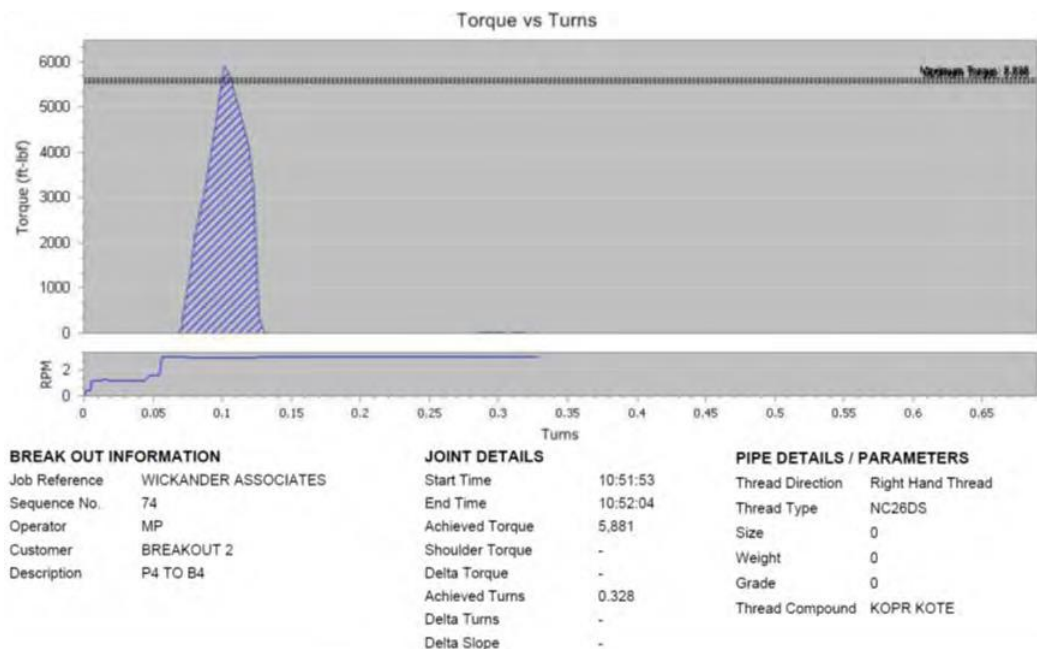


Figure B.14—NC26DS P4–B4 Break-in Cycle, Break-out No. 2

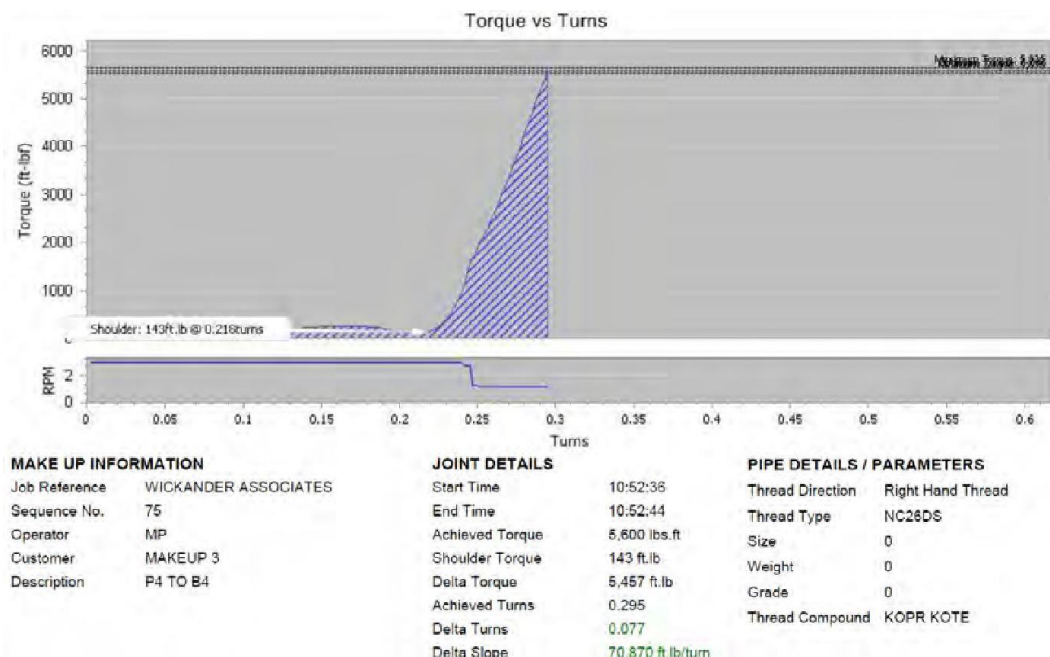


Figure B.15—NC26DS P4—B4 Break-in Cycle, Make-up No. 3

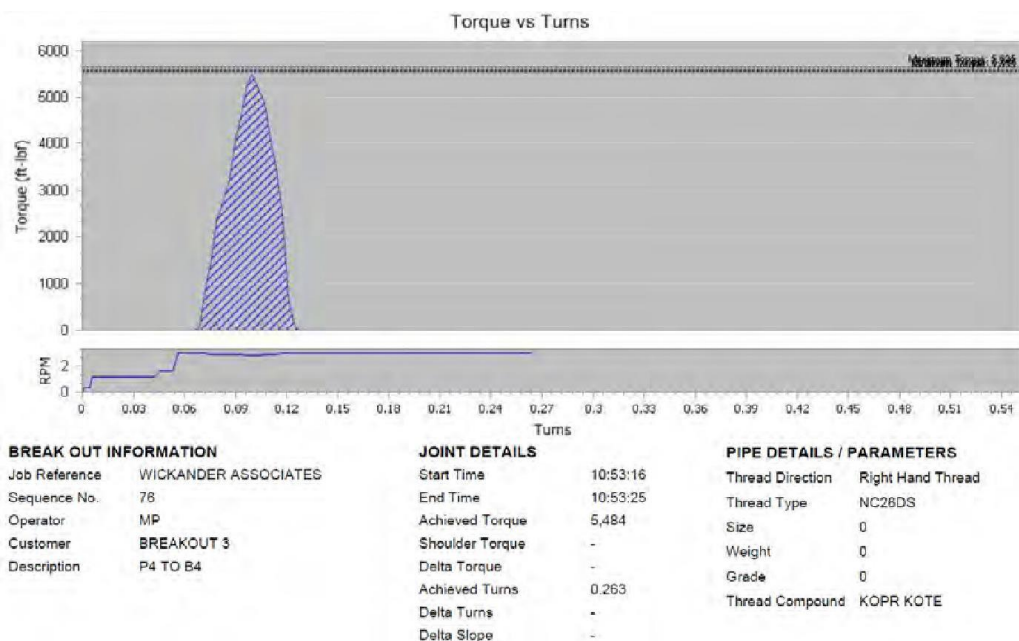


Figure B.16—NC26DS P4—B4 Break-in Cycle, Break-out No. 3

## Annex C (informative) NC26DS Torque to Yield Curves

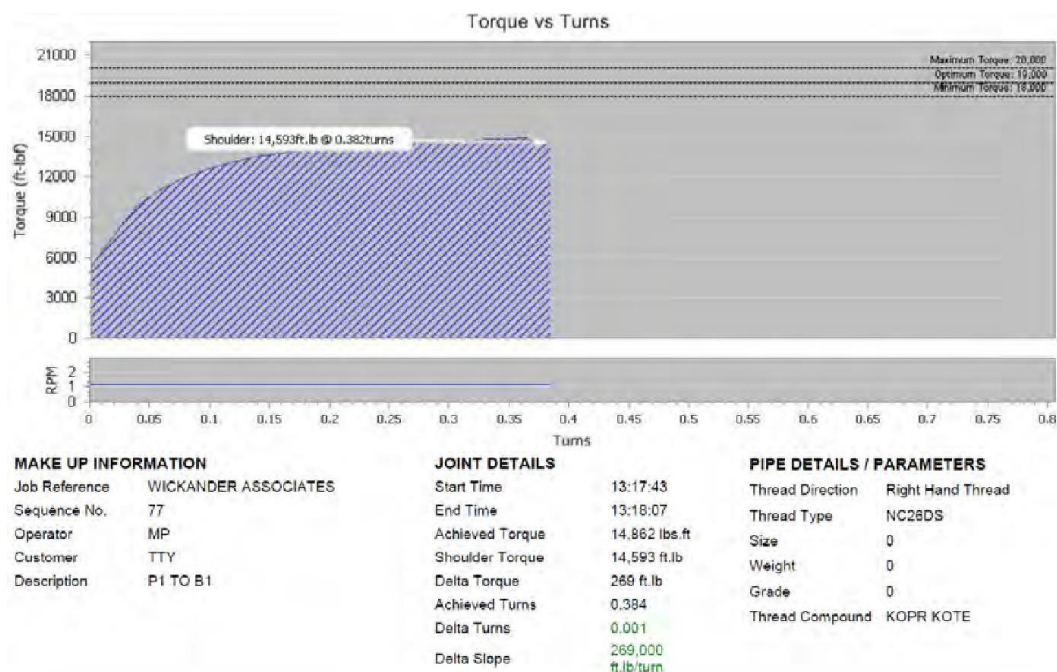


Figure C.1—NC26DS P1–B1 Torque-to-yield (Make-up Torque 14,862 ft-lbs)

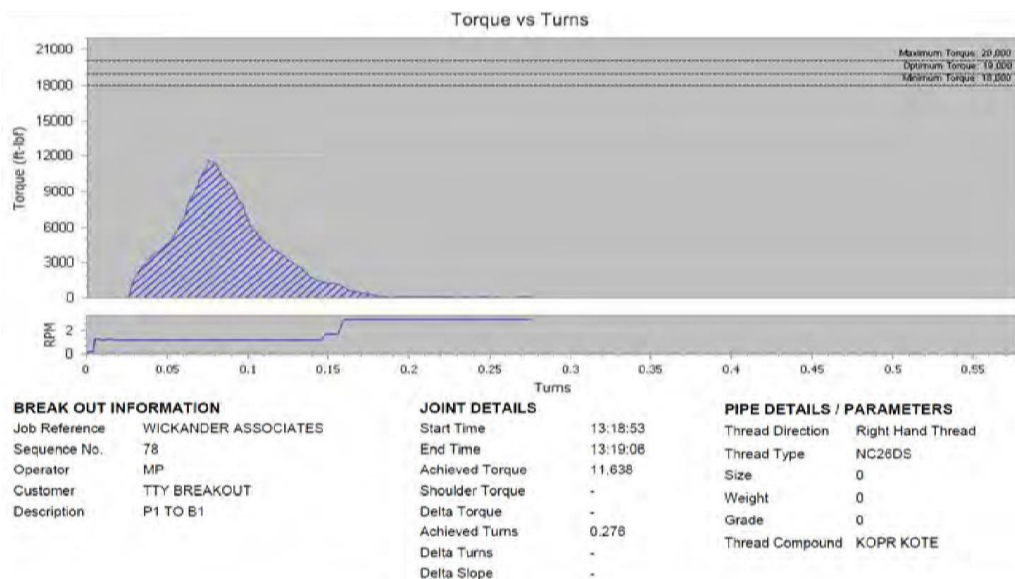
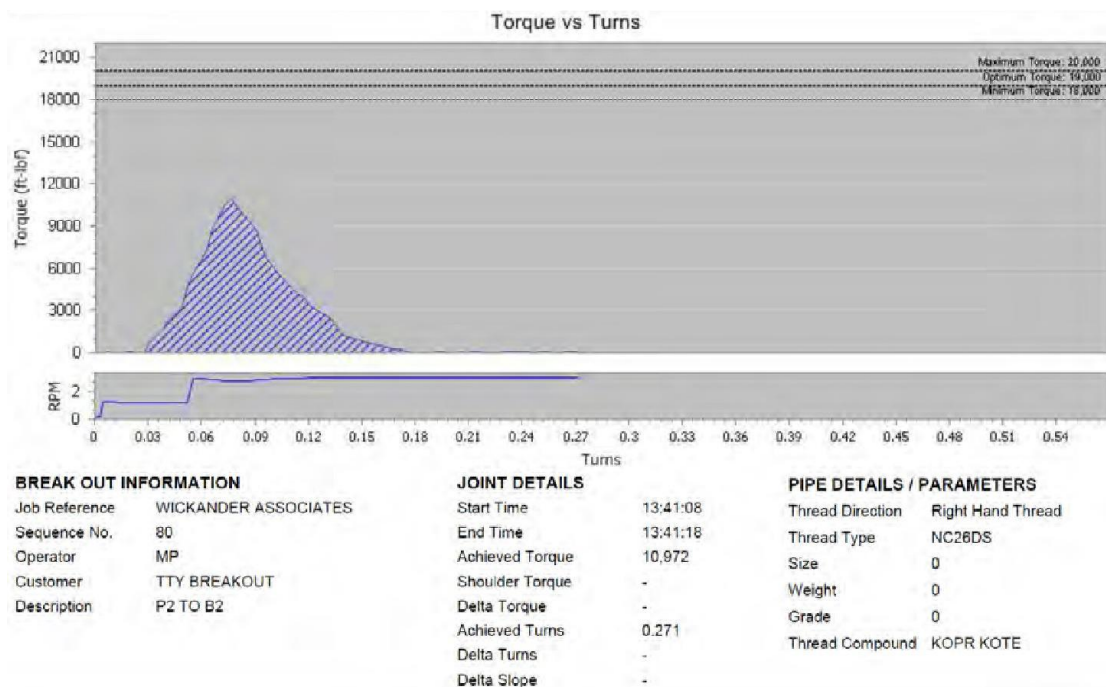


Figure C.2—NC26DS P1–B1 Torque-to-yield (Break-out Torque 11,638 ft-lbs)



**Figure C.3—NC26DS P2–B2 Torque-to-yield (Max Torque 14,070 ft-lbs)**



**Figure C.4—NC26DS P2–B2 Torque-to-yield (Break-out Torque 10,972 ft-lbs)**



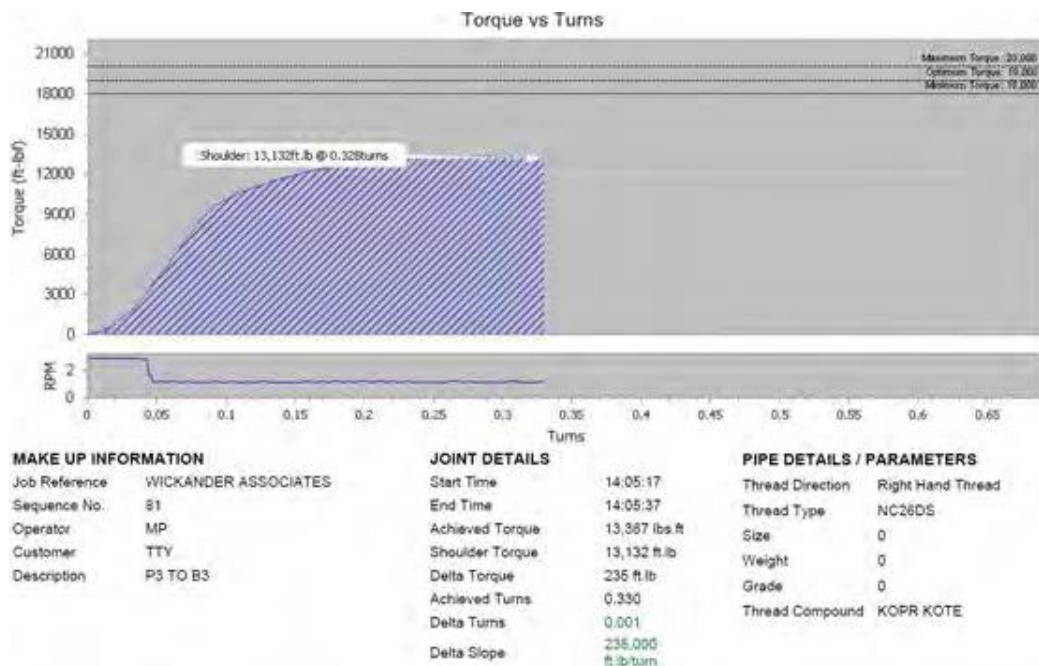


Figure C.5—NC26DS P3–B3 Torque to-yield (Max Torque 13,367 ft-lbs)

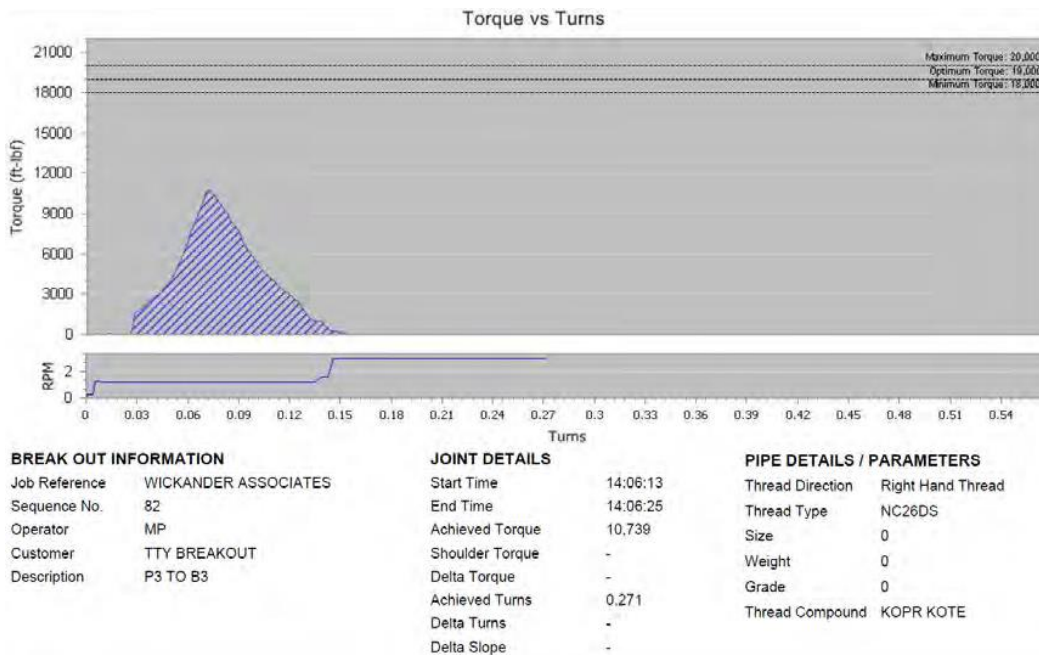
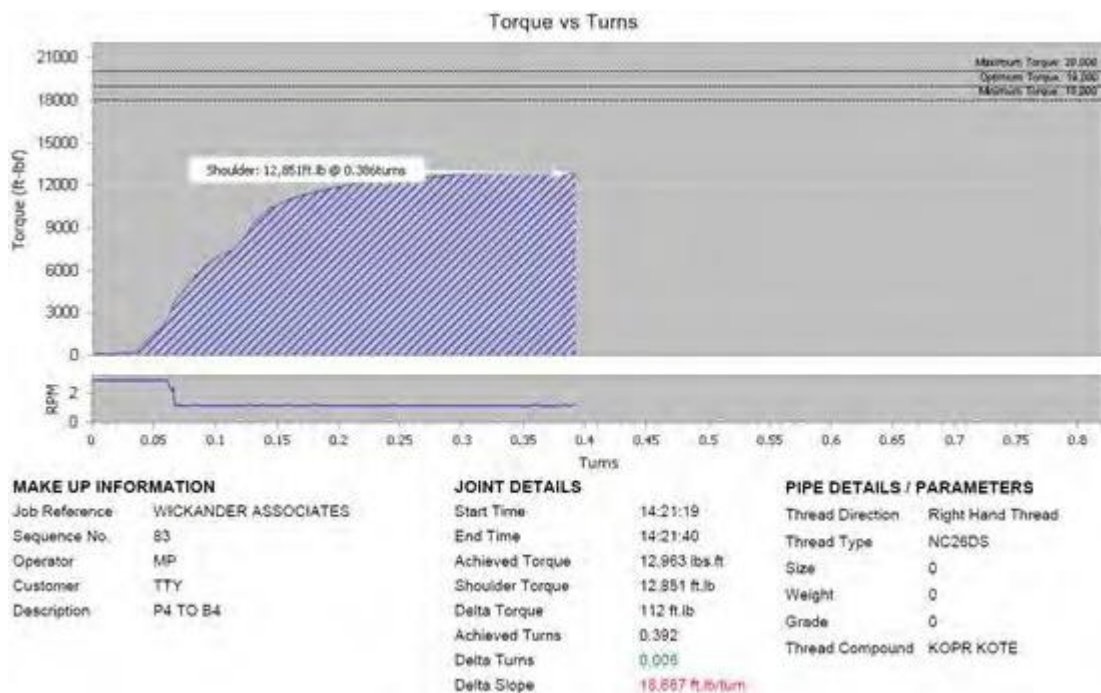
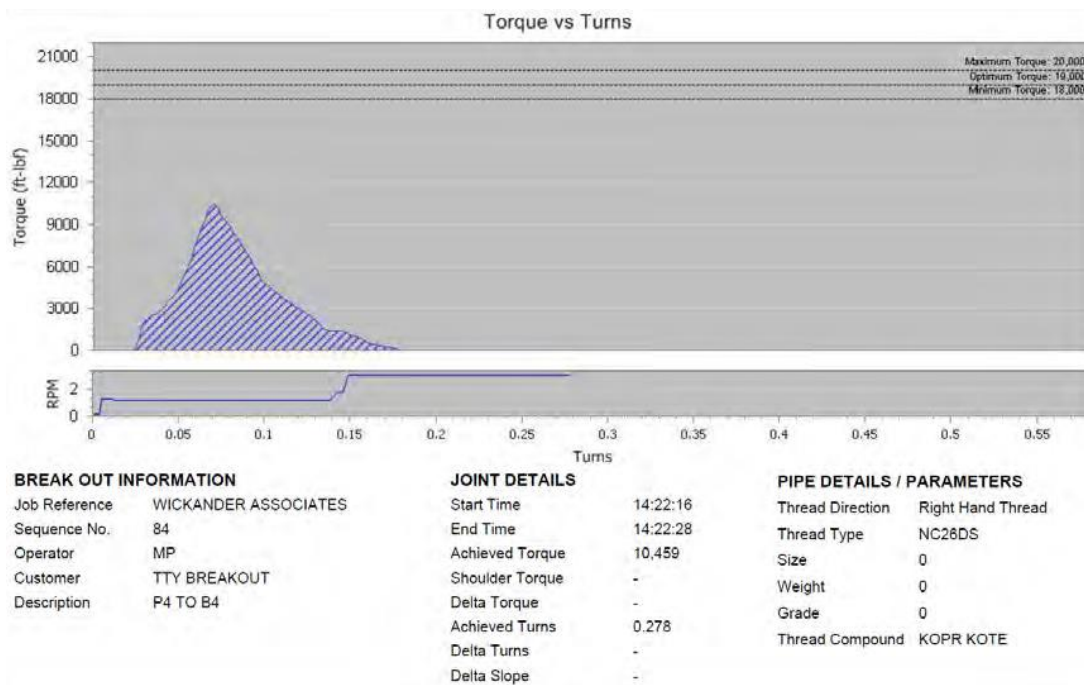


Figure C.6— NC26DS P3–B3 Torque-to-yield (Break-out Torque 10,739 ft-lbs)



**Figure C.7—NC26DS P4–B4 Torque-to-yield (Max Torque 12,963 ft-lbs)**



**Figure C.8—NC26DS P4–B4 Torque-to-yield (Break-out Torque 10,459 ft-lbs)**

## Annex D (informative) 6<sup>5</sup>/<sub>8</sub> FHDS Break-in Curves

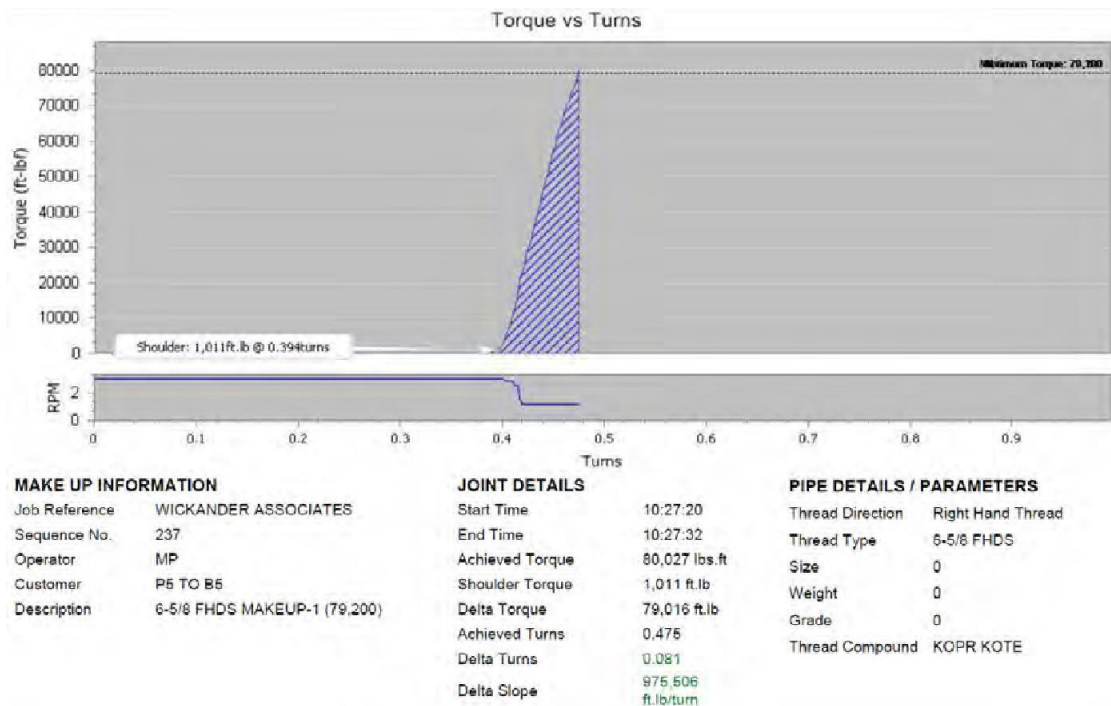


**Figure D.1—6-5/8 FHDS P5–B5 Break-in Cycle, Make-up No. 1**

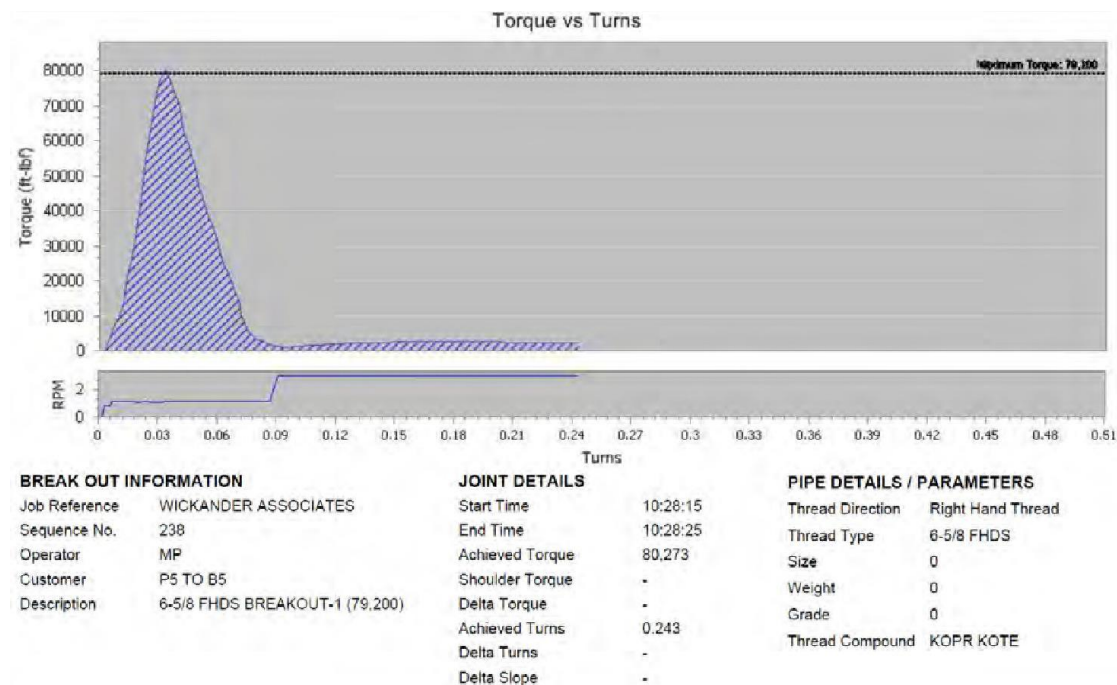


**Figure D.2—6-5/8 FHDS P5–B5 Break-in Cycle, Break-out No. 1**

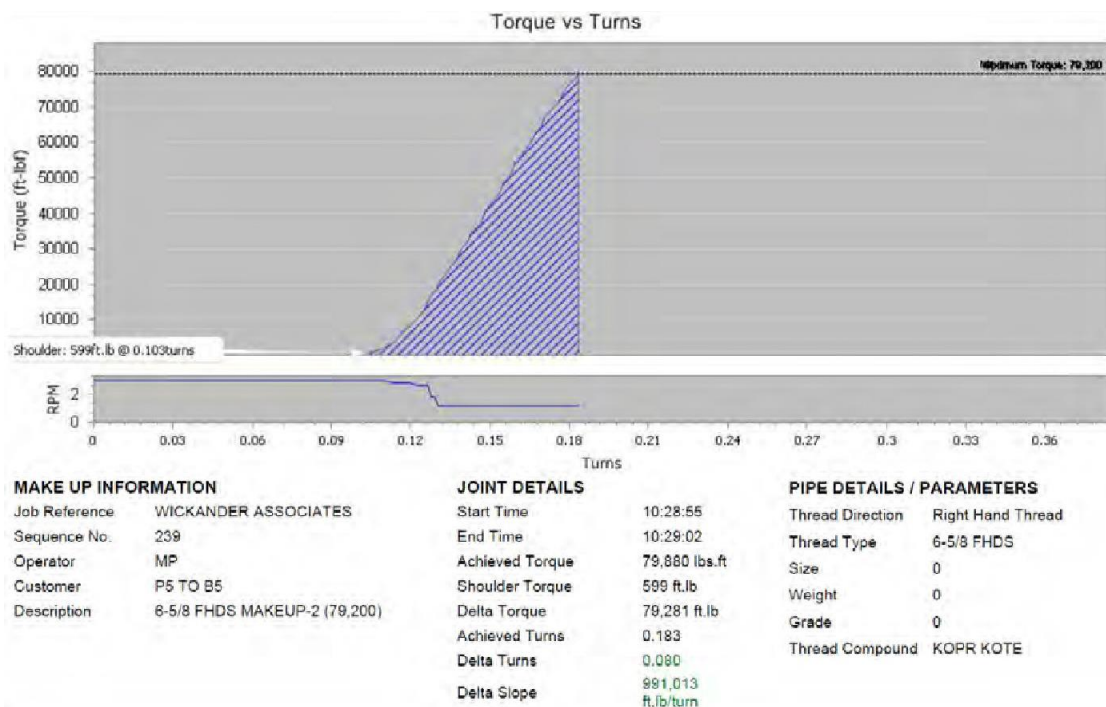


**Figure D.3—6-5/8 FHDS P5-B5 Break-in Cycle, Make-up No. 2**

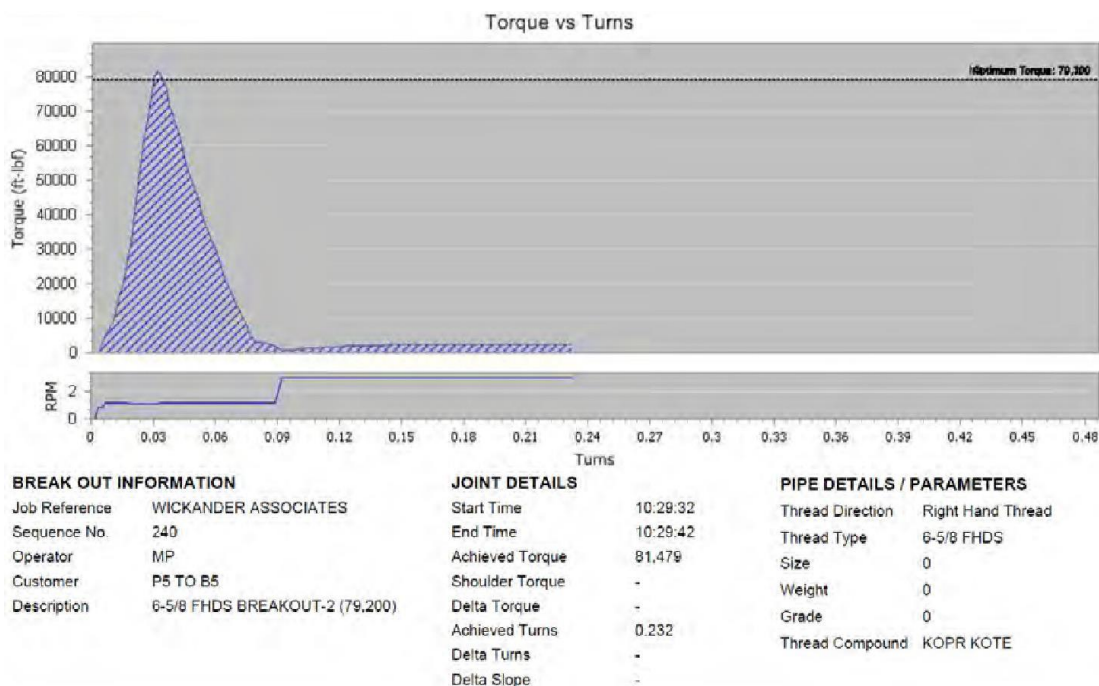


**Figure D.4—6-5/8 FHDS P5-B5 Break-in Cycle, Break-out No. 2**



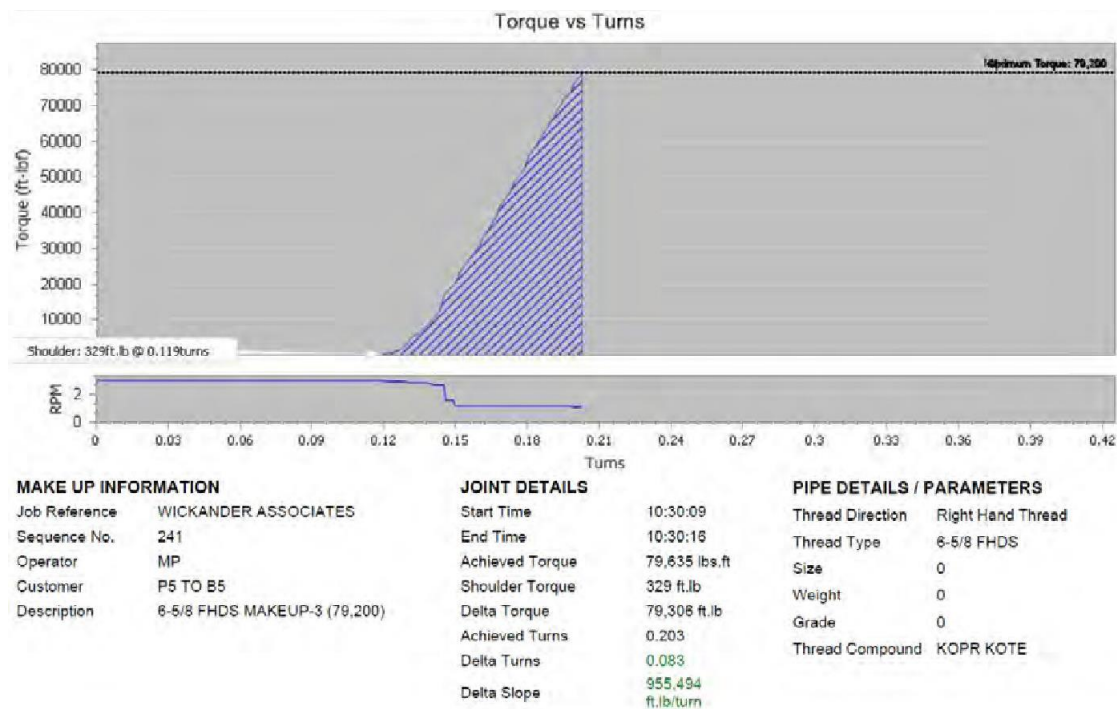


Figure D.5—6-5/8 FHDS P5–B5 Break-in Cycle, Make-up No. 3

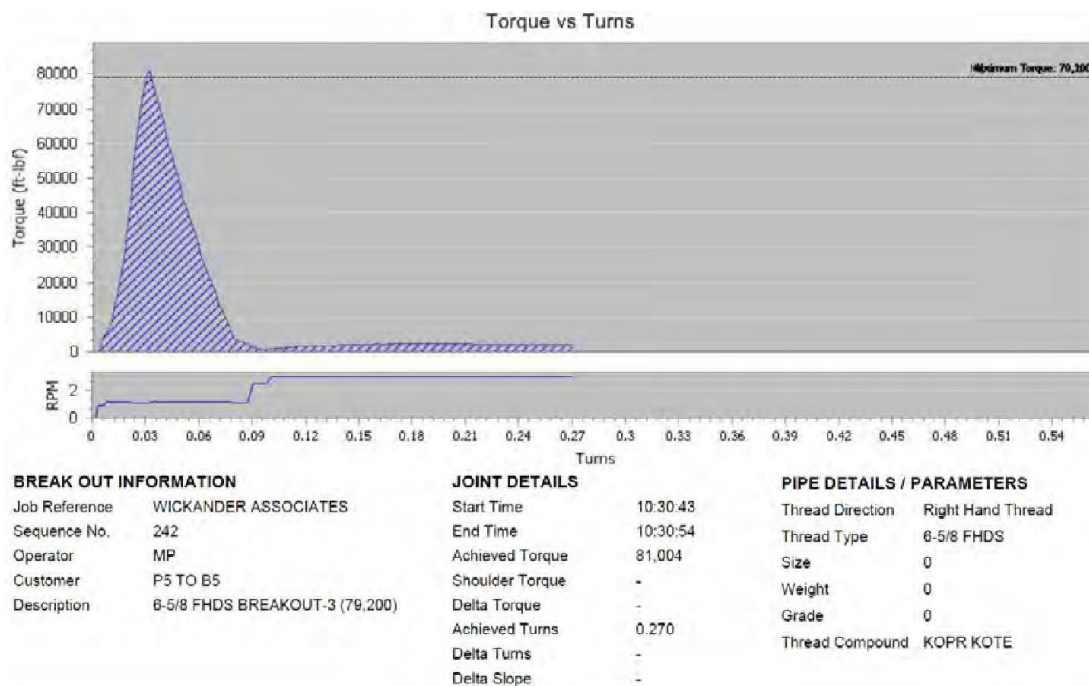
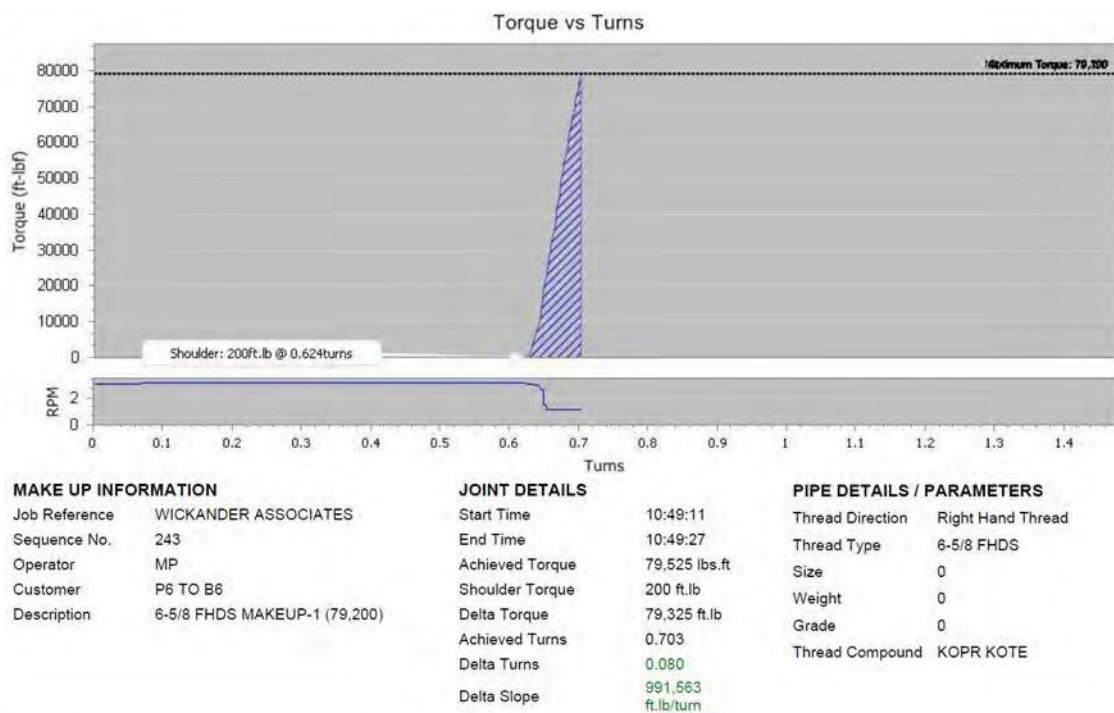
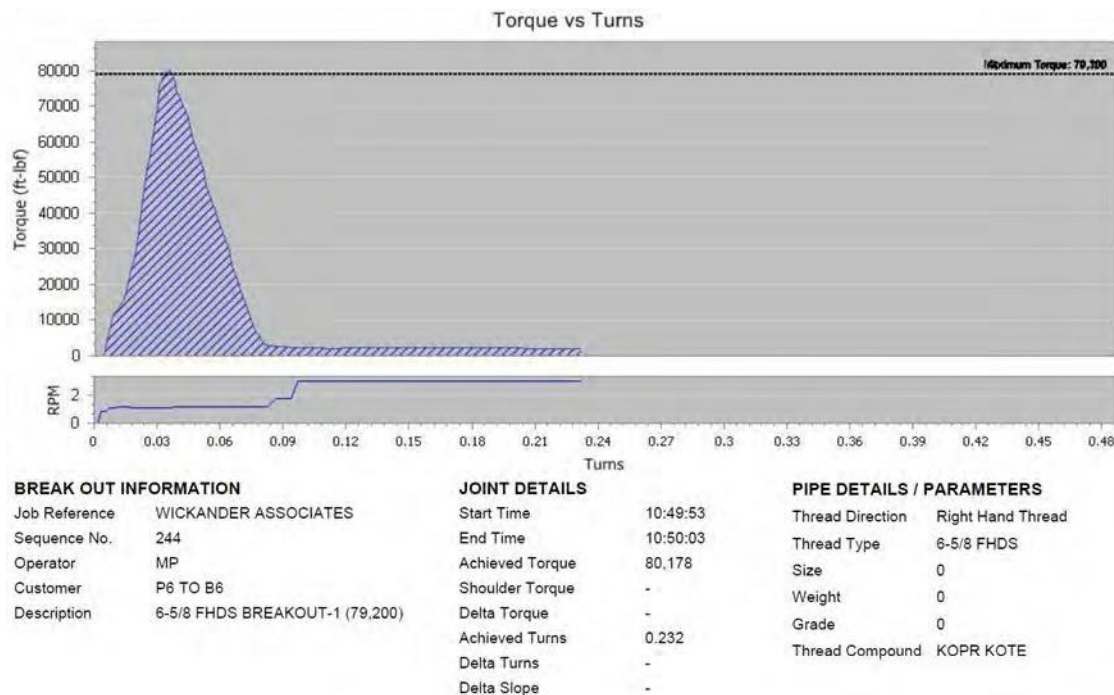


Figure D.6—6-5/8 FHDS P5–B5 Break-in Cycle, Break-out No. 3



**Figure D.7—6-5/8 FHDS P6–B6 Break-in Cycle, Make-up No. 1**



**Figure D.8—6-5/8 FHDS P6–B6 Break-in Cycle, Break-out No. 1**

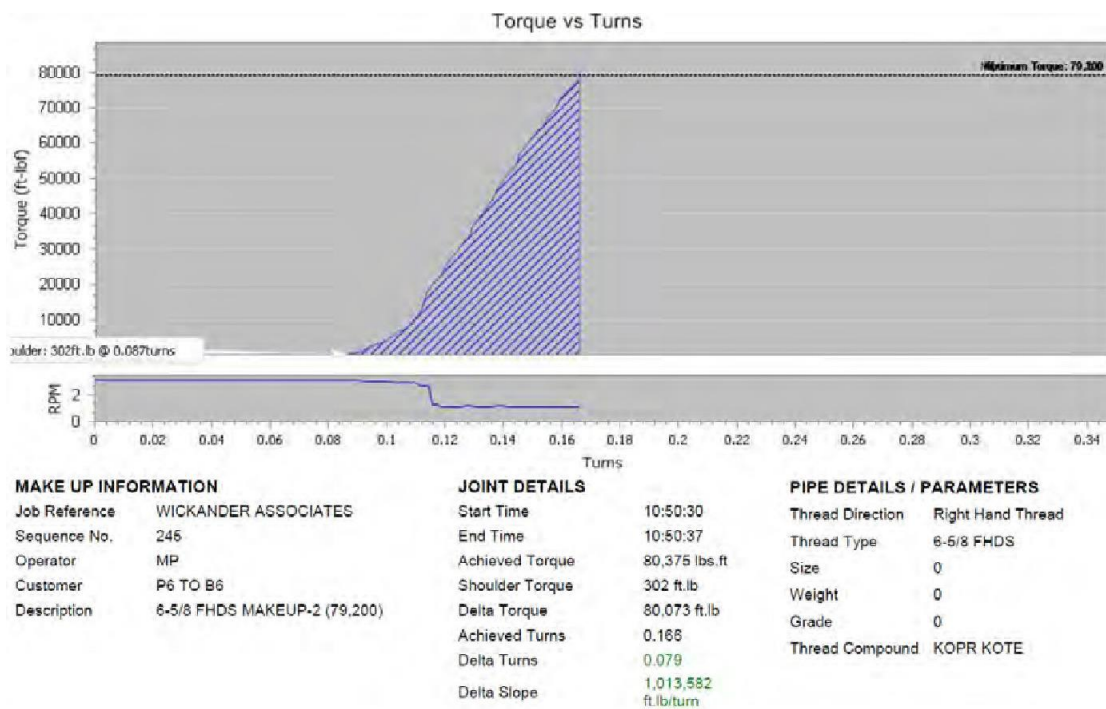


**Figure D.9—6-5/8 FHDS P6–B6 Break-in Cycle, Make-up No. 2**

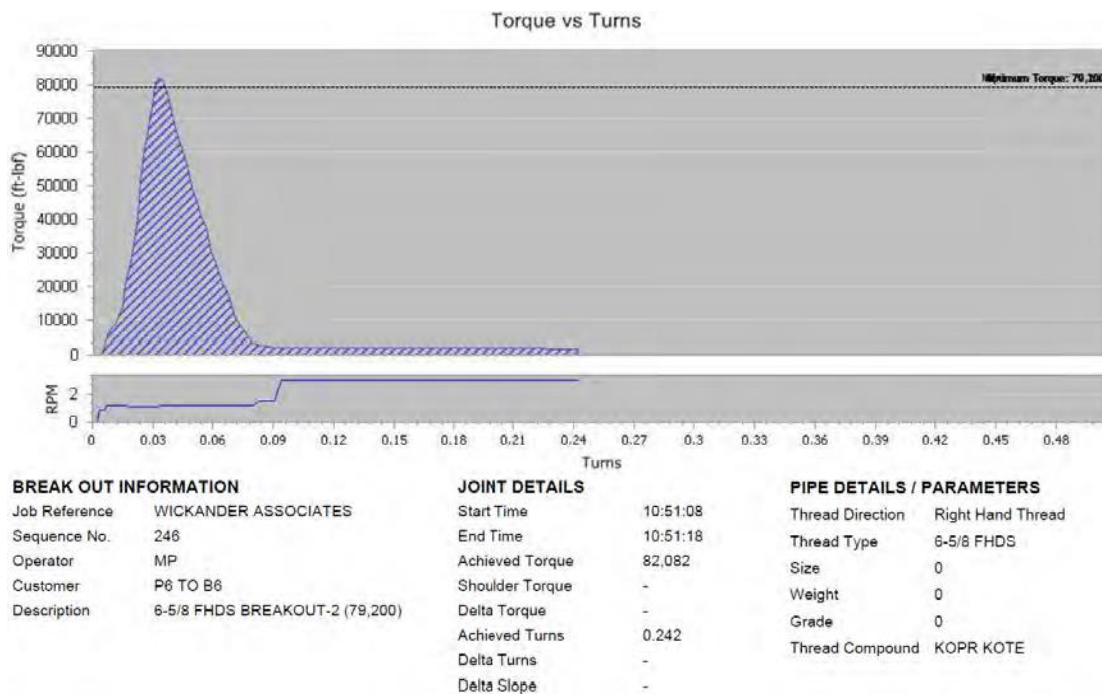


**Figure D.10—6-5/8 FHDS P6–B6 Break-in Cycle, Break-out No. 2**



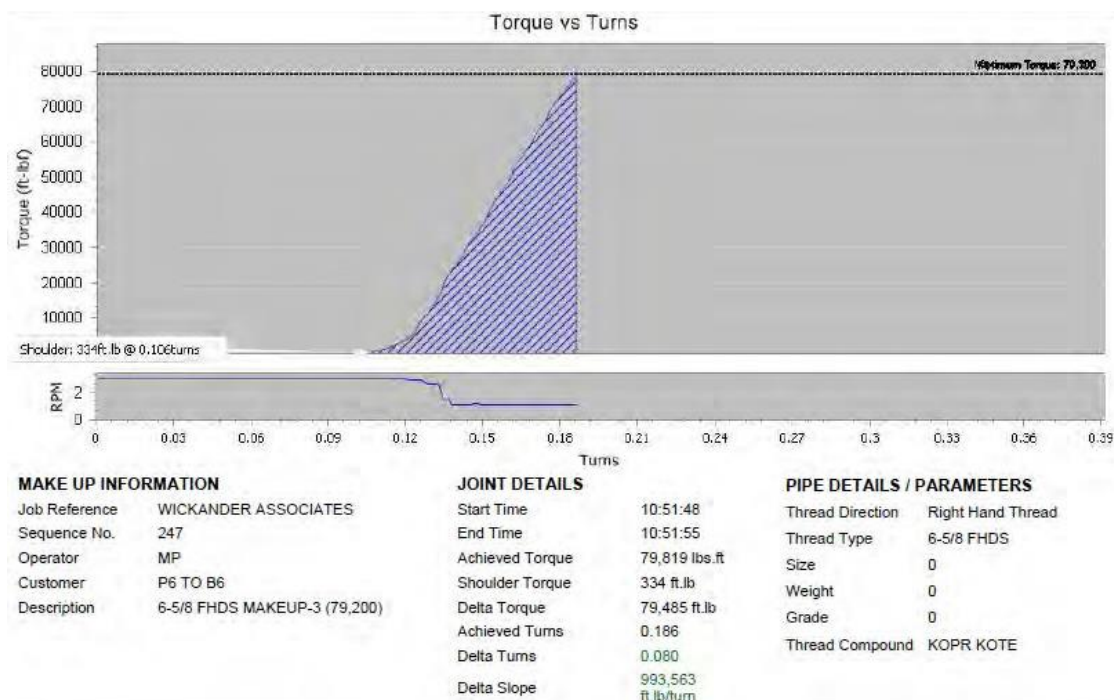


**Figure D.11—6-5/8 FHDS P6–B6 Break-in Cycle, Make-up No. 3**

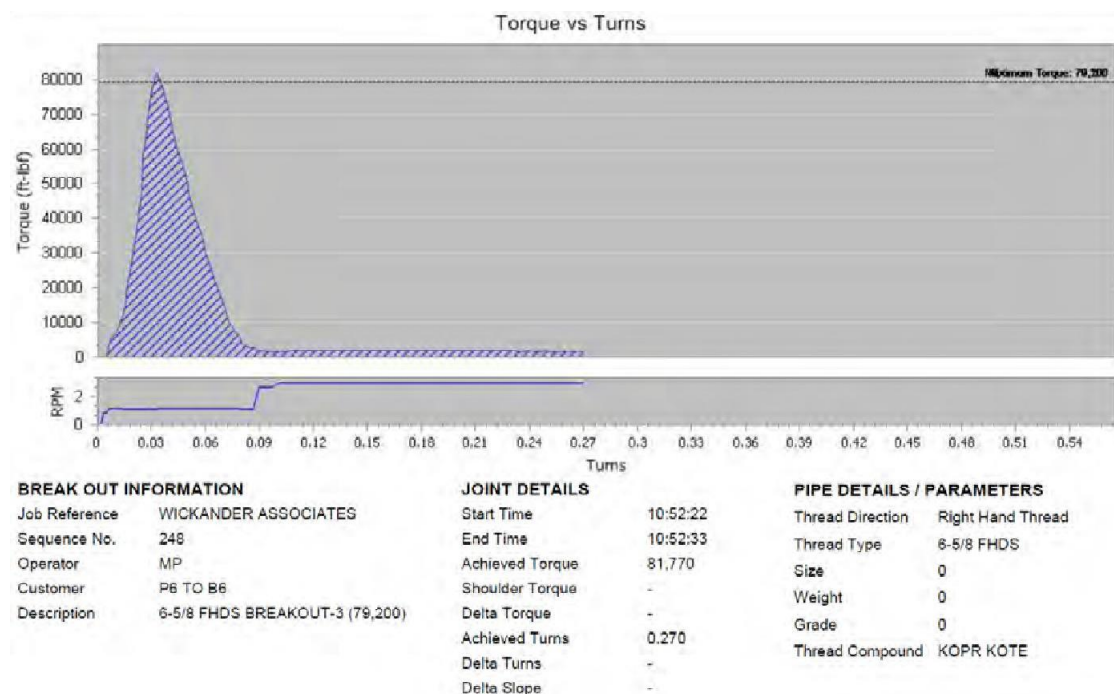


**Figure D.12—6-5/8 FHDS P6–B6 Break-in Cycle, Break-out No. 3**



**Figure D.13—6-5/8 FHDS P7–B7 Break-in Cycle, Make-up No. 1**

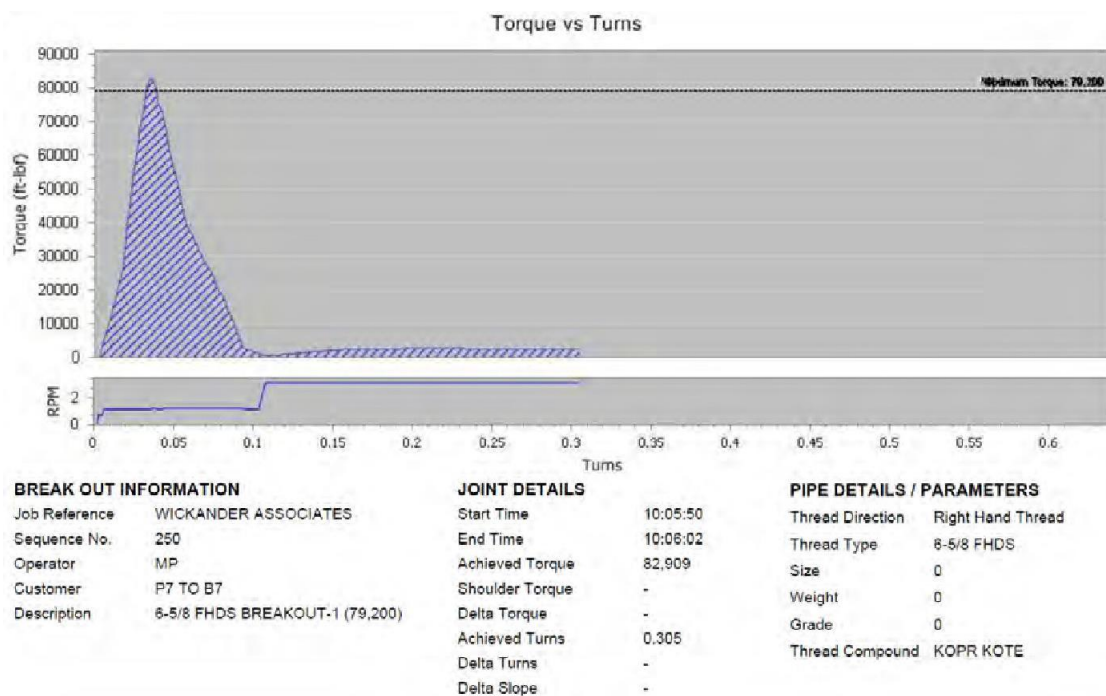


**Figure D.14—6-5/8 FHDS P7–B7 Break-in Cycle, Break-out No. 1**

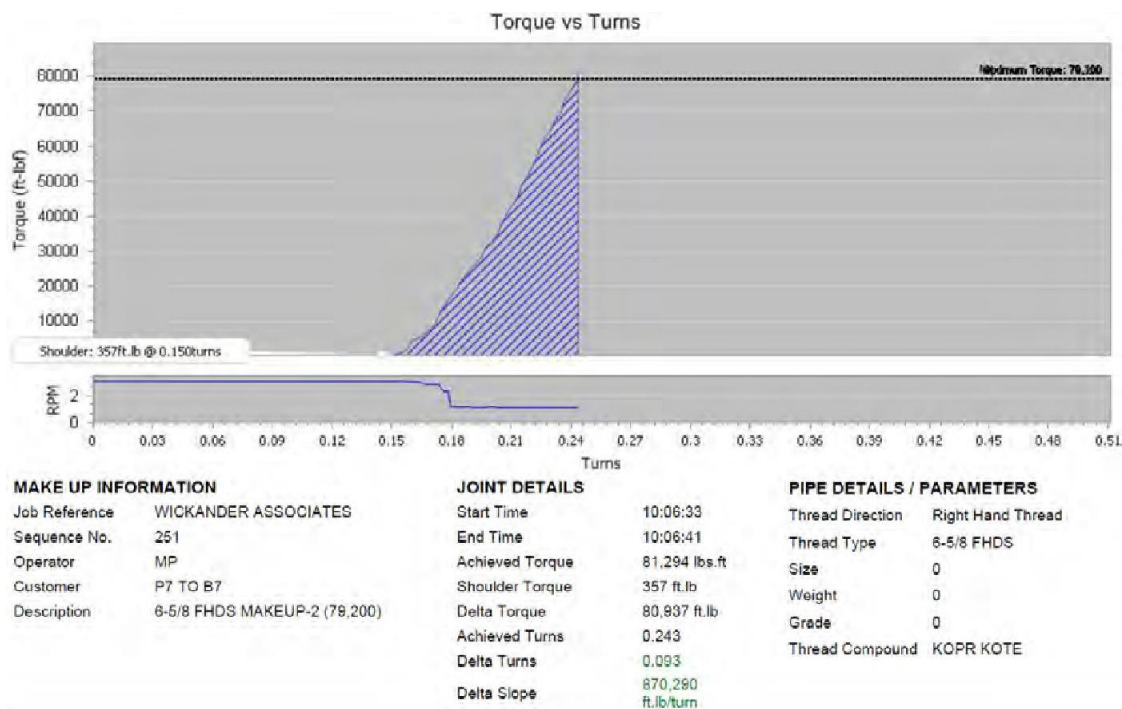


**Figure D.15—6-5/8 FHDS P7–B7 Break-in Cycle, Make-up No. 2**

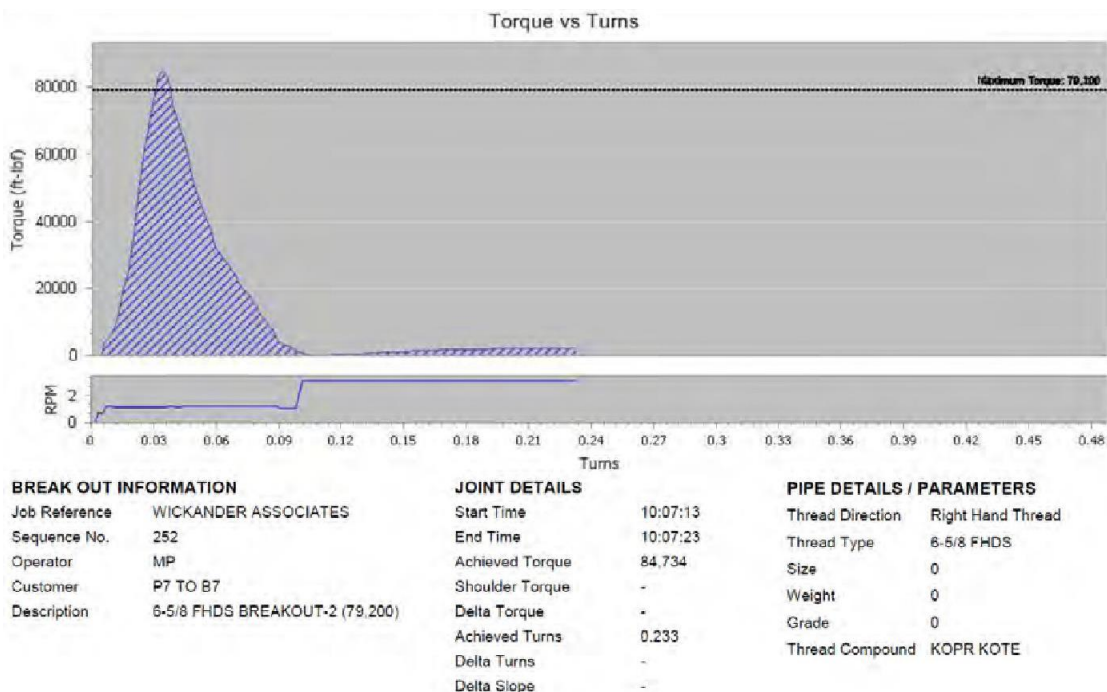


**Figure D.16—6-5/8 FHDS P7–B7 Break-in Cycle, Break-out No. 2**

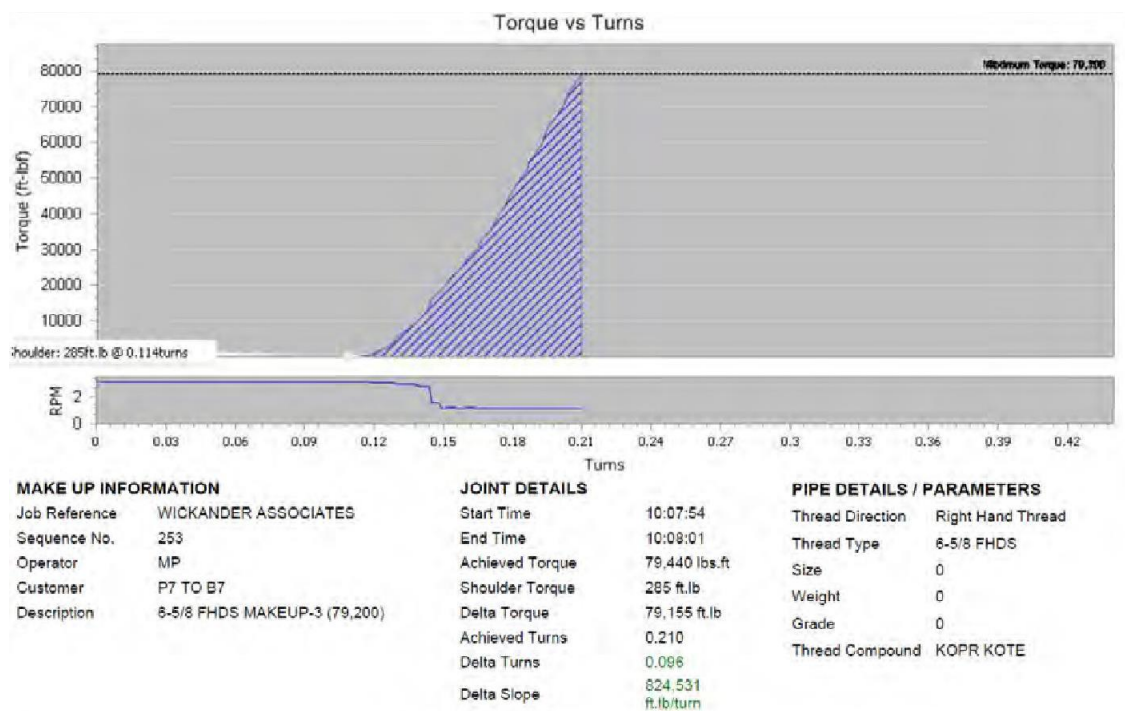


**Figure D.17—6-5/8 FHDS P7–B7 Break-in Cycle, Make-up No. 3**

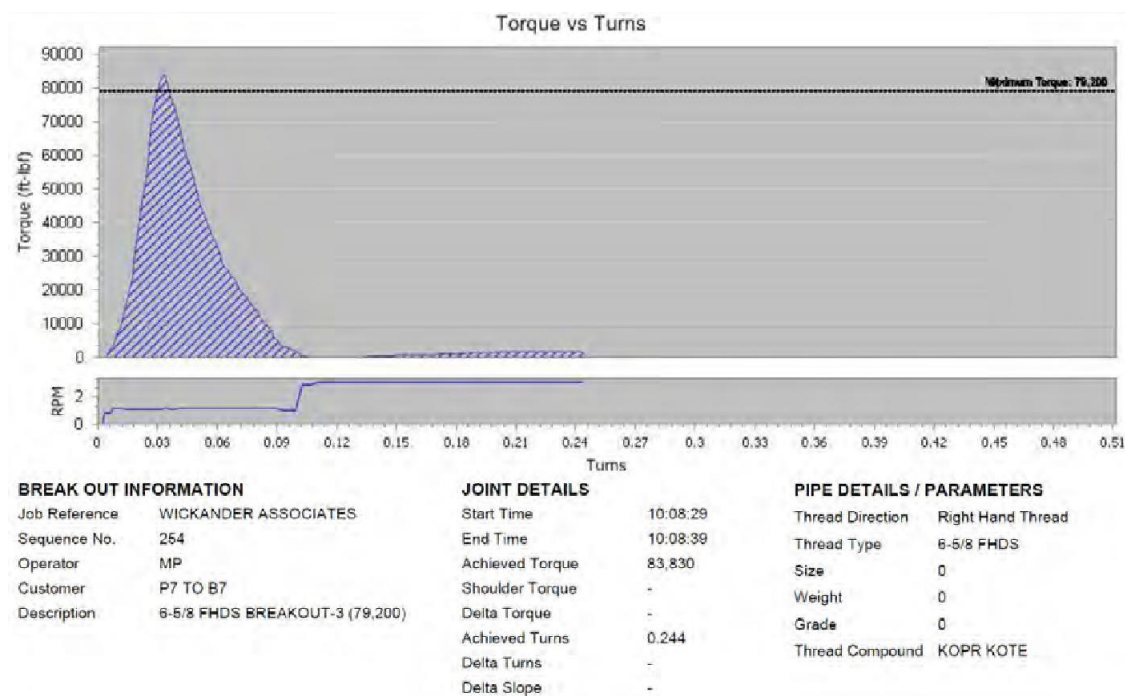


**Figure D.18—6-5/8 FHDS P7–B7 Break-in Cycle, Break-out No. 3**



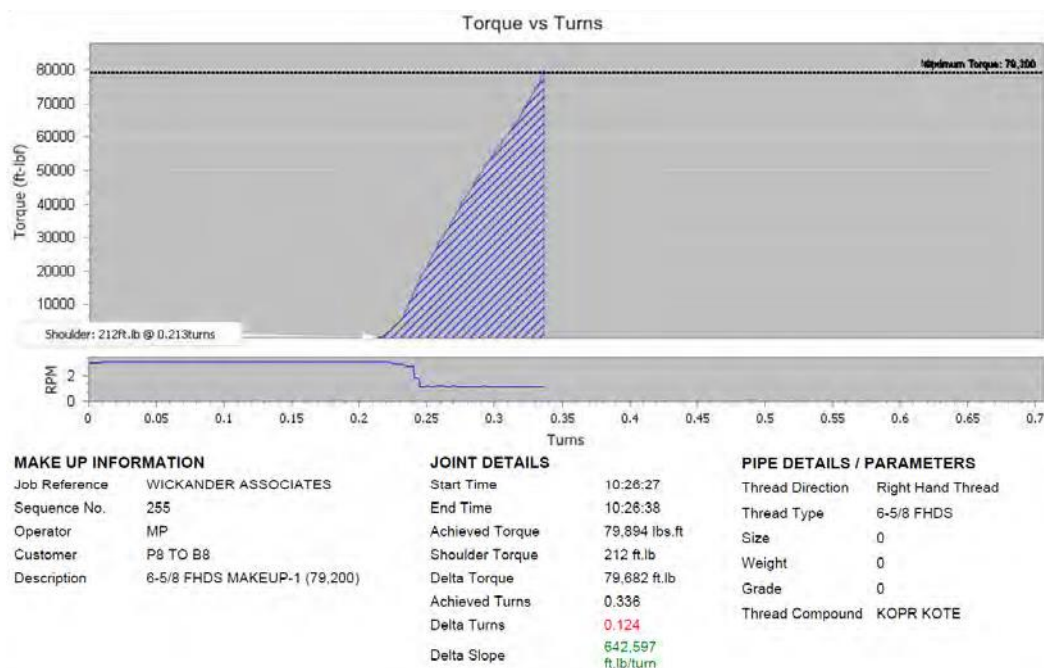


**Figure D.19—6-5/8 FHDS P8–B8 Break-in Cycle, Make-up No. 1**

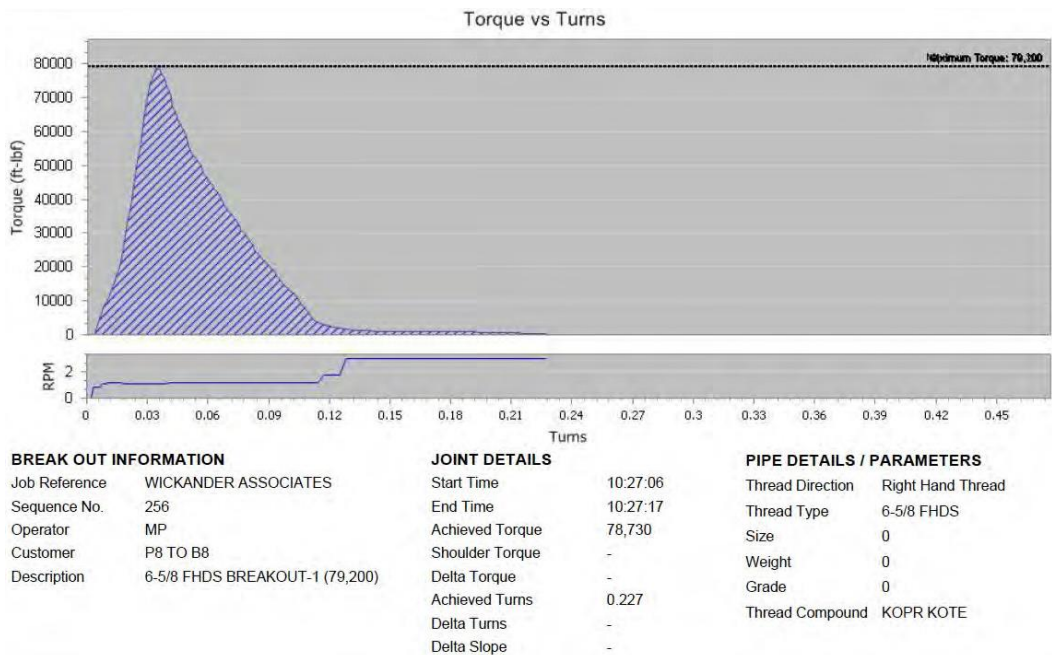


**Figure D.20—6-5/8 FHDS P8–B8 Break-in Cycle, Break-out No. 1**

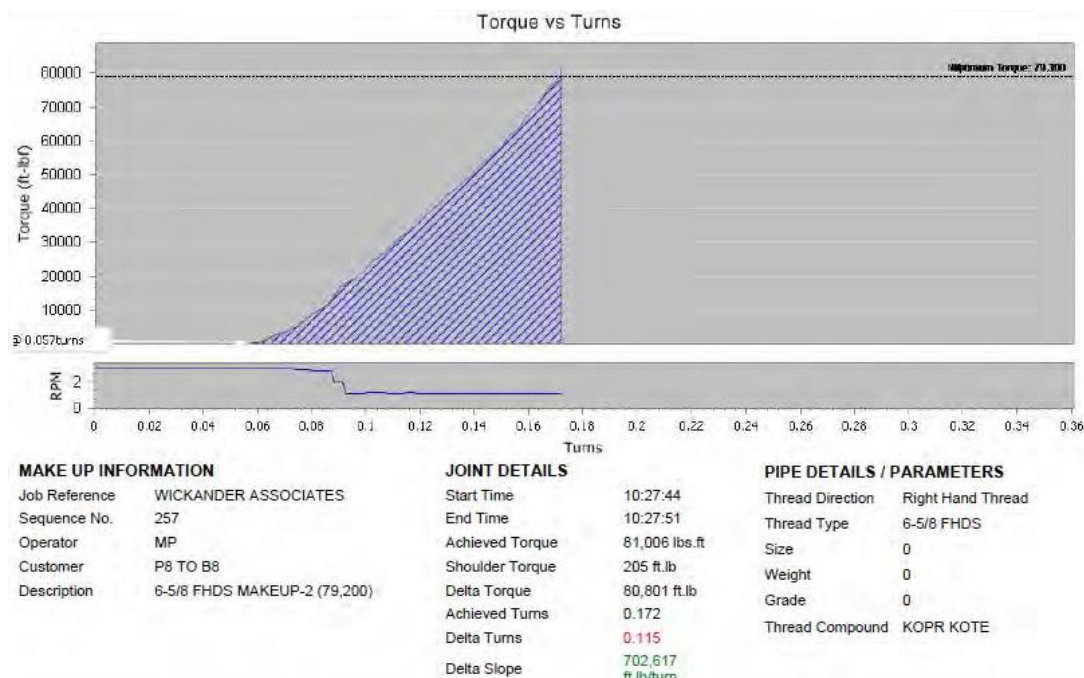


Figure D.21—6-5/8 FHDS P8–B8 Break-in Cycle, Make-up No. 2

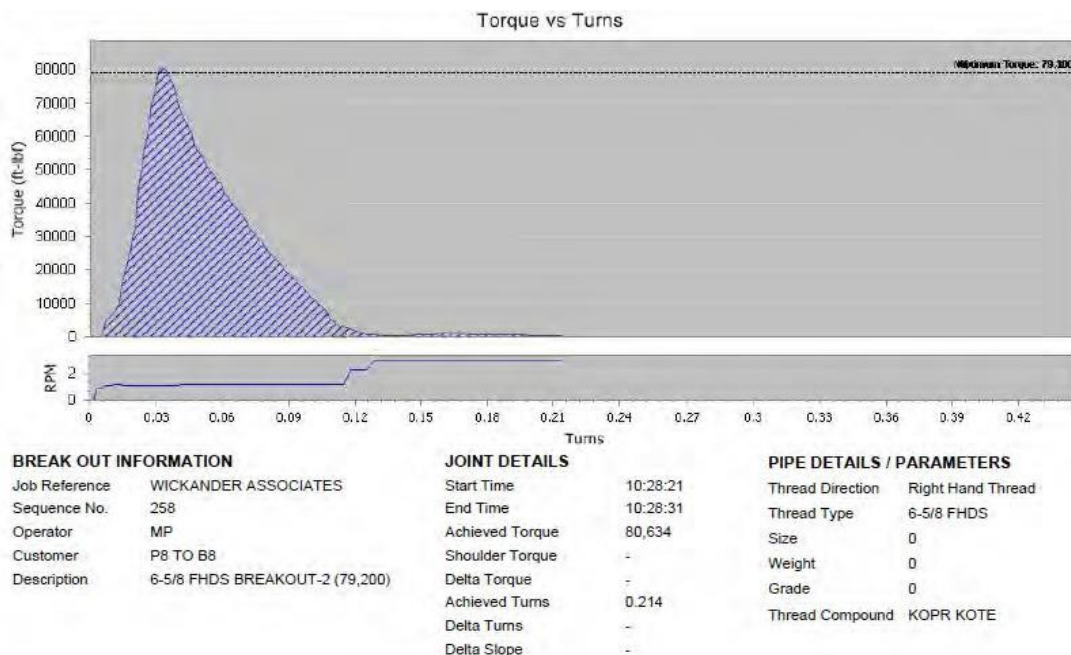
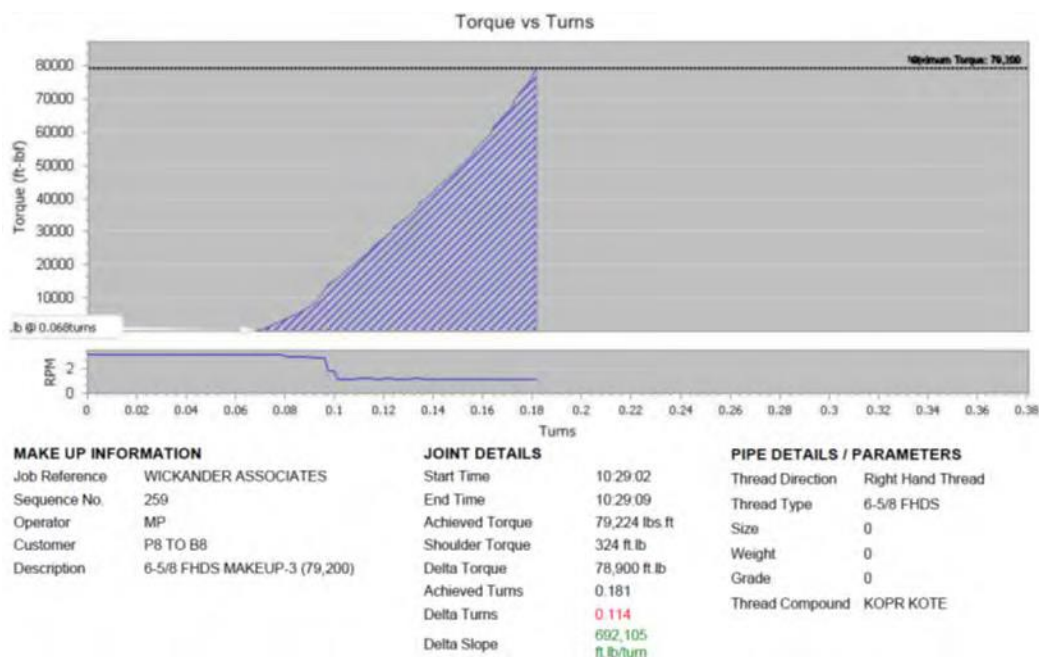
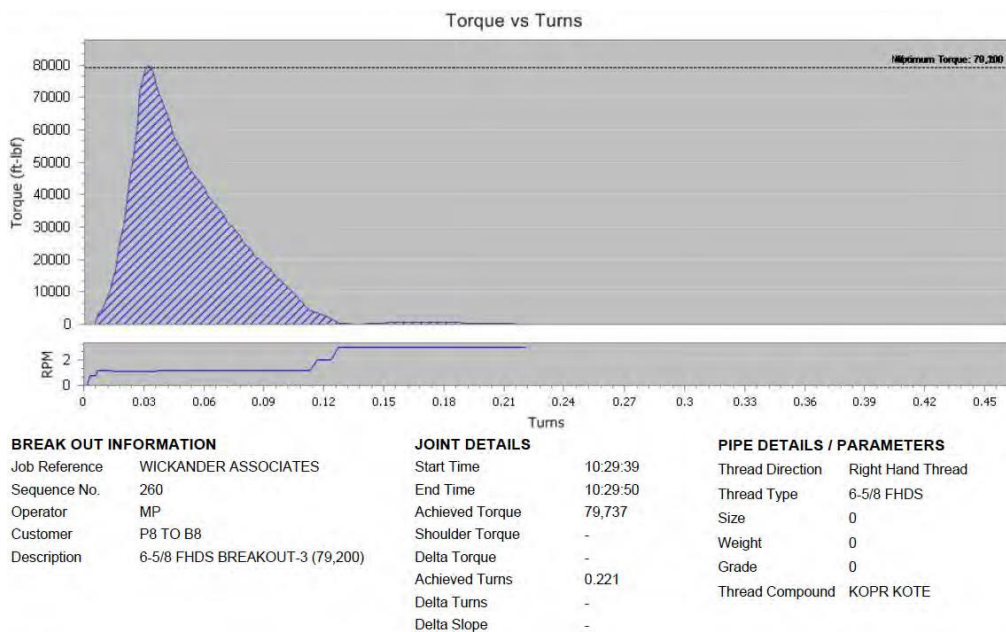


Figure D.22—6-5/8 FHDS P8–B8 Break-in Cycle, Break-out No. 2



**Figure D.23—6-5/8 FHDS P8–B8 Break-in Cycle, Make-up No. 3**



**Figure D.24—6-5/8 FHDS P8–B8 Break-in Cycle, Break-out No. 3**



## Annex E (informative) 6<sup>5</sup>/<sub>8</sub> FHDS Torque-to-yield Curves

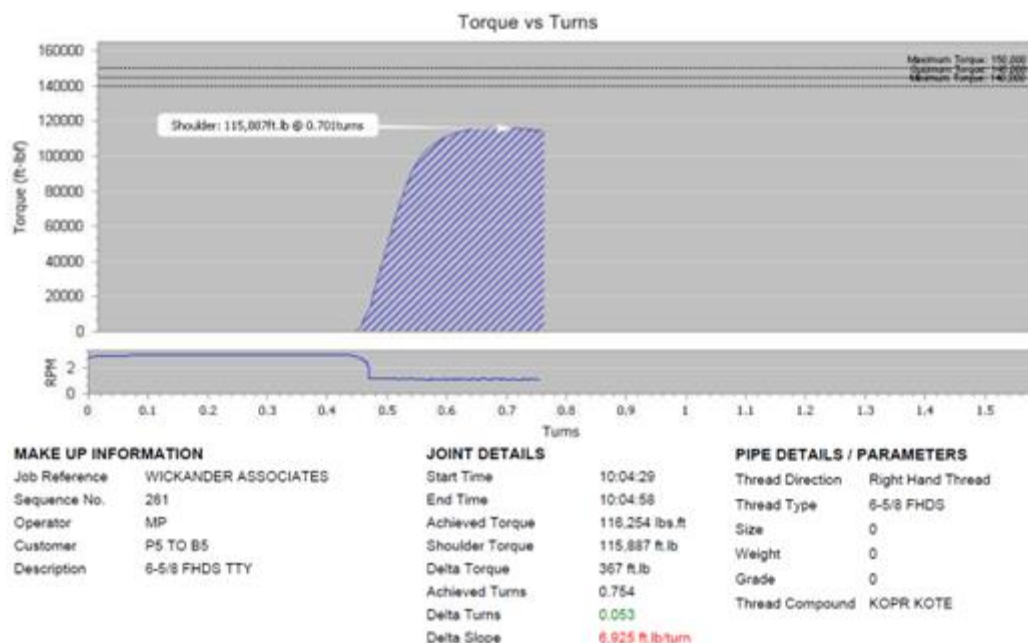


**Figure E.1—6-5/8 FHDS P5–B5 Torque-to-yield (Max Torque 116,254 ft-lbs)**

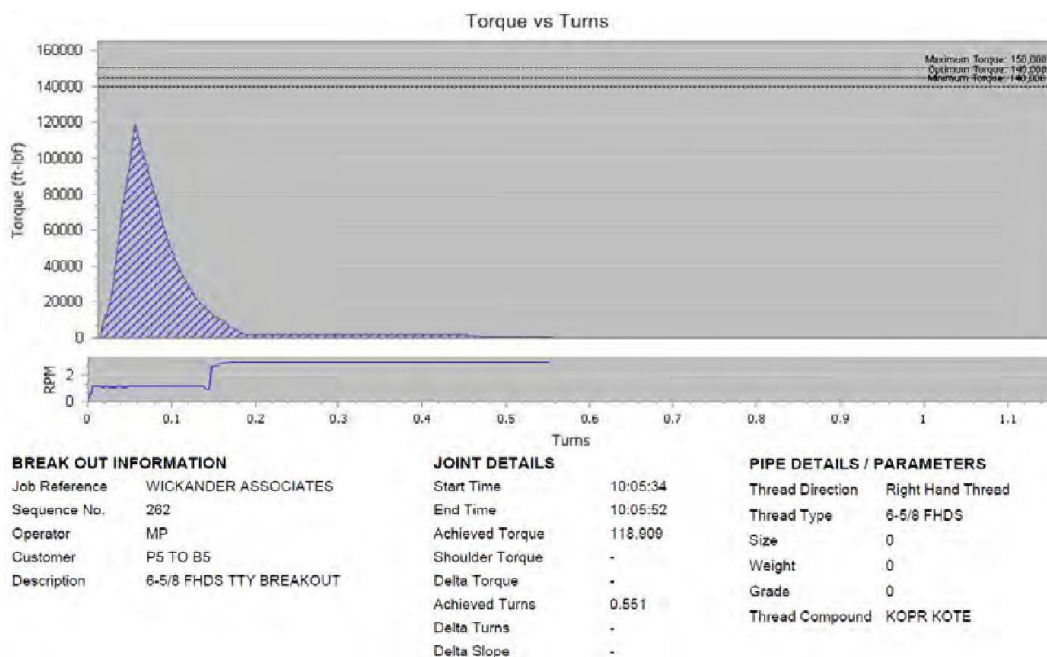


**Figure E.2—6-5/8 FHDS P5–B5 Torque-to-yield (Break-out Torque 118,909 ft-lbs)**

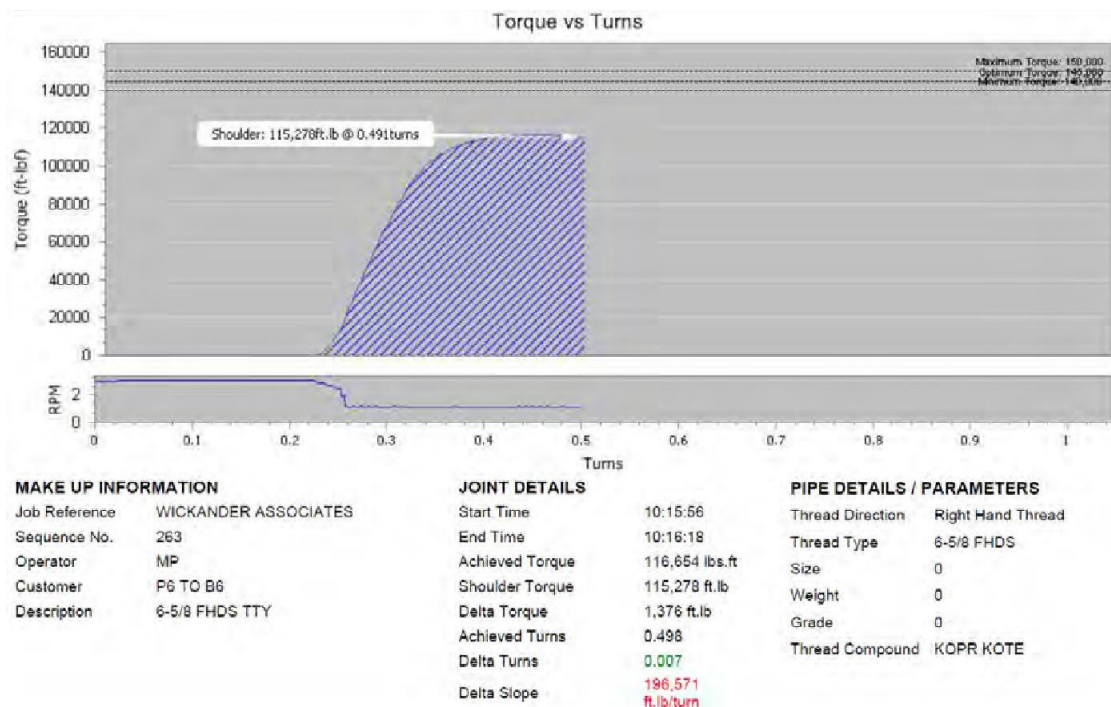


**Figure E.3—6-5/8 FHDS P6–B6 Torque-to-yield (Max Torque 116,654 ft-lbs)**

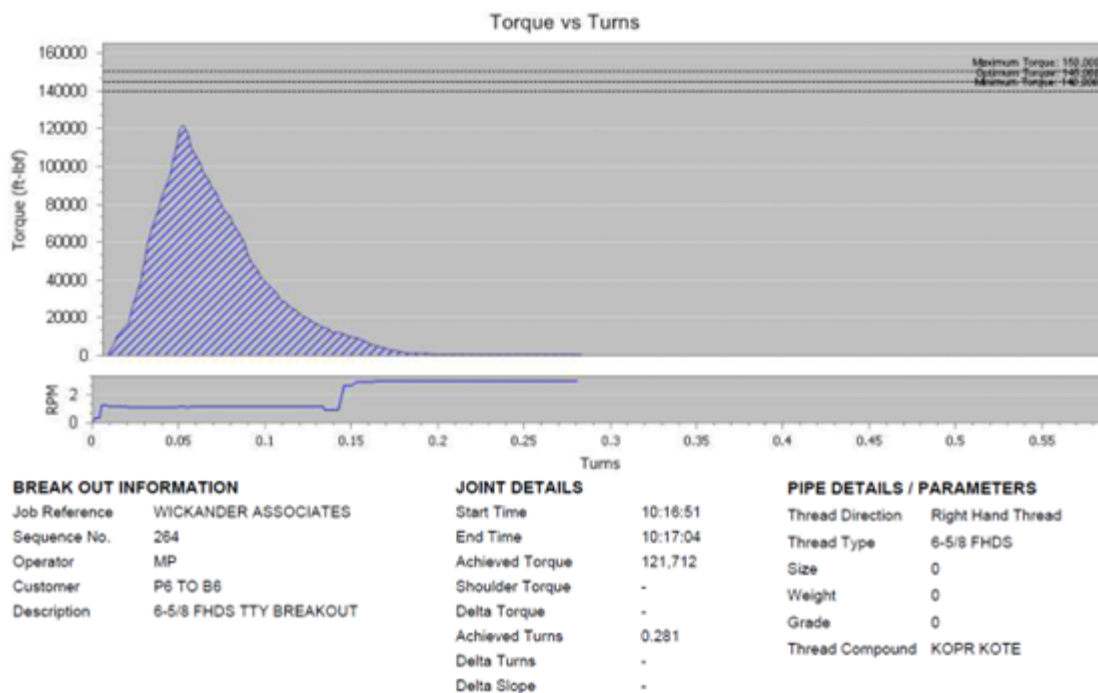


**Figure E.4—6-5/8 FHDS P6–B6 Torque-to-yield (Break-out Torque 121,712 ft-lbs)**

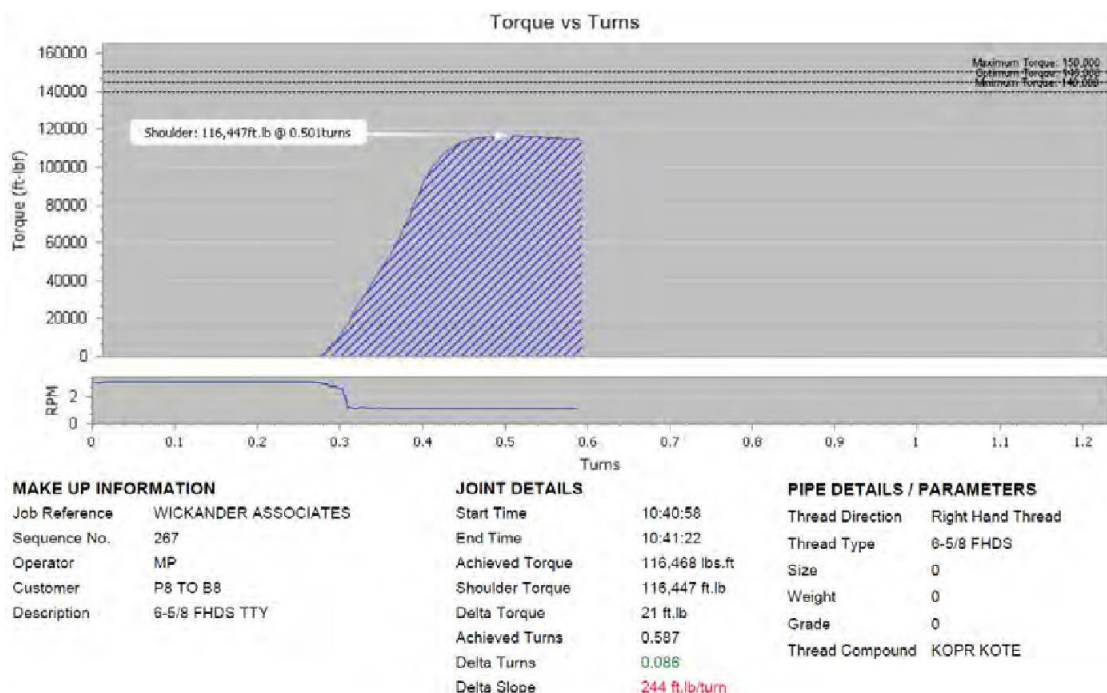


**Figure E.5—6-5/8 FHDS P8–B8 Torque-to-yield (Max Torque 116,468 ft-lbs)**

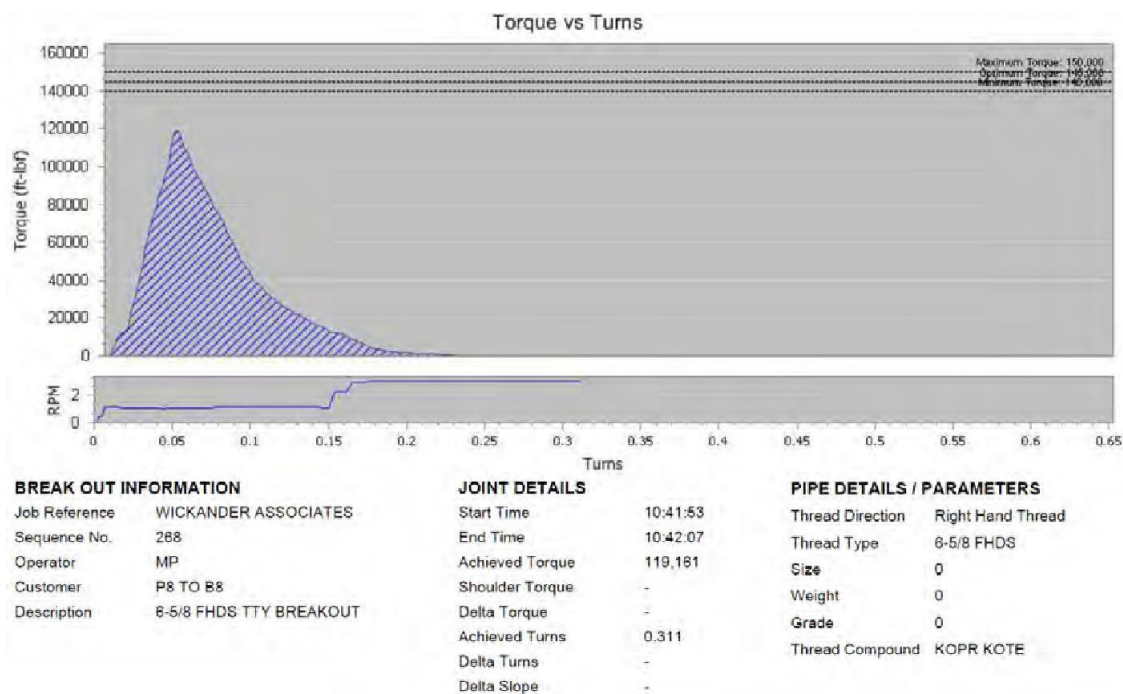



**Figure E.6—6-5/8 FHDS P8–B8 Torque-to-yield (Break-out Torque 119,161 ft-lbs)**

**Annex F**  
**(informative)**  
**Derivation of Tool Joint Torque Formula**

**THE AMERICAN SOCIETY OF  
MECHANICAL ENGINEERS**

29 WEST 39TH STREET • NEW YORK 18, N. Y.

**Paper No.  
57-PET-19**



## Torque Requirements For Rotary Shouldered Connections And Selection of Connections For Drill Collars

**A. P. FARR, Assistant Chief Product Engineer**  
HUGHES TOOL COMPANY  
P. O. Box 2539  
Houston 1, Texas

Contributed by the Petroleum Division for presentation at the ASME Petroleum Mechanical Engineering Conference, Tulsa, Oklahoma, September 22-25, 1957.  
(Manuscript received at ASME Headquarters July 29, 1957)  
Written discussion on this paper will be accepted up to October 28, 1957.  
(Copies will be available until July 1, 1958)

**50 cents per copy**  
To ASME members **25c**  
Released for general publication upon presentation  
Printed in U.S.A.

The Society shall not be responsible for statements or opinions advanced in papers or in discussion at meetings of the Society or of its Divisions or Sections, or printed in its publications.

Decision on publication of this paper in an ASME journal had not been taken when this pamphlet was prepared. Discussion is printed only if the paper is published in an ASME journal.

**Figure F.1—Derivation of Simplified Torque Formula for Rotary Shouldered Connections**



$S$  = Stress.  
 $F_s$  = Total axial resisting load, lb.  
 $F_n$  = Total force normal to thread surface, lb.  
 $R_t$  = Average mean radius of thread, inches.  
 $R_s$  = Mean radius of shoulder, inches.  
 $f$  = Coefficient of friction on mating surfaces, threads or shoulder.  
 $A$  = Tension area of pin at thread root  $\frac{3}{4}$ " from shoulder or compression area of box at an arbitrary point  $\frac{3}{8}$ " from shoulder—whichever area is less, square inches.  
 $p$  = Lead of threads, inches.  
 $W$  = Work done, inches—lb., subscripts  $a$ ,  $f$ ,  $s$ , refer to useful work, thread friction, and shoulder friction.  
 $T$  = Turning moment or torque required for makeup, lb.—inches.  
 $\alpha$  = Average helix angle or lead angle at mean diameter, degrees.

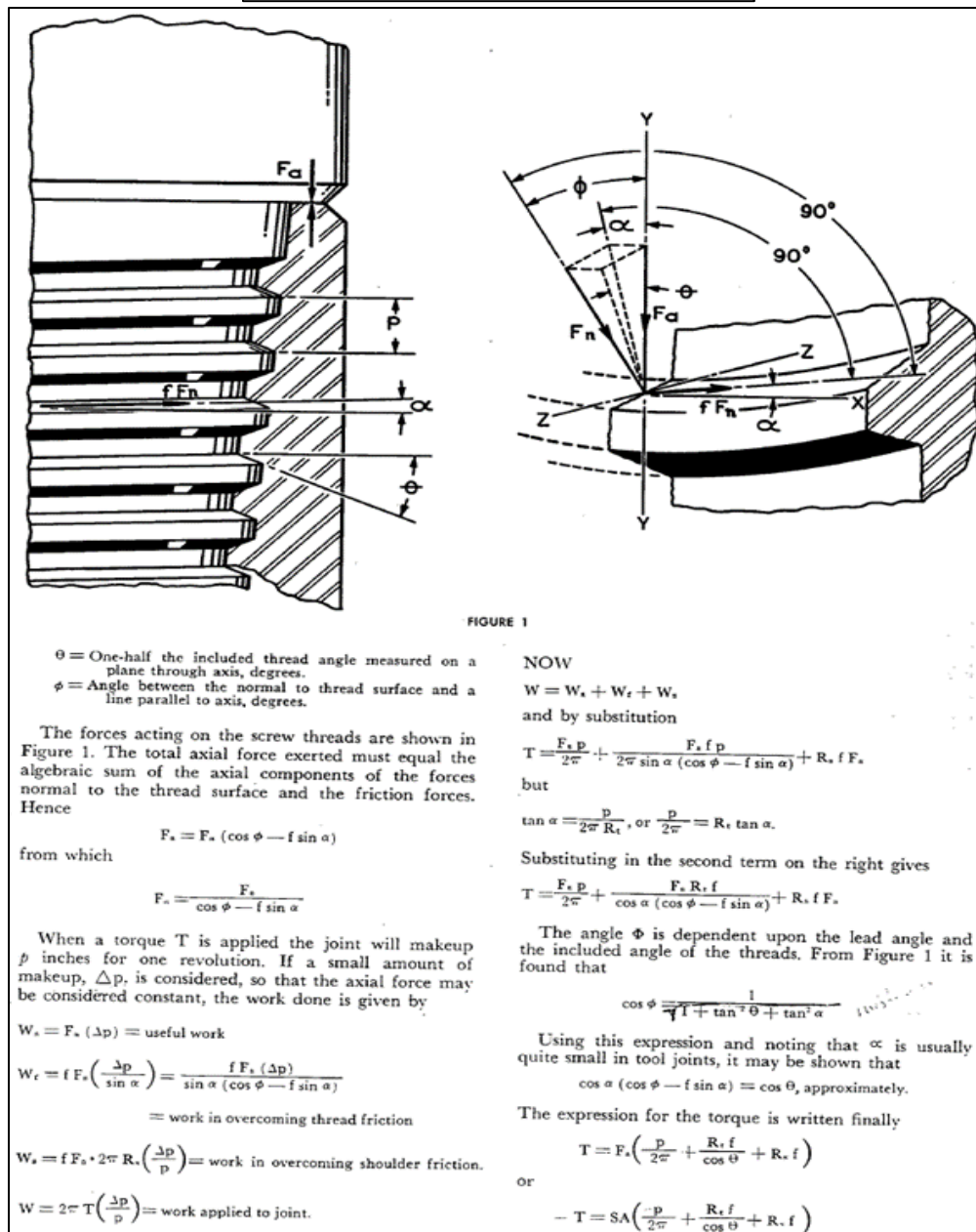


Figure F.1—Derivation of Simplified Torque Formula for Rotary Shouldered Connections (cont.)

## Annex G (informative) Calibration Certificates of Torque-turn Unit

Calibration Certificate			
Certificate No:	CC20066	Client:	DRIL-QUIP
Certificate Valid From:	28 February 2020	Client Department:	DRILLING
Certificate Valid To:	27 May 2020	Client PO:	7420740
Certification Frequency:	3 MONTHS	Machine Type:	AMC RT24:200 TO*
Torque Range:	0-200,000 ft.lb	Machine Serial No:	24:200/9131
EnerQuip Job No:	FSO03578	Customer Reference No:	N/A
Adjustments Made:	NO	Location:	HOUSTON

Calibration Details		Calibration Equipment	
Load Cell Type:	COMPRESSIVE	Manufacturer:	NORBAR
Rotation Direction:	Anti-Clockwise/Break-Out	Model No:	50637.LOG
Encoder PPR:	500	Serial No:	97682/98123**
Gear Ratio:	93.75	Accuracy:	+/- 0.84%
Headstock PPR:	46875.0	EnerQuip Serial No:	EQ-CT07
10 Turns (Tolerance 9.950 - 10.050) =	10	Calibration Date:	09 May 2019

Pre Calibration					Adjusted Calibration				
Applied (ft.lb)	Result (ft.lb)	Error (ft.lb)	Error (%)	Hydraulic Force (PSI)	Applied (ft.lb)	Result (ft.lb)	Error (ft.lb)	Error (%)	Hydraulic Force (PSI)
0	0	0	-	100	WITHIN TOLERANCE - NO ADJUSTMENTS NEEDED				
2,500	2,584	84	3.36%	150					
5,000	5,110	110	2.20%	175					
7,500	7,610	110	1.47%	200					
10,000	9,831	-169	-1.69%	225					
12,500	12,694	194	1.55%	275					
15,000	15,286	286	1.91%	300					
17,500	17,435	-65	-0.37%	325					
20,000	20,357	357	1.78%	350					
25,000	24,683	-317	-1.27%	400					
30,000	29,619	-381	-1.27%	500					
35,000	34,506	-494	-1.41%	550					
40,000	39,850	-150	-0.38%	600					
50,000	50,020	20	0.04%	700					
60,000	59,942	-58	-0.10%	850					
70,000	69,774	-226	-0.32%	1,000					
80,000	80,241	241	0.30%	1,175					
100,000	101,900	1900	1.90%	1,400					
150,000	151,021***	1021	0.00%	2,022***					
200,000	201,420***	1420	0.00%	2,653***					
Tolerance		0-2300 ft.lb = ±5%			2300-5750 ft.lb = ±115 ft.lb		Above 5750 ft.lb = ±2%		

\* The Machine was calibrated to manufacturers specifications IAW EQQP-Service-002-Calibration Procedure

\*\* The equipment used to calibrate this machine is traceable to National Standards or equivalent

\*\*\* The calibration point has been extrapolated using a linear calculation based on the previous calibrated points.

The equipment used to calibrate this machine is traceable to National Standards or equivalent

Figure G.1—Certificate of Calibration

Turns Calibration							
READING	ANGLE	TURN	ACTUAL READING ON TORQUE UNIT	TOLERANCE	DIFFERENCE	DIFFERENCE	ACC/REJ
	Degrees	Turns	Turns	+/- %	Turns	+/- %	
1	90	0.250	0.250	1%	0.000	0.00%	ACC
2	180	0.500	0.500	1%	0.000	0.00%	ACC
3	270	0.750	0.749	1%	0.001	-0.13%	ACC
4	360	1.000	1.000	1%	0.000	0.00%	ACC
5	720	2.000	2.000	1%	0.000	0.00%	ACC
6	1080	3.000	3.000	1%	0.000	0.00%	ACC
7	1140	4.000	4.000	1%	0.000	0.00%	ACC
8	1800	5.000	5.001	1%	-0.001	0.02%	ACC
9	2160	6.000	6.000	1%	0.000	0.00%	ACC
10	2520	7.000	7.000	1%	0.000	0.00%	ACC
11	2880	8.000	8.000	1%	0.000	0.00%	ACC
12	3240	9.000	9.000	1%	0.000	0.00%	ACC
13	3600	10.000	10.000	1%	0.000	0.00%	ACC

Speed Calibration							
TURNS	STOPWATCH		SPEED RPM MEASURED	SPEED RPM DISPLAYED	TOLLERANCE	DIFFERENCE	ACC/REJ
	second	minute	turn/min	turn/min	+/- %	+/- %	
1	21	0.35	2.86	3.00	10%	5.00%	ACC
2	41	0.68	2.93	3.00	10%	2.50%	ACC
3	61	1.02	2.95	3.00	10%	1.67%	ACC
4	82	1.37	2.93	3.00	10%	2.50%	ACC
5	105	1.75	2.86	3.00	10%	5.00%	ACC
6	124	2.07	2.90	3.00	10%	3.33%	ACC
7	146	2.43	2.88	3.00	10%	4.29%	ACC
8	167	2.78	2.87	3.00	10%	4.38%	ACC
9	188	3.13	2.87	3.00	10%	4.44%	ACC
10	209	3.48	2.87	3.00	10%	4.50%	ACC

**Figure G.1—Certificate of Calibration (cont.)**



## **Bibliography**

- [1] API Recommended Practice 7G, *Drill Stem Design and Operating Limits*, 16<sup>th</sup> Edition